THE UNIVERSITY
OF MICHIGAN
MAY 23 1960
ENGINEERING
LIBRARY

Number 3

March 1959

ИЗМЕРИТЕЛЬНАЯ
ТЕХНИКА

SOVIET INSTRUMENTATION AND
CONTROL TRANSLATION SERIES

Measurement Techniques

(The Soviet Journal *Izmeritel'naya Tekhnika* in English Translation)

■ This translation of a Soviet journal on instrumentation is published as a service to American science and industry. It is sponsored by the Instrument Society of America under a grant in aid from the National Science Foundation with additional assistance from the National Bureau of Standards.

SOVIET INSTRUMENTATION AND CONTROL TRANSLATION SERIES

Instrument Society of America Executive Board

John Johnston, Jr.
President
Henry C. Frost
Past President
Dr. Ralph H. Tripp
President-Elect-Secretary
Thomas C. Wherry
Dept. Vice President
Glen G. Gallagher
Dept. Vice President
Adelbert Carpenter
Dept. Vice President
Nathan Cohn
Dept. Vice President
John C. Koch
Treasurer
Nelson Gildersleeve
Dist. I Vice President
Charles A. Kohr
Dist. II Vice President
John R. Mahoney
Dist. III Vice President
George L. Kellner
Dist. IV Vice President
Milton M. McMillen
Dist. V Vice President
Glenn F. Brockett
Dist. VI Vice President
Thomas H. Pierson
Dist. VII Vice President
John A. See
Dist. VIII Vice President
Robert C. Mann
Dist. IX Vice President
Joseph R. Rogers
Dist. X Vice President
John J. McDonald
Dist. XI Vice President

Headquarters Office

William H. Kushnick
Executive Director
Charles W. Covey
Editor, ISA Journal
George A. Hall, Jr.
Assistant Editor, ISA Journal
Herbert S. Kindler
Director, Tech. & Educ. Services
Ralph M. Stotsenburg
Director, Promotional Services
William F. Minnick, Jr.
Director, Public Relations

ISA Publications Committee

Nathan Cohn, *Chairman*
Jere E. Brophy, Enoch J. Durbin, George R. Feeley, Richard W. Jones, George A. Larsen, Thomas G. MacAnespie, John E. Read, Joshua Stern, Frank S. Swaney, Richard A. Terry

Translations Advisory Board of the Publications Committee

Jere E. Brophy, *Chairman*
T. J. Higgins, S. G. Eskin, G. Werbizky

■ This translation of the Soviet Journal *Izmeritel'naya Tekhnika* is published and distributed at nominal subscription rates under a grant in aid to the Instrument Society of America from the National Science Foundation. This translated journal, and others in the Series (see back cover), will enable American scientists and engineers to be informed of work in the fields of instrumentation, measurement techniques, and automatic control reported in the Soviet Union.

The original Russian articles are translated by competent technical personnel. The translations are on a cover-to-cover basis, permitting readers to appraise for themselves the scope, status, and importance of the Soviet work.

Publication of *Izmeritel'naya Tekhnika* in English translation started under the present auspices in August, 1959, with Russian issue No. 1 of Jan.-Feb. 1958. The six issues of the 1958 volume year were published in English translation by February, 1960. Russian issue No. 1 of January, 1959 will be published in March, 1960, and the twelve issues of 1959 will be published in English translation by December, 1960.

Transliteration of the names of Russian authors follows the system known as the British Standard. This system has recently achieved wide adoption in the United Kingdom, and is being adopted in 1959 by a large number of scientific journals in the United States.

All views expressed in the translated material are intended to be those of the original authors, and not those of the translators, nor the Instrument Society of America.

Readers are invited to submit communications on the quality of the translations and the content of the articles to ISA headquarters. Pertinent correspondence will be published in the "Letters" section of the ISA Journal. Space will also be made available in the ISA Journal for such replies as may be received from Russian authors to comments or questions by American readers.

1959 Issue Subscription Prices:

Per year (12 issues), starting with 1959, No. 1

General: United States and Canada	$25.00
Elsewhere	28.00
Libraries of nonprofit academic institutions:	
United States and Canada	$12.50
Elsewhere	15.50
Single issues to everyone, each	$ 6.00

1958 issues also available. Prices upon request.

See back cover for combined subscription to entire Series.

Subscriptions and requests for information on back issues should be addressed to the:

Instrument Society of America
313 Sixth Avenue, Pittsburgh 22, Penna.

Translated and printed by Consultants Bureau, Inc.

Number 3—March, 1959

English Translation Published May, 1960

Measurement Techniques

The Soviet Journal Izmeritel'naya Tekhnika in English Translation

Reported circulation of the Russian original 8,000.

Izmeritel'naya Tekhnika is an organ of the Academy of Sciences, USSR

EDITORIAL BOARD
as Listed in the Original Soviet Journal

G. D. Burdun, *Editor*
I. I. Chechik, *Asst. Editor*
V. O. Arutyunov
N. M. Karelin
B. M. Leonov
M. I. Levin
V. F. Lubentsov
P. G. Strelkov
B. M. Yanovskii
M. K. Zhokhovskii
N. I. Zimin

See following page for Table of Contents.

Copyright by Instrument Society of America 1960

MEASUREMENT TECHNIQUES

1959 Number 3 March

CONTENTS

	PAGE	RUSS. PAGE
Improvement in the Supervision of Measurement Technology. Ya. I. Kazovskii	155	1
A General Approach to the Analysis of Static and Dynamic Errors. N. A. Chekhonadskii	156	2
Linear Measurements		
Inspection of Gas Turbine Blade Blanks. B. I. Pikalov and V. V. Petrosov	161	5
A Recording Extensometer. A. D. Martynov	163	7
A New Dividing Head. E. I. Finkel'shtein	164	8
A Theodolite Apparatus for Checking Angle Gages. N. P. Konovalov	166	9
A Miniature Portable Piezoelectric Profilograph. E. I. Regirer	168	11
A Modification to the MIS-11 Double Microscope. F. P. Volosevich	172	14
Determination of Undesirable Tapering in Punching. P. U. Markov	174	15
Device for Polishing Large Micrometers. A. F. Chadaev and E. V. Navskii	174	16
Systematic Inspection of Gages. V. G. Shtein	175	16
The Piston-Balancing Errors of Weight-and-Piston Pressure Gages. V. N. Samoilov	178	19
Investigation of the Reasons for the Instability of Various Tensiometer Systems at High Temperatures. E. Yu. Nekhendzi	182	21
An Electromechanical Tension Dynamometer for 50,000 kg Loads. O. N. Fofanov	187	25
Electrical Measurements		
Convergence of Automatic Balancing in Measuring Circuits with Two Balancing Elements. V. Yu. Kneller	189	27
Automatic Testing Equipment of the "Elektroschetchik" Plant. I. N. Osher	196	32
Maximum Sensitivity of a Simple Bridge Circuit at Balance. V. A. Kochan	200	36

CONTENTS (continued)

	PAGE	RUSS. PAGE
Moving Coil Loop Vibrator With Concentrated Liquid Damping. S. N. Gural'nik and A. N. Zaslavskii	206	39
High and Ultrahigh Frequency Measurements		
A Standard Pulse-Series Generator for Checking Discrete-Operation Computers in Measuring Instruments. G. L. Grin and M. A. Zemel'man	209	42
Impedance Measurements by Means of Directional Couplers. A. I. Zykov	211	44
Calculation of Errors in Comparing Frequencies by Means of Lissajous Figures. M. I. Shatalov	215	46
A V. T. Voltmeter for a Radio Noise Measuring Device with Internationally Recommended Parameters. I. M. Furmanov	218	48
Application of High Precision 44-I Wavemeters. V. Ya. Volodarskii	221	51
Radiation Measurements		
Assaying Radium Preparations for Radium Content. G. V. Gorshkov, F. M. Karavaev, and N. S. Shimanskaya	222	52
A Portable Electroviscometer. P. A. Ivanov	224	54
Essays and Reviews		
Dynamic Properties of Devices for Measuring Unstable Temperatures. G. P. Katys	230	58
Committee of Measures Standards, Measures, and Measuring Devices		
I. New Standards for Measures and Measuring Devices Approved by the Committee	237	63
II. Measures and Measuring Devices Approved by the Committee on the Basis of Official Tests and Admitted for Use in the USSR	237	63
Amendments to the Instructions now in Operation for the Inspection of Measures and Measuring Devices. N. N. Staroverov	238	63

IMPROVEMENT IN THE SUPERVISION OF MEASUREMENT TECHNOLOGY*

Ya. I. Kazovskii

A number of commercial enterprises until recently had established workshops and laboratories for checking and repairing apparatus. The establishment of these workshops resulted in unnecessary expenditure of resources and also lowered the quality of apparatus maintenance. For example, the cost of a three phase stand for checking electric meters and other electric apparatus varied in different workshops from 20,000 to 80,000 rubles. Some 50 to 500 meters and perhaps about 500 other pieces of electric apparatus have to be checked by departmental inspectors once a year and by the inspectors of the Committee on Standards, Measures and Measuring Devices once every two years. The rest of the time the stand was not in use.

Each economic administrative region (or group of regions) should have one large workshop for the maintenance of apparatus, rather than a number of separate workshops and laboratories. The Council of National Economy (sovnarkhoz) could supply individual enterprises with various pieces of equipment through this workshop.

Assembling points and organizations had been set up at various times by several different ministries for the assembly of apparatus and automatic devices. These organizations carried out departmental inspection of measuring devices. The trusts and companies presently in existence (for example, "Yuvmetallurgavtomatika", "Stroiteplokontrol," "Remenergomontazh" and "Promstroiavtomatika") do the same work, but very often they do it badly. The branches of these trusts should be organized into one large assembling organization under the direction of the Council of National Economy.

The RTC (Regional Technical Council) should have charge of maintenance and departmental supervision of the rural districts; this would improve the quality of supervision and would likewise decrease maintenance costs.

Committee units in charge of inspection should also be examined. According to workers at the Stalinsk, Odessa, Sumy, Ternopol'sk, Vinnitsa and Chernovitsy GKL (State Control Laboratories) the establishment of temporary departments was not completely justified.

As the quantity of apparatus being used in the national economy is increasing, it is necessary to increase both the staffs of the existing temporary departments and the stock of standardizing apparatus, automotive devices, etc.

Temporary departments should be abolished, and State Control Laboratories should take over the inspection of base laboratories of the Council of National Economy, while the Regional Technical Council would take charge of the standardizing apparatus (stands and devices designed for the checking of apparatus).

In order that the standardizing apparatus can be used in its greatest advantage and in order that the full potential of government inspectors might be realized, it is necessary to reorganize the structure of the State Control Laboratories for Measurement Technology. The State Control Laboratory must be divided into sections (departments): one of standards and technical conditions, one for research, one in charge of inspections and one dealing with operations.

* Now being discussed.

The section on standards and technical conditions must control and check the quality of production, encourage the introduction of new methods in the field of manufacture, check the accuracy of manufacturing processes, introduce technical improvements, and point out obsolete standards and terminology.

The research section would study the influence of measuring devices on the quality of production, it would bring to light obsolete apparatus and would investigate means of replacing them with newer models; it would also study new measuring devices.

The inspection section would inspect standardizing apparatus belonging to the State Control Laboratories and would inspect the apparatus of the base laboratories; it would make arbitration inspections and would keep charts and graphs of its work.

The operations section would provide a constant, uninterrupted system of controls and inspection of departmental supervision both from a quantitative and a qualitative point of view.

This proposal would not only improve work on inspection and control but would also provide a greater choice of facilities.

A GENERAL APPROACH TO THE ANALYSIS OF STATIC AND DYNAMIC ERRORS

N. A. Chekhonadskii

Results of any measurement usually contain a certain amount of error. Depending on the nature of changes in the quantity being measured, measurement errors can be divided into static errors and dynamic errors.

Static measurement errors, can now be analyzed by means of metrology [1] using special methods.

Dynamic errors are basically studied by means of automatic control, and little metrological attention has been given to the analysis of such errors.

It must be noted that in accordance with contemporary terminology, dynamic errors are those which occur as a result of distortion of the quantity being measured, this distortion having been produced by the apparatus. The reason why such distortions occur lies in the presence of linkages in the construction of the apparatus; these linkages possess a certain dynamic "inertia." If the structure of the apparatus contains only "noninertia" linkages, these dynamic errors can not possibly arise.

Dynamic apparatus errors may be determined by calculation or by experimental methods.

The experimental method for determining dynamic errors is based on the determination of the dynamic characteristics of the apparatus being studied; in this case methods developed by the theory of automatic control are used. Amplitude-phase characteristics are most frequently used; they are determined by studying the periodic oscillations in the measured quantity as it passes through the apparatus.

In order to determine the dynamic errors of an apparatus, the transition process is studied when an input quantity in the form of a unit function [2] is applied at the input.

In the case of an experimental determination of a dynamic error in an apparatus, the analysis of the input quantity of the apparatus being studied is closely linked with the properties of the apparatus under working conditions which is not the case in an analysis of static errors. However, in contrast to the method of determining static errors (which presumes the separation of such errors into systematic and random ones), in the case of the determination of dynamic error the question of division into components has not been studied.

Thus, when static and dynamic apparatus errors are analyzed, completely different methods are used at present and, as a result, as has been noted in [3], static errors have not been considered in close enough relationship to problems of dynamics.

Therefore, it would be useful to examine theoretically the question of a general approach to the analysis of both static and dynamic apparatus errors, in the absence of which approach the above-mentioned difficulties are encountered.

General expression for the output of the experimental apparatus.* Let us consider in a general way, the process of measuring a certain physical quantity $\underline{x}$, by means of the apparatus we are studying. The quantity $\underline{x}$, which is being measured, may remain constant or may change arbitrarily with time.

Such a study of the quantity being measured also includes its constant value. Therefore, in a general analysis of the process of measurement, we shall study the quantity being measured as some function of time [4].

In both cases, the measurements will always contain a certain amount of error.

The process of measurement consists in the transposition by the apparatus of the quantity measured $x(t)$ from now on referred to as the input function, into a certain output function $y(t)$ which represents the results of measurement. Between these two functions there exists a definite relation which in the general case can be represented by:

$$y(t)=F[x(t)]+\varepsilon(t), \tag{1}$$

where $\epsilon(t)$ is the error in the measurement of $x(t)$.

The form of the functional transformation, carried out by the given apparatus during a measurement, will depend on the nature of the quantity being measured. Thus, in the case of measurement by the apparatus of a constant value of a certain quantity x_1, the output y_1 can be written as:

$$y_1=k_1x_1+\epsilon, \tag{2}$$

where k_1 is the sensitivity of the apparatus at a given point on the scale;

ϵ is the error at the given point on the scale.

If the input fed to the apparatus changes with time thus producing dynamic errors, then the functional transformation, carried out in this case by the apparatus, will be rather complicated.

However, the relation between the output and input functions of the apparatus (with any arbitrary change in input) may be expressed in a relatively simple way if the impulse response function of the apparatus is known; i.e., the reaction of the apparatus to a unit impulse input function [5].

The output of the apparatus for a known impulse response function may be determined as follows:

$$y(t)=\int_0^t \lambda(t-\tau)\,x(\tau)\,d\tau+\varepsilon(t), \tag{3}$$

where $\lambda(t)$ is the impulse response function of the apparatus.

The impulse response function $\lambda(t)$ may be found by applying the inverse Laplace transform to the transfer function for the same apparatus; this is determined by the following relation:

$$L(p)=\frac{y(p)}{x(p)}. \tag{4}$$

* We have studied only linear systems, i.e., systems possessing such a property that the result of the effect on them of certain perturbations represents a superposition of the effect of individual perturbations.

where $y(p)$ represents the output function of the apparatus; and

$x(p)$ represents the input function of the apparatus.

The general expression for static and dynamic errors. Let us consider the question of the transformation of the input function by the apparatus when this function happens to be a random function of time.

It is easy to see that in this case the error of measurement $\epsilon(t)$ in (3) will be a random function of time and the function $\lambda(t)$ is a known function of time.

In order to solve the given question let us find the output function of the apparatus determined by (3), using in this case methods developed in the theory of random functions [6].

The mathematical expectation of the apparatus output function is determined by the relation

$$M[y(t)] = \int_0^t \lambda(t-\tau)\, M[x(\tau)]\, d\tau + M[\epsilon(t)]. \tag{5}$$

where $M[x(t)]$ is the mathematical expectation of the input function; and

$M[\epsilon(t)]$ is the mathematical expectation of measurement error.

The correlation function for the output function will be given by the relation

$$K[y(t, t')] = \int_0^t \int_0^{t'} \lambda(t-\tau)\, \lambda(t'-\tau')\, K[x(\tau, \tau')]\, d\tau\, d\tau' + K[\epsilon(t, t')] + R_{x\epsilon}(t, t'), \tag{6}$$

where $Kx(t, t')$ is the correlation function of the input function;

$K[\epsilon(t, t')]$ is the correlation function of the measurement error; and

$R_x\epsilon(t, t')$ is the correlation function of the relation between the input function and the measurement error.

As is well known, when $t' = t$, the correlation function becomes the dispersion

$$K[y(t, t')] = D[y(t)]. \tag{7}$$

The general expressions (5) and (6) that we obtained defining the mathematical expectation and correlation function of the apparatus output in terms of the same characteristics for the input function and the impulse response function of the apparatus, permit an analysis of the errors which arise in various individual cases when the apparatus is used.

Analysis of static error in measurement. If the measuring apparatus that we have been studying is used for repeated measurements of a certain constant quantity $\underline{x}$, then the mathematical expectation of the output, i.e., the results of the measurements, will be determined by the following expression:

$$M[y_1] = \int_0^t \lambda(t-\tau)\, x_1\, d\tau + M[\epsilon]. \tag{8}$$

To determine the impulse response function let us find, first of all, the transfer function $L(p)$ of the apparatus used for measuring. It is easy to prove that the transfer function of the apparatus will be expressed in this case as follows:

$$L(p) = k, \tag{9}$$

where $\underline{k}$ is the sensitivity of the apparatus.

Applying the inverse Laplace transform to the above expression, we find that its original is a pulse function of the first order multiplied by the constant value $\underline{k}$:

$$L(t)=k\delta(t-\tau). \tag{10}$$

Substituting this relation into (8), we obtain:

$$M[y_1]=x_1\int_0^t k\delta(t-\tau)\,d\tau+M[\varepsilon]. \tag{11}$$

It is well known that the integral contained in (11) is equal to the value $\underline{k}$ when $t > \quad > 0$. Therefore (11) finally assumes the form

$$M[y_1]=kx_1+M[\varepsilon]. \tag{12}$$

The dispersion $D[y_1]$ in the apparatus output may be found from (6) in the form of:

$$D[y_1]=D[\varepsilon]. \tag{13}$$

The other components, contained in (6), become zero, as the dispersion of the constant value x_1 is equal to zero, and the correlation link of this value with the error ϵ is absent.

It is easy to see that (12) expresses the relation which exists between the actual (and most probable) value of the desired quantity when it has been measured many times and the systematic error of measurement. This expression shows that the mathematical expectation of the quantity measured after repeated measurements differs in the general case from its actual value by a systematic error.

Expression (13) (from which it follows that the dispersion of the quantity measured, determined as a result of many measurements, is equal to the dispersion of the error of the apparatus used for the measurement) is never emphasized in the literature.

Analysis of dynamic errors of measurement. Let us determine the dynamic error of the apparatus using the previously obtained expressions (5) and (6). We will apply repeatedly to the apparatus input the same input function, determined to a high degree of accuracy.

Let us study the case of applying to the apparatus input a changing input function, determined by the following relation:

$$x(t)=0 \quad \text{when} \quad t<0;$$

$$x(t)=x \quad \text{when} \quad t\geq 0.$$

The mathematical expectation of the apparatus output function in this case will be expressed as follows:

$$M[y(t)]=\int_0^t \lambda(t-\tau)\,x\,d\tau+M[\varepsilon(t)]. \tag{14}$$

It is easy to see that the mathematical expectation of error $\epsilon(t)$ may be expressed from this equation by the relation

$$M[\varepsilon(t)]=M[y(t)]-kx. \tag{15}$$

And the dispersion of error $\epsilon(t)$ will be expressed by the relation

$$D[\varepsilon(t)]=D[y(t)]. \tag{16}$$

In the last expression the other two members present in (6) are missing, for in the case we have studied, a certain known function was applied many times with a high degree of accuracy to the input of the apparatus, as a result of which the correlation function of this function as well as the correlation function of the link with the error ϵ (t) are equal to zero.

When (15) is analyzed, it is easy to see an interesting property of the experimental determination of dynamic error which consists in the fact that the dynamic error found by this method represents by its value a systematic error of the apparatus operating dynamically. In addition to this systematic dynamic error (when measurements are carried out dynamically), a random error occurs which is determined by (16). This error characterizes the dispersion of the output function of the apparatus in relation to its mathematical expectation when the same input function is applied many times to the input of the apparatus.

SUMMARY

1. The laws operating when measurements are carried out both statically and dynamically may be expressed by general relationships.

2. As a result of an application of the expressions obtained for the dynamic error analysis, it can be established that the dynamic error determined experimentally is, by its meaning, a systematic error of an apparatus operating dynamically. In addition to this error, a random error also arises when measurements are made dynamically.

3. Results of measurements carried out by the apparatus both statically and dynamically may be expressed by similar expressions containing the basic characteristics of the apparatus for these operating conditions; this should make it easier to resolve static and dynamic problems involved in the construction of apparatus.

LITERATURE CITED

[1] M. F. Malikov, Principles of Metrology, Committee on Measures and Measuring Devices (1949).

[2] V. V. Solodnikov, Automation and Remote Control No. 5 (1949).

[3] N. N. Shumilovskii and B. S. Sinitsyn, Basic Problems of the Theory of Automatic Measurements, Scientific Principles Underlying the Construction of Technical Means of Automation (AN SSSR Press, Moscow, 1957).

[4] B. S. Sinitsyn, On Automatic Control Terminology, Doklady LPTI 1, 2 (1955).

[5] V. V. Solodnikov, Automatic Control in the Statistical Dynamic Systems GITTL (1952).

[6] V. S. Pugachev, Theory of Random Functions and Its Application to Problems of Automatic Control GITTL (1957).

LINEAR MEASUREMENTS

INSPECTION OF GAS TURBINE BLADE BLANKS

B. I. Pikalov and V. V. Petrosov

Gas turbines are now increasingly used in various branches of the national economy. The production of compressor and turbine blades is one of the most labor-consuming operations in their manufacturing process.

The use of advanced methods of production (precision drop-forging, shell casting with 0.3-1 mm allowances) considerably reduces the amount of labor involved in the production of blades, and enables an economy in the use of expensive heat-resisting and titanium alloys to be effected; but at the same time it calls for a more stringent inspection of blade dimensions.

The uniformity of distribution of allowances and their absolute sizes are determined by the quality of the dimensional inspection of forgings and castings in the process of finishing the dies.

The consequence of the use of new materials for casting and forging the blades of modern gas turbines is that some residual stresses are left in the blade blanks; it becomes necessary to determine the actual residual deformations of the blade blanks and to take them into account in finishing the dies.

At present, three principal methods are used in measuring the forgings and castings of blades.

One of these methods is based on cutting the first blade blank in a direction perpendicular to its axis. The sections along which the forging (casting) of the blade is to be cut is marked on it (Fig. 1). Thereupon, the tip section 1-1 of the blade is machined, the blade placed upon the projector work table and the light directed onto it from above. The contour of the section and the stem of the blade is marked on the tracing paper placed on the projector screen to the scale 10:1. The machining and projection procedure is then repeated for all the other sections of the blade (2-2, 3-3, etc.). The actual contours obtained from the sections of the blade blanks in this way are compared with the theoretical profiles by placing them on top of these profiles which have been drawn to the same scale on drawing paper.

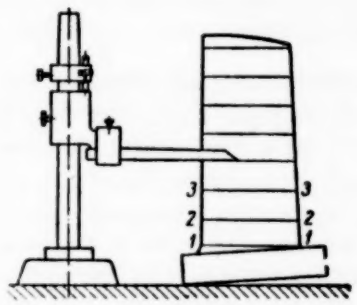

Fig. 1

This method of inspection is very laborious and fails to produce reliable results since the cutting of blanks may produce additional deformations.

Another method of inspection of blanks ("point-by-point") is shown diagrammatically in Fig. 2. The blade blank is clamped between centers and all its sections marked off. Then equidistant points 1, 2, ... 8 are marked on the concave and convex sides of the blade. The blank thus prepared is mounted in the center of an optical dividing head and the distances between the points, the position of the leading and tail edges of the blade (contours 10 and 11), the size of the chord 1, and the angle of the twist of the blade are measured by means of an indicator gage with a pointed plunger.

This method of inspection of blades is unproductive and less accurate than the method involving the cutting of the blade.

The third method of inspection which involves checking against light with rigid profile gages is only suitable for the inspection of blade blanks with allowances exceeding 2 mm.

We have tried out, and are now introducing at our plant, a new method of inspection of blade blanks which involves the use of USSh needle-type gages, in place of rigid profile gages, for application as a general assembly. The needle gages are mounted in a universal inspection-assembly device developed by B. I. Pikalov through the USP* system.

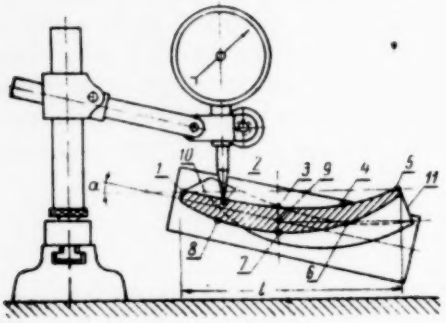

Fig. 2

The device consists of interchangeable standard components and units which enables the required inspection gage for a new blade to be assembled in 1-2 hours. This device with its needle gages ensures a high-quality inspection of blades with an allowance of less than 1 mm.

Figure 3 shows the device with needle gages for the inspection of the blade blank for the working blade of a compressor.

The blade 1 is surrounded by the points of needles 2 which copy the full profile of the sections of the blade. The needles are clamped to the body of the gage by means of the plate 3.

With respect to the data elements for correct setting, there is no difference between the needle gage and the rigid profile gage, which makes possible the use of both types of gages in the same device 4.

During the inspection of a blade forging, the plate with needles is placed onto the base plate of the device. The freely moving needles are shifted until they touch the profile of the blade; after setting they are fixed to the plate.

The needle gages for assembly purposes are set in a similar manner for all sections of the blade on its concave and convex sides. The set needle gages are mounted in pairs (concave and convex sides) on the work table of the projector onto which the setting gage, with the data plane corresponding to that of the base plate of the device, has previously been placed.

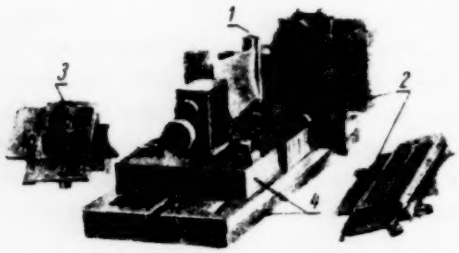

Fig. 3

Cartridge paper with profiles of blade sections drawn to the scale 10 :1 is now placed on the projector screen.

The presence on the screen of the theoretical profile of the blade forging, and of the profile obtained by projecting the needle gages set to the blade, makes possible the comparison of the theoretical and actual cross section of the blade, which in effect amounts to the qualitative inspection of the blade blank within fine limits.

The inspection of a number of blade forgings to fine tolerances by means of needle gages showed that this method, which has been suggested by the authors, produces a clear picture of the actual profile of the blade. It is easy to ascertain the uniformity of the distribution of tolerance and the existence in the forging of a displacement of the profile with respect to the stem. This method also makes possible the detection of residual deformations in the blade forging and the determination of the size of these deformations for each section. On the basis of deformations so determined, it is possible to finish the profile of the die in all its sections with the corresponding "advance tolerance." The "advance tolerance" of the die profile is given in finishing the profile in order to allow for the distortion of the blade due to residual deformations.

The accuracy with which the profile is measured is ± 0.1 mm.

The diameter of the needles should be 1.2-1.5 mm and the length 100 mm. The working end of the needles should be finished to a hemispherical shape. In order to increase the resistance to wear, the needles should be chromium plated, while for the easier determination of the gap between the needle and the component they should be oxidized.

* V. S. Kuznetsov and V. A. Ponomarev, Universal and Assembly Devices in Mechanical Engineering, (Mashgiz, Moscow, 1952).

In addition to the inspection of blade blank profiles the needle gages have begun to be used in the inspection of the rough-machined blades during the setting of the copying milling machine to new components.

If it is necessary to give blades which have been made earlier an additional twist, which often happens at various factories, the needle gages help to complete this work in a short time, since the setting of one pair of needle gages to a new blade profile does not take more than one hour.

The needle gages can be successfully used in the inspection of drop-forging dies for complex components, of casting dies for blades, grooved rollers for rolling guide vanes, of copy templets and other devices of complicated form, during their manufacture in the tool room.

From the Editorial Board. The positive results obtained in the standardization of special gages for the inspection of dimensions described in this article point the way to rationalization in this field of measurements by the standardization of measuring equipment. This will make possible its centralized production in special tool factories in the form of standard units, thus relieving the machine manufacturers of the need to develop and make for their own use measuring equipment for the production of which they are not equipped.

If this solution is adopted, the optimum results can be expected with respect to the cheap and rapid manufacture of high-quality measuring devices for the inspection of the dimensions of components during their manufacture.

The Editorial Board invites the readers of this journal, and in particular those who work at the Council of the National Economy, to discuss this problem in the pages of our journal.

A RECORDING EXTENSOMETER

A. D. Martynov

Dimensional parameters are usually measured by means of electrical recording instruments provided in the form of separate units for attachment to various checking and measuring devices (for instance, recorders BV-562). In some cases, however, it is desirable to be able to build the recorders into the checking and measuring devices (for instance, ininstruments for checking gears, such as evolventometers, pitch gages, wobble gages, etc.).

The possibility and advisability of inclusion depends in the first place on the dimensions of the recorder. Miniaturization of recorders facilitates their inclusion in the checking and measuring devices. It is therefore desirable to strive for the greatest simplicity in the mechanism for multiplying the measured dimension.

The simplest is the mechanical principle of multiplication which was adopted in the miniature recorder developed by the All-Union Scientific Research Institute for Instruments.

The mechanism of a conventional extensometer is used in this recorder as a multiplying gear. An ink pen is used for recording the readings on a paper chart.

The construction of this recording extensometer is shown in the figure attached.

The instrument is built around a measuring tube 1 of the "Kalibr" extensometer with a scale division of 0.001 mm. The extensometer tube is screwed on to the instrument base 2 to which the sides 3 and 4 and back 5 walls are fixed. The front of the instrument is covered by lid 6 which is made detachable to provide access to the internal parts of the instrument. Pen 8 is attached to the extensometer pointer in such a way that their sweeps are equal. The bottom of the pen is immersed in an inkwell which is fixed to the base of the instrument. The pointer sweeps over scale 10, which is the same as in a conventional extensometer with a division of 0.001 mm.

The readings are recorded on a paper chart 60 mm wide. When passing under the pen the chart is supported by plate 11 which is fixed by means of angle brackets to walls 3 and 4.

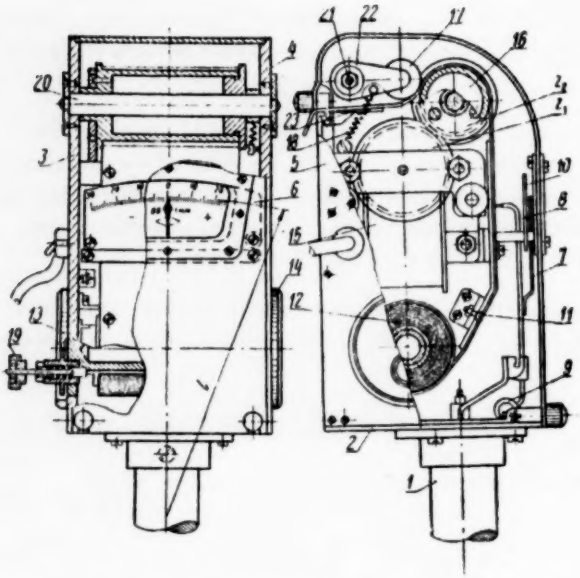

The paper chart is wound on spool 12, which revolves freely on spindle 13. The spindle is fixed at its ends to walls 3 and 4; it can be removed together with the spool from the recorder. Spindle 13 is fixed in the recorder by means of screw 14.

The chart-propelling mechanism consists of a synchronous motor 15 type SD-2 which drives by means of gears $z_1 = 84$ and $z_2 = 50$ the drum 16. The speed of the chart is 5.275 mm/sec.

In order to provide driving friction the chart is pressed against the drum by roller 17, which is held under constant tension by spring 18 fixed to the side wall by a screw. The driving drum revolves together with its spindle 20, whose ends pass through the side walls. Spindle 21 with its holder 22 and roller 17 is also fixed to the side walls. From the driving drum the chart passes outside the recorder along trough 23. In order to be able to rewind the used chart back on to the spool the latter is connected to spindle 13 by catch 19.

Recording extensometers can be produced with any of the scales of the conventional extensometers, for which purpose the measuring tubes and scales of the conventional extensometers are used.

Metrological tests of recording extensometers have shown that the error and instability of their readings do not exceed those specified for conventional extensometers.

For field testing the recording extensometer was attached to an instrument of the All-Union Research Institute of Instruments for checking gears and gear-wheel cutters. The tests revealed a sufficiently reliable and accurate recording of the measurement results.

A NEW DIVIDING HEAD

E. I. Finkel'shtein

The accuracy of optical dividing heads with single-sided reading can be increased by introducing a more sensitive reading device such as an optical micrometer and simultaneously raising the accuracy of the circular dial scale and improving its centering with respect to the axis of rotation.

Double-sided reading by means of graduations placed at both ends of the dial diameter, similar to the arrangement of an optical theodolite, considerably reduces unnecessary accuracy in centering the circular scale, and makes the device less sensitive to small scale eccentricities arising in the course of the instrument's use. This constitutes the main advantage of double-sided reading instruments, which makes their use indispensable where the reading error must not exceed 2-5". The production of such a head, however, involves the development of a new instrument design with a new optical arrangement.

Below, a modernized optical dividing head is described which has half the error of the old-type instrument, yet preserves the old construction, changing only the optical system. The diagram of the optical head ODG-1, improved in that manner, is shown in Fig. 1.

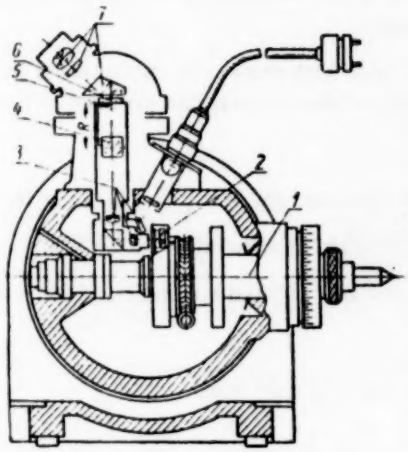

Fig. 1

The graduations of the angular scale of dial 2, fixed to spindle 1, are projected by objective 3 into the field of vision of the reading microscope. Grid 6 with seven pairs of parallel lines is placed in the focal plane of eyepiece 7. The distance between any two centers of the parallel line pairs is equal to 10° of the dial rotation, i.e., when the spindle with dial 2 is turned through 10°, the image of the angular scale graduations is displaced in the field of vision by an amount equal to the distance between the centers.

At a certain distance from the eyepiece focal plane the instrument has a block gage 4 of a certain thickness which can be turned through ± 5° about an axis perpendicular to that of the microscope. When it is turned through an angle α, the angular graduations will appear to be displaced by $A = \frac{d\alpha n}{n-1}$, where d is the thickness of the block and n is the refractive index of the block-gage glass (if this approximate formula is replaced by the exact formula $A = \frac{d \sin(\alpha - \alpha_1)}{\cos \alpha_1}$, where α_1 is found from the equation $\sin \alpha = n \sin \alpha_1$, it will be found that the approximate formula gives an error of 0.3% which can be neglected).

The block gage is rigidly connected to scale 5 which has divisions proportional to angles of rotation of the gage. The scale is so arranged that when the block is turned through one division the image of the dial angular graduations will be displaced by a distance corresponding to a rotation of the spindle and dial through 10°. The angle of rotation of the block gage is read against a stationary mark on the grid.

In order to try and avoid parallax between the grid and the scale, the latter is drawn on a cylindrically-shaped glass with radius R of the cylinder equal to the distance between the axis of rotation of the block and the focal plane of the eyepiece. For zero setting, the block is adjusted to the zero position on the scale and the angular scale zero line image is made to coincide with the middle of the zero pair of parallel lines.

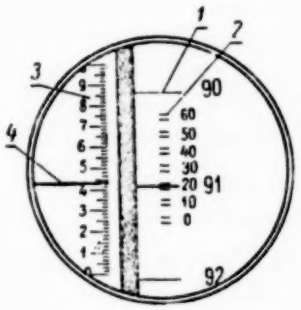

Fig. 2

When the spindle is turned through any angle, one of the lines of the angular scale corresponding to a whole number of degrees will take up a position in the field of vision somewhere between two sets of parallel lines. By rotating the block gage, the image of the degree scale graduation is placed in the center between the two nearest parallel lines. Then the pair of lines to which the degree scale was adjusted will read the tens of minutes, and the number of minutes and seconds will be read on the other scale against the stationary mark. The reading will have a single value since the whole scale over its entire length strictly corresponds to 10°, i.e., to the distance between the centers of two adjacent pairs of parallel lines.

Figure 2 (where 1 are the graduations of the degrees scale, 2 are the sets of paired parallel lines, 3 the minutes and seconds scale, and 4 the stationary mark) shows a setting of 91° 24' 20".

Samples of the ODG-1 recorder showed fairly high metrological qualities. The measurement error was found to be within 12", the spindle position is not changed by more than 4" during tightening, the change in the reading of the optical scale when the direction of rotation of the spindle is reversed does not exceed 3". The sensitivity of the system owing to the use of the optical micrometer is increased by a factor of 12 as compared with dividing heads ODG (in the ODG type the sensitivity is equal to 60 and in ODG-1 it is 720).

The sensitivity limit of this system depends on the limit of sensitivity in placing the degree scale graduation centrally between the two parallel lines, thus depending on the magnification of the microscope. If, for instance, the microscope magnification is × 60 and the subjective sensitivity limit of the observer in correctly adjusting the scale is 250 tan 10" = 0.012 mm, the error of correctly placing the graduation between the parallel lines, which we can call the adjustment error, is 0.012/60 = 0.0002 mm. With a dial diameter of 80 mm, this corresponds to an error of 1". This calculation was confirmed by measurement.

The accuracy of the system depends on the accuracy of the block gage with respect to its thickness and refractive index, on the accuracy of scale calibration and on the accuracy of determining the distance between the scale and the axis of rotation of the block gage.

Since the size of the scale corresponds to 10' (600") of the spindle rotation, and $A = \frac{d\alpha n}{n-1}$, the error of each element of the system must not exceed 1/600 or 0.17% in order to attain an over-all error of 1".

With a block gage thickness d = 10 mm, a total deviation of the block of 10", and a distance of the scale from the axis of rotation of the block gage R = 40 mm, we have:

$$\Delta d = \pm 0.017 \text{ mm}, \quad \Delta\alpha = \pm 1', \text{ and } \Delta R = \pm 0.07 \text{ mm}.$$

It will not be difficult to attain these tolerances in production especially if it is taken into consideration that distance R can be made adjustable in order to be able to compensate for discrepancies in other parameters.

Externally, the new ODG-1 with its scale division value of 10" differs from the old ODG with the value of 1' only by the knob attached to the eyepiece for turning the glass block gage.

In conclusion, a Table of parameters by which ODG-1 differs from ODG is attached.

	ODG	ODG-1
Value of a division in the field of vision	1'	10'
Observed size of the division	0.75 mm	1.4 mm
Sensitivity	60	720
Limit of sensitivity	6"	1"
Actual accuracy of measurement	25"	12"

A THEODOLITE APPARATUS FOR CHECKING ANGLE GAGES

N. P. Konovalov

The "Bol'chevik" plant in Leningrad has developed and is using an apparatus which incorporates theodolite TB-I, calibrated in seconds, and used as a goniometer for checking angle gages according to the method developed by the Khar'kov State Institute of Measures and Measuring Instruments.

The equipment's diagram is shown in Fig. 1. The gage 1 under test is placed on tripod 2, which can be revolved about the vertical axis of theodolite 3. The dial of the theodolite is fixed on the same axle as the tripod and rotates together with it.

The precise positioning of the gage faces which is required in measurements is attained by the beam of light from collimator 4 being reflected from one of the gage faces into telescope 5. It is obvious that in this arrangement the alignment of the collimator cross hairs, as seen in the telescope, with those of the telescope eyepiece, will correspond to a strictly defined position of the gage face with respect to the remaining components of the optical system (collimator 4, auxiliary mirror 6 and telescope 5), which determine the path of the beam.

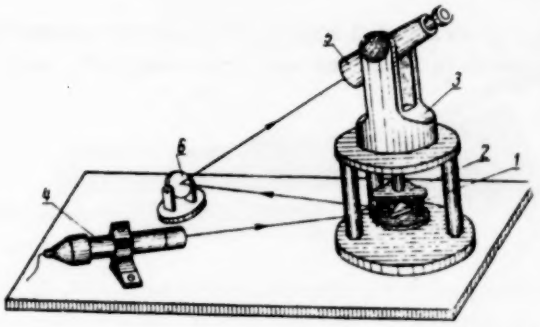

Fig. 1

The equipment (Fig. 2) consists of base plate 1, which carries the auxiliary mirror fixture 2, with a device for turning and tilting the mirror, collimator 3 with cross hairs and a millimeter scale, the theodolite stand and the tripod. The stand consists of two disks 4 and 7 connected by three posts 5.

The bottom disk 4 is fixed rigidly to the base plate. The top disk 7 has three screws 8 for fixing the theodolite rigidly to it. Spiral springs placed inside posts 5 press upwards hinged levers 10 which carry ball bearings. One of the posts also has a bracket to which a lever-type extensometer 6 is fixed.

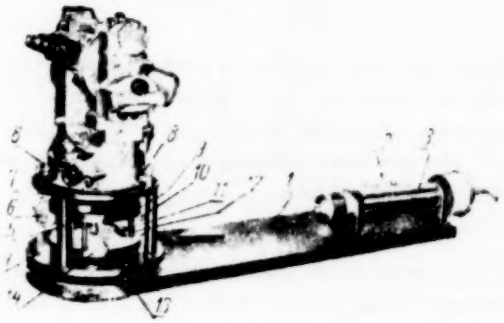

Fig. 2

The tripod consists of disk 9 and table 14. The disk is rigidly fixed by its upper surface to the bottom flange of the theodolite, and its lower surface rests on the ball bearings of levers 10 and is free to revolve about its axis. The bottom surface of the disk carries a clamping bracket 11 for holding the angle gage 13 against the lapped upper surface of table 14. The tripod table is fixed to the disk by three posts 12 with screws and springs by means of which the top face of the table can be adjusted to be normal to the axis of rotation of the tripod.

For checking angle gages the following preparations are made: The theodolite is separated from its tripod and fixed to that of the testing equipment; the theodolite together with the test tripod is placed on the top disk of the stand and fixed to it by means of three screws with cleats. The bottom surface of the tripod disk rests against the ball bearings of the levers, which press the lower part of the theodolite toward its upper part under the thrust of their springs. The necessity of pressing the tripod against the theodolite is caused by the unusual fixing of the theodolite in this equipment; the theodolite is not placed on its tripod in the normal manner, but screwed on by its body to the stand, the test tripod remaining suspended. Therefore, in order to provide normal operating conditions for the theodolite, it is necessary to use a device which presses the tripod against the upper part of the theodolite.

By rotating the tripod the upper face of its table is adjusted by means of the extensometer and the three screws, so that in a complete revolution of the table the extensometer deviations do not exceed 0.01 mm.

In order to be able to align the gage face during testing in a strictly determined position, the mirror is adjusted to throw the collimator light beam, which is reflected from the gage face, into the theodolite telescope.

This concludes the setting of the equipment for checking angle gages.

The checking of angle gages consists of the following; the gage under test is placed on the tripod table, with its inoperative (unmarked) surface facing the table and fixed in position by means of the clamping bracket to prevent it from moving when the tripod is rotated. The tripod is rotated by its upper disk until the collimator light beam, reflected from one of the gage faces, appears in the telescope (seen thru the eyepiece). Then, by means of the micrometer drive of the theodolite dial, the image of the collimator cross hairs is superposed on the telescope eyepiece cross hairs, and the first reading of the number of degrees, minutes and seconds is taken from the horizontal dial of the theodolite. Similarly, the collimator cross hairs' image is made to coincide with

the eyepiece cross hairs for the second face of the gage, and another reading is taken. The difference between the two readings measures the external angle of the gage, hence by subtracting it from 180°, we obtain the required angle of the gage under test.

In order to determine the perpendicularity of the operative faces of the gage to its inoperative face, the vertical displacement of the collimator cross hairs' image with respect to the eyepiece cross hairs is observed during testing. The value of this deviation is read off the millimeter scale of the collimator on which one millimeter corresponds to 1' of the arc.

Tests have shown that the checking of an angle gage by means of this equipment, with the measurements and readings taken three times for each face, can be completed in 5 minutes with an accuracy of ± 4 sec of the arc.

A MINIATURE PORTABLE PIEZOELECTRIC PROFILOGRAPH

E. I. Regirer

The Institute of Sound Recording has developed, in connection with research in sound reproduction, a portable piezoelectric profilograph * (Fig. 1). In constructing the instrument the experience of the LIAP and the improvements introduced by the Brush Company to their instrument, in which the piezoelectric recorder was replaced by a magnetoelectric one, were taken into account. The described profilograph, however, is not identical to the existing instruments and differs from them in many constructional details.

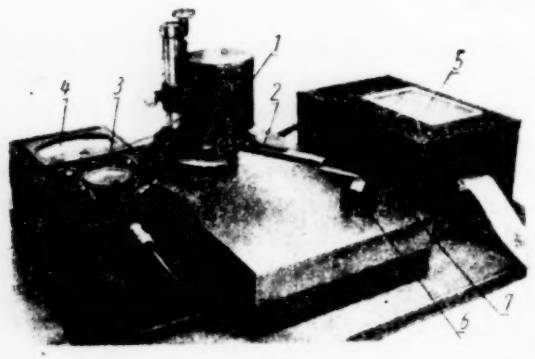

Fig. 1. General view of the profilograph. 1) Driving mechanism; 2) pickup; 3) amplifier; 4) indicating instrument; 5) recorder; 6) sample under test; 7) base plate on shock absorber.

The instrument's pickup (Fig. 2) is not articulated; the suspension works like an elastic system. In order to decrease its inertia, the mass of the system is reduced to a minimum. It consists of the mass of the crystal, the tube with the needle, and the metal head which connects the crystal to the tube (in fact only a small part of the total mass is involved in vibration, since both the end of the tube and the crystal are rigidly fixed).

A bimorphous Rochelle salt crystal of 0.7 × 30 × × 10 mm operated by flexing serves as the piezoelectric element; one of its leadouts is connected to the outside plate and ground and the other to the foil at the splice. We also tried other piezoelectric elements including a barium titanate one.

The stress gradient in the pickup is equal to 8 mg/μ. The needle normally protrudes by less than 0.1 mm, and the total probing effort as a rule does not exceed 0.1 g. Microscopic inspection has shown that a noticeable trace is left on a mild steel sample, especially if instead of the feeler needle of 10 μ radius, which we normally used, a needle with a radius of 1-2 μ was used. The presence of traces is not only due to the greater

* I. F. Kadushin, P. G. Zon, M. I. Strelkov, N. N. Lukhmanova, and V. I. Ul'yanov participated in the development of the instrument. The calibration of the instrument was carried out by means of vibration equipment certified by the Committee of Standards, Measures and Measuring Instruments.

pressure, but also to the poor technological method of obtaining a needle point with a radius R = 1-2 μ, a method which only provides an indefinite shape for the blunted point whose size is of the above order with an angle of 60° at the apex.

According to our observations, a decrease in speed does not lead to a drop in the scratching effect.

The pickup has one resting spherical surface which takes a total load of 25 g.

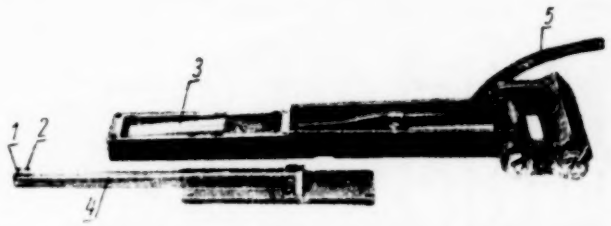

Fig. 2. Pickup (external appearance, partly dismounted). 1) Diamond needle; 2) rest cushion; 3) crystal; 4) tube; 5) lead to the amplifier.

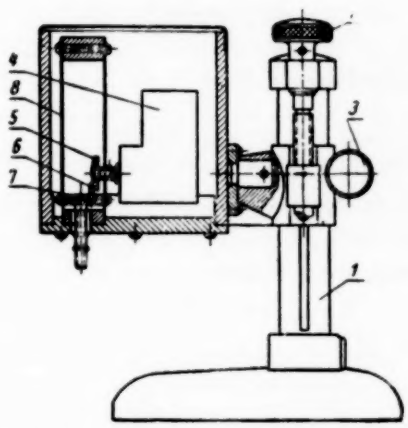

Fig. 3. Driving mechanism. 1) Stand; 2) vertical displacement screw; 3) locking screw; 4) motor; 5) cam; 6) pin which is operated by the cam; 7) pickup carrier; 8) suspension on flat springs.

The probing is carried out by means of a driving mechanism (Fig. 3). The track we selected amounts to 1.5 mm, the duration of the total run there and back is 0.2 min, the speed of probing 0.25 mm/sec. The forward movement is provided by a cam, which determines the length of the probing run and is actuated by a synchronous motor SD-2; the return movement is provided by an elastic suspension on flat springs which press the pin of the suspension against the cam.

The vertical adjustment of the pickup is made by means of a screw which is mounted on the stand column. The driving mechanism with the pickup is mounted on a massive plate which rests on a shock absorber consisting of a porous rubber cushion 50 mm thick.

The schematic of the amplifier is shown in Fig. 4. It has four stages. Its input decade potentiometer provides an attenuation ratio of 10^{-5}.

The first three stages are RC coupled; the last stage consists of a cathode follower in order to obtain a small output impedance.

The amplifier has a negative voltage feedback which is taken off the cathode of tube 6P6S and connected to the cathode of tube 6G2. The feedback contains correcting networks, one of which extends the amplifier low frequency range down to 0.5 cps and the other provides a rising characteristic at 120 cps, compensating for the decreased sensitivity of the oscillograph in this frequency range. This frequency boost and the amount of feedback is made adjustable within wide enough limits for calibration purposes.

The gain of the amplifier amounts to 2000; the circuit contains a means for calibrating it. The calibration voltage is set on a copper-oxide rectifier voltmeter and fed through a potential divider to the amplifier input by pressing a special push-button marked "Cal."

A V_{rms} vacuum tube voltmeter is connected to the output of the amplifier. The voltmeter input has a correcting network which provides a linear frequency characteristic at the grid of tube 6N8S with respect to the input of the amplifier.

The amplified voltage is fed from the anode of the first triode through a capacitor to the cathode of the second half of the tube, which is connected as a diode and serves to detect the voltage and deflect the voltmeter pointer.

The voltmeter circuit has a sensitivity control for the circuit as a whole and a separate one for the second scale. Owing to the presence of coupling capacitors in the circuit, the mean values of the positive and negative half cycles are equal, thus making it possible to use half-wave rectification for the voltmeter.

The anode voltage is stabilized by means of a gas-discharge stabilizer SG-4S and a neon tube MN-7.

The graduations of the output instrument, which reads V_{rms} values, are proportional to the area enclosed by the voltage curve and the time axis; the square-law detecting characteristic makes the pointer deflections proportional to the mean square values of voltages instead of their mean values. The extraction of the root required for obtaining the V_{rms} values is accomplished by an appropriate calibration of the scale.

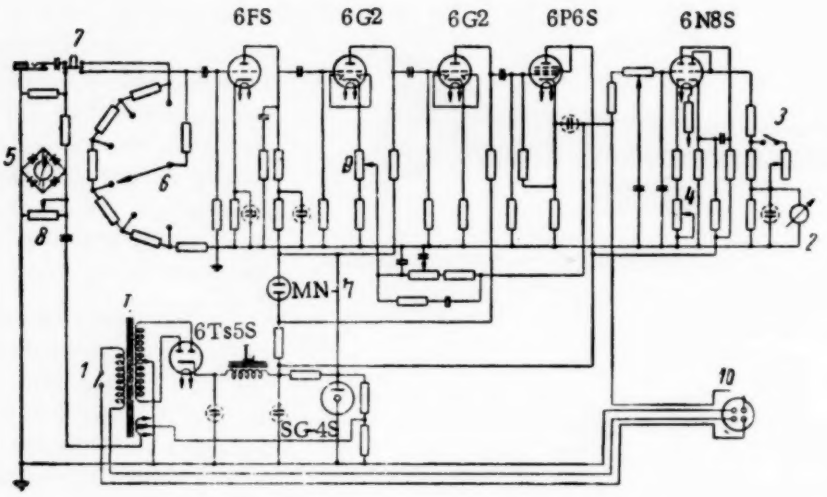

Fig. 4. Schematic of the electronic unit. 1) Supply switch; 2) V_{rms} reading voltmeter; 3) scale-switching push-button; 4) V_{rms} voltmeter gain adjustment; 5) calibration voltmeter; 6) input potentiometer knob; 7) calibration voltage push-button; 8) calibration-voltage adjustment; 9) common gain control; 10) four-pin plug.

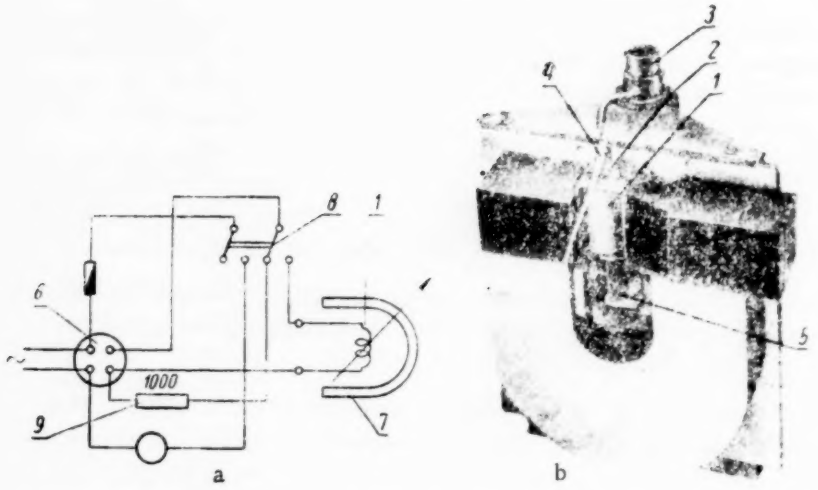

Fig. 5. Ink recording oscillograph (a) circuit; b) external appearance with cover removed). 1) Coil; 2) cushion with a spring clip fixed to the coil spindle; 3) inkwell; 4) pen whose ink supply is cut off for convenience by means of a pinchcock (removed); 5) block whose rotation serves to adjust the zero reading and is accomplished by means of an external lever; 6) four pin plug; 7) recorder head; 8) double-pole tumbler switch; 9) equivalent resistance.

Microammeter MS-50 is used as an indicating instrument. The shunting capacitor of 2000 μf and resistor of 500 ohm increase the instrument's decay time to 10 sec, i.e., cover practically the whole duration of the run.

The instrument's sensitivity can be made 5 times greater by pressing a push-button, which cuts out the resistance in the diode circuit, and then reading off the bottom scale. The upper scale is graduated to 0.25 μ and the bottom one to 0.05 μ.

The paper for recording profilograms is propelled by means of a paper-feed mechanism. Any well-sized and smooth paper, for instance, tracing paper is suitable for recording. The paper is cut into 60 mm wide unperforated rolls.

The paper strip is unwound from the feeding roller round the guiding roller, passed under the pen, over the table which exposes the last recording, and then, having passed between the receiving rollers which pull the strip along its edges, the paper comes out of the instrument; the fresh recording does not come into contact with anything and the smearing of undried ink is prevented.

The paper-feeding mechanism can drive the paper strip at three speeds: 5, 25, and 125 mm/sec, thus producing a horizontal magnification of 20, 100, and 5000. The gear box changes are controlled by means of a push-button.

The schematic and external appearance of the recorder are given in Fig. 5. The recording device is of the moving-coil type, has a power of some 0.2 w, and overcomes easily the pressure of the pen against the paper, which is considerably smaller than 1 g. The coil of the instrument is in the field of a strong magneco alloy magnet. The coil spindle carries small cushions on which rest the knife-edge bearings of the recording pen device; it is dismountable and can be easily cleaned outside the instrument, or replaced if required. The recording pen consists of a light, strong, seamless metal tube with a capillary 0.4 mm diameter hole.

The ink is fed to the pen by means of rubber tubing connected to the inkwell.

The circuit of the instrument contains a double pole switch which connects,simultaneously,power to the motor of the paper-feeding mechanism and the oscillograph coil to the amplifier output and in disconnecting the power from the motor, it switches the amplifier output from the coil to a 1000 ohm resistor, which is equal to the oscillograph coil resistance.

The weight of the profilograph (excluding that of the base plate, since the latter can be of different sizes according to the requirements of the details under test) amounts to 24.5 kg only. The external dimensions of the instrument are in unit sizes: the pickup is 40 x 240 x 40 mm, the driving mechanism 205 x 255 x 140 mm, the electronic unit 170 x 355 x 175 mm, the recorder 235 x 350 x 175 mm. In operating conditions (with the base plate used by us) the over-all dimensions are 800 x 500 x 300 mm.

The instrument works on 127 v ac supplies consuming 85 w.

Its sensitivity is 20 mv/μ. The amplifier input voltage is 0.001 v, its maximum output voltage is 13 v. The recorder sensitivity is 1.3 mm/v.

The amplifier frequency characteristic is linear from 0.3 to 100 cps within 1 db; the frequency characteristic of the electronic unit with the indicating instrument is linear from 0.3 to 50 cps,and that of the oscillograph from 0 to 30 cps,falling by 12 db at 120 cps. The calibration of the instrument in the initial stage and during periodic checks is carried out by means of a graduated sample or a vibration apparatus.

The determination of the surface roughness is done by placing the pickup on the sample, obtaining the profilogram and reading the V_{rms} instrument.

The sample is placed on the base plate with the help of a stand, or wax seating, if required.

The pickup is lowered onto the sample in such a manner that the pickup needle is in a vertical position, which is achieved by means of the vertical displacement screw on the stand column. Having adjusted the height of the pickup it is fixed in position by means of the locking screw.

Having placed the input potentiometer in position "1", without connecting the driving mechanism, the recorder double-pole switch is thrown to the recording position; the recording thus obtained indicates the presence of interfering vibrations, which could be picked up by the base plate (the presence of vibrations is especially

noticeable when working with high gain). If there are no noticeable vibrations, the driving mechanism is connected and the recording started with a maximum swing of the pen of ± 20 mm. Two complete cycles of the pickup movements are recorded and then the recording and driving mechanisms switched off; the profilogram of the second cycle serves to check the absence of random noise and must repeat the shape of the first profilogram. In the "1" position of the input potentiometer the gain is equal to 1000; in positions denoted by other numerals the gain is equal to 1000 multiplied by the numeral of the setting; for instance, in position "100" the gain is 100,000, and in position "0.001" it is 1. For very smooth surfaces, the gain may be raised to 200,000.

Such high gain can only be used when distortions of the probing process itself are permissible.

The recording is made with circular ordinates, with the radius of the circle equal to 75 mm, the length of the pen.

The reading of the V_{rms} instrument is carried out simultaneously with the recording. The correct reading is obtained by using a factor whose numerator is 100 and whose denominator is equal to the numeral of the input potentiometer setting. For instance, if the input potentiometer is in position "100" the factor is 1, if it is in position "0.1" the factor is 1000, etc. If the pointer does not reach 0.05 μ, push button " × 5" is pressed down and the reading taken on the bottom scale.

A shock to the pickup or an incorrect setting of the input potentiometer may overload the amplifier and the voltmeter, although it will not produce at the output an excessive voltage; it may, however, take the instrument several minutes to return to normal.

If required, it is possible to record only one run in one direction (for a horizontal magnification of 500, we shall obtain a completely satisfactory recording length of 750 mm). The instrument can also record both directions of probing, and this is essential for analyzing diffraction defects and establishing the actual profile.

The study of the possibility of different "recordings" of a surface depending on the conditions of its probing by a needle are of interest in sound recording, especially from the point of view of the effect of local irregularities on sound reproduction. The relation between the methods of evaluating a surface and sound recording was noted by us a long time ago. At present the Institute of Sound Recording is extending the probe method to recording of soft (wax) and resilient (elastic plastics) materials; this research is carried out by the process of making a hard copy by means of galvanoplastic processes and subsequent probing of the hard copy instead of the original, which is subject to deformations.

Such investigations also provide for the same surface forward-and reverse-representations in which diffraction conditions are replaced by their images. By means of this technique, it appears to be possible to investigate the effect of elasto-plastic deformations on the diffraction distortions.

A MODIFICATION OF THE MIS-11 DOUBLE MICROSCOPE

F. P. Volosevich

A disadvantage of the MIS-11 double microscope is that it often cannot be used with large specimens. In practice, one often wants to examine the surfaces of parts whose sizes are much larger than that of the stage (100 × 100 mm) and which are rather heavy.

To partly overcome this difficulty, we have modified an MIS-11 in the Central Test Laboratory of the Kirov Works (Leningrad). We used the base and stage of a large instrument microscope (Fig. 1). To this base is fixed a rod whose diameter and height are larger than those of the rod in the MIS-11. This rod carries a strong boss, to which the MIS-11 is fixed. The presence of the strong base enables one to examine large and heavy parts with the MIS-11. Figure 1 shows the ordinary MIS-11, and the same microscope mounted on its new base.

Much time may be wasted in setting-up when shaped parts (e.g., turbine blades) have to be examined. In the Testing Laboratory we have used universal ball joints with this microscope, in which the part may be fixed in any position quickly. These ball joint devices consist of a base in which a hollow sphere fitted with a clamp at the top may rotate. The jaws of the clamp are closed symmetrically by a screw with right- and left-hand threads. The ball is held by a special clamp fitted in the base.

To extend the uses of the MIS-11, G. Ya. Maiorov has made special prismatic supports that may be used with the MIS-11 to examine the surface of a shaft of any diameter and length directly on the lathe.

These supports (Fig. 2) consist of two halves joined by screws with a special adaptor having dovetail joints to take the MIS-11.

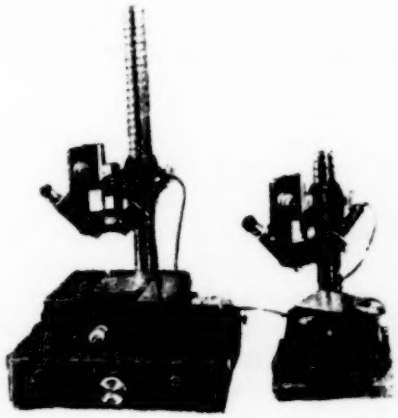

Fig. 1

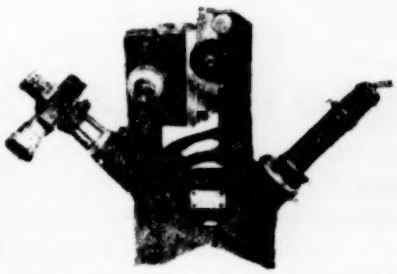

Fig. 2

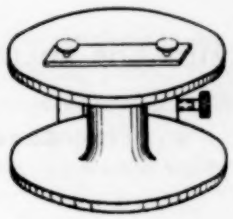

Fig. 3

These same supports can also be used to examine large flat surfaces (surface plates, sheets, and large parts).

A special stage (Fig. 3) has been made to hold parts of awkward shape on the ordinary MIS-11; this stage can be used to vary the tilt and mode of fixing, since a plate and two screws are employed.

To examine the parts of surfaces not directly accessible with the microscope, we have used replicas. These are usually of irregular shape on the back, and much time is wasted in setting them up with packing pieces on the stage. A cylindrical support is used to set them up rapidly and correctly; this has a spherical recess at the working end. The replica is then rapidly and safely set parallel to the stage by sliding it about in the sphere.

G. Ya. Maiorov has drawn up special tables to simplify the method of calculating H_{av} for any pair of interchangeable objectives. The Leningrad Office of Scientific and Technical Propaganda has issued an information sheet (No. 76) on these tables.

The above devices have made the MIS-11 much more useful.

DETERMINATION OF UNDESIRABLE TAPERING IN PUNCHING

P. U. Markov

It is necessary to check tapering used in punching die holes. Such checking can be successfully achieved by means of a measuring microscope. Observations are made both in reflected and direct lighting. First, the instrument is focused on the upper edge of the hole, then, without changing the position of the die, the microscope tube is lowered to the level of the top edge of the hole.

If the contour of the bottom edge of the hole is then seen through that of the top edge, the die should be discarded.

DEVICE FOR POLISHING LARGE MICROMETERS

A. F. Chadaev and E. V. Navskii

A device developed by the authors (see figure) is used at the Gor'kii automobile plant for polishing working surfaces of repaired micrometers with measuring limits of 100 mm and more.

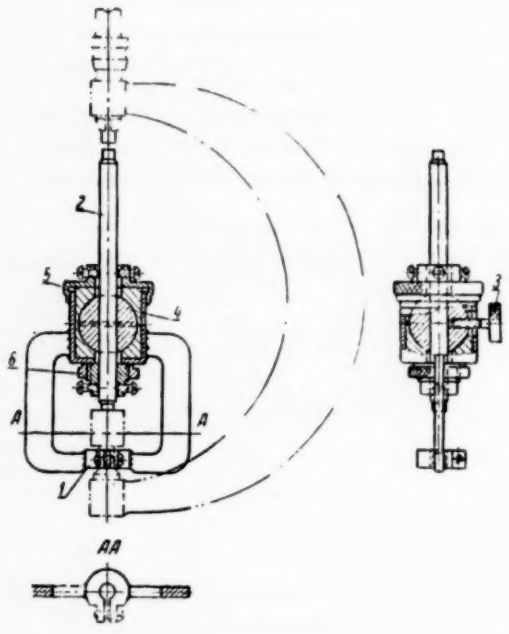

First the face of the micrometer spindle is polished. For this purpose the micrometer screw is taken out of the micrometer and the spindle face lapped and polished in a prism or a 0-25 micrometer and then the screw is replaced in the micrometer under repair. The micrometer is then held in a vise by its frame. The device is fixed by means of the fitting ring 1 on the anvil of the micrometer and secured by a screw. Rod 2 whose length depends on the size of the micrometer under repair is then lifted toward the micrometer spindle and secured by screw 3. A glass block gage is then placed between the ends of the rod and the spindle. The working surfaces of the micrometer spindle and the rod are adjusted to be parallel by means of the ball and socket joint in which the rod moves.

After ascertaining that the surfaces are parallel, the ball 4 is tightened up by means of its holder, screw 3 is released, and rod 2 is lowered for lapping and polishing the anvil in the same manner as it is done in the 0.25 mm micrometers.

The pressure required for lapping is obtained by means of the nut 6. In order to prevent the end surface of the rod wearing, the lap surface is oiled.

Polishing is done by means of a cast-iron lap. Laps made of grey cast iron of a hardness of 90-120 H_B are recommended.

The lapping paste should consist of fine and medium grained graphite, with a metallic base of ferrite; pearlite remnants should not exceed 25%.

The chemical composition of the lapping mixture should be: carbon – 4%, silicon – 2.8%, manganese – 0.7%, phosphorus – 0.12%, sulfur – not more than 0.016% and chromium – 0.02%.

The lap is round, 30-35 mm in diameter; deviations of its surfaces from parallelism must not exceed 3 μ.

For rough lapping GOI 30-40 μ paste should be used; for lapping, GOI 7-10 μ paste, and for polishing, GOI 3-4 μ paste. In lapping and polishing the lap is moved in a to-and-fro and circular manner.

SYSTEMATIC INSPECTION OF GAGES

V. G. Shtein

The organization of the inspection of limit gages is one of the least adequately solved problems in the work of inspection units (IU) and service tool stores (STS) in the production shops of engineering plants. However, this is probably the most labor-consuming inspection operation of IU, since normally, limit gages represent 70-80% and more of all measuring tools in use. Thus, from the point of view of ensuring the interchangeability and uniformity of measures, as well as from the point of view of saving time needed for general inspection work, a correct organization of gage inspection is a matter of great importance.

In the following, we suggest an efficient system of organizing the systematic inspection of gages, which is based on the experience in the field of inspection of several plants.

Period Between Inspections. At present, the periods between the regular inspections of gages adopted at different plants vary from a month to a year. At some plants the need for inspection is determined by visual examination after use, while at other plants this need is determined from the dimensions.

Screw-thread gages are examined visually after use and inspected regularly once in 4-6 months.

The following three alternative methods of regular inspection of gages may be considered most satisfactory:

1) the dimensions of gages are checked after use and regularly once a year;

2) the gages are examined visually after use and inspected regularly once in 3 months;

3) the second alternative, with an additional checking of dimensions after use in the case of gages of the first and second class of accuracy, gages rejected by the inspector of the inspection department (which will be discussed below), and gages which have been used extensively.

The lists of gages of the last category are compiled by the inspector for each workshop, and the neck of their "Not Go" end marked with a painted ring. Thus, every limit gage which must be checked after use is marked. All other limit gages are examined only visually.

This regulation applies only to smooth gages. All screw-thread gages undergo a visual examination after use (screw-thread gage rings are checked with master gages), while the regular inspection is carried out once in 4-6 months.

Registration of Inspection of Limit Gages. At some plants, each gage is given an individual number and entered into special books, while other plants (the majority) note the regular inspections on a chart. These very labor-consuming methods can be avoided when a gage is provided with a mark indicating the period of inspection (for example, one month, or quarter of a year). In order to ensure the inspection after the required period without using the chart, all gages issued to the shop must be returned to the STS within 2-3 weeks after the work is completed; if a small number of gages are issued for continuous use a special procedure is applied to them, and they can be inspected according to the list held at the IU or STS.

The inspection period is marked on the gage in various ways; at the IU of the shops of a diesel-locomotive works the date of the next inspection is marked on the gage by means of an electrograph; Czechoslovakian plants drill a conical 2 mm diameter hole in the handle of the gage and fill it with paint of different colors, corresponding to the month of inspection; Riga plants apply a strip of agreed color to the handle of a gage, which denotes the quarter-year of inspection (only two alternating colors are used). The mark indicating the inspection period can be applied to all external gages and plug gages of over 10 mm diameter by means of a rubber stamp, using the following compound; for marking purposes: 1 liter of blue vitriol (saturated solution), 0.1 liter nitric acid (spec. gravity 1.4), 0.2 liter potassium bichromate, and 0.1 liter water. After an inspection, this mark is easily removed with fine emery paper. All these methods ensure a correct inspection without charts and without marking each gage with an individual number.

It is wrong to mark the period of regular inspection with paraffin wax as is being done at many plants because the marking disappears quickly, since the operator removes the paraffin wax on receiving the gage from the STS. A positive inspection can only be ensured when the inspectors of the inspection department are instructed not to accept components made with the use of gages carrying an out-of-date mark.

If this method is used, the need to use certificates for smooth and screw-thread limit plug gages is obviated; they were officially abolished by the Committee of Standards, Measures and Measuring Instruments in 1957.

The gages which pass the inspection (inspection after use or regular inspection) are paraffinized; this kind of marking serves as an indication that the gage is suitable for use, and is a substitute for greasing; the shelves at the STS should contain only the paraffinized gages.

This method has been known for a long time, but some plants stopped the marking of gages with paraffin wax because the wax sticks firmly to the gage and must be removed with a knife; operators reject such gages and the IU ceases to paraffinize them. Paraffin wax adheres to the gage surface and at the same time is easy to remove when the following rules are observed during the paraffinization:

1) the temperature of the molten paraffin wax should not exceed 40-45° C (the pan with paraffin wax can still be held in the hand);

2) commercial vaseline (not more than 5% of the total) is added to the paraffin wax; the vaseline is not added into the fatty paraffin wax (if the compound is difficult to remove, pure paraffin wax is added; if it fails to adhere, vaseline is added);

3) the gage is washed before the paraffinization but not greased, since grease added to the paraffin wax increases its viscosity.

Often the paraffin wax is melted on an electric hot plate; this is unsatisfactory because the paraffin wax then becomes overheated and the first of the above conditions remains unfulfilled. It is recommended that a device made with a 150 or 200 w electric lamp enclosed in a 140 mm diameter and 240 mm long sheet-metal casing should be used; the lampholder is secured to the bottom of the casing by means of a sleeve with two nuts. A 140 mm diameter, 1 liter capacity aluminum cooking pan is placed onto this device. The electric lamp melts paraffin wax in 20 minutes and maintains it at a constant temperature of 40-45° C; the paraffin wax will not become overheated even if the lamp is left burning. The device is also fireproof. It is already in use in a number of plants.

The Allocation of Gages to Various Stages of Inspection. The test workshop gages are not handed over to the inspectors of the inspection department for two reasons; those concerned are afraid that this will require the erection of a new store in the inspection department, and they believe that this system would not work in cases when the STS has only one gage of a given dimension which cannot be shared between the operator and the inspection department.

These fears are unfounded and can be alleviated if the system described below is used; it has been introduced at a number of plants by the VPTI of heavy machine construction in cooperation with the staff of the TsIL and IU.

First of all, tables of internal standards are compiled which contain the sizes of gages allocated to various stages of inspection. These tables include the dimensions of the "Go" as well as the "Not Go" gages (although the latter are not issued), which replace all other tables giving the sizes of gages.

The tables* give data for various measurement ranges in accordance with the following form (example for plug limit gages):

Measurement range, mm	"Go"			"Not Go"	
	size when new	when handed over to insp. dept.	finally rejected	maximum size	allowance, μ
	Plug gages A_3				
1-3	0.004	.999	.997	.022	4
1-6	0.005	.999	.997	.027	4
		etc.			

If the first decimal figure is 0 then the nominal dimension is written before the decimal point; if, however, the first figure is 9 then the figure before the point is the nominal dimension minus one.

On a sheet of the size A_4, the data are entered vertically in two columns; one table deals with all classes of accuracy for the system "hole" and all dimensions from 1 to 180 mm. For external gages all fits of the system "hole" are contained in three tables.

These four tables replace thick volumes of gage sizes; at the diesel-locomotive plant, for example, the volume of departmental standard specifications containing the gage sizes has 240 sheets. The use of the suggested standard tables obviates the need for gage certificates; the size of a gage can now be taken from the standard tables, and it is clear without the certificate that if the gage has been handed over to the inspection department then it has nearly reached the limit of wear and must be inspected more frequently.

The gages are allocated as follows; if the size of the gage does not exceed the limits specified for the workshop gages, then it is paraffinized and handed over to the STS; if the gage is unsuitable for workshop use but is still within the limits specified for use by the inspectors of the inspection department, it is paraffinized and its handle painted yellow, meaning that it can only be issued to an inspector of the inspection department. If the gage is worn beyond the size specified for the workshop gage, it is rejected and written off.

Owing to the use of the field of tolerances of a workshop gage for the operators as well as for the inspectors of the inspection department, both types of gages can be stored in the STS in the same boxes, thus eliminating the need for the erection of special stores in the inspection departments; if only one gage is left in a box for the inspector of the inspection department it can also be issued, for the reasons discussed above, to operators; this will not produce rejects.

The effectiveness of the suggested system is summarized by the following points:

a) the need for the use of certificates for gages which at large plants are issued in enormous quantities is obviated; at the same time this system ensures that every gage is inspected in time;

b) the abolition of charts which were used at many plants simplifies the procedure for checking that all gages are regularly inspected;

c) with the new system it is possible to ascertain at the workplace whether every gage has been inspected in time;

d) the paraffinization of every gage is improved; and

e) the allocation of gages to various stages of inspection reduces the danger of rejects due to the incorrect use of gages, and increases the productivity of inspectors in determining the actual sizes of gages, as they have to handle only 4 instead of 240 sheets.

* The described system of organization of the regular inspection of gages results in an increase of the productivity of inspectors and ensures a higher degree of uniformity of measures at engineering plants, by using simpler methods of work organization.

* They are suitable only for the standard diameters complying with GOST-6636-53. Separate tables are compiled for special diameters.

MECHANICAL MEASUREMENTS

THE PISTON-BALANCING ERRORS OF WEIGHT-AND-PISTON PRESSURE GAGES

V. N. Samoilov

The accuracy of a weight-and-piston gage depends mainly on how accurately the effective area of the piston is known. It is usual to measure the effective area by balancing hydrostatically the pistons of two gages connected to a single pressure source. Therefore, the accuracy of the area depends on the sensitivity of the system, which consists of the two gages, the pressure source, and the connecting tubes. The sensitivity of the whole system, and not that of any one part, is the important feature. Therefore, the maximum accuracy attainable with such gages can be estimated only by considering the sensitivity; this we shall do here.

We may derive parameters that indicate the sensitivity and may estimate the errors by considering the motion of the piston.

To do this, we must first define what we mean by equilibrium in the piston-liquid-piston system.

The equilibrium state is that state in which the liquid in the source, in the tubes, and under the pistons is at rest, and each piston is falling slowly at its natural rate on account of the leak in the working gap. This rate is given by

$$v = \frac{ph^3}{6\mu bl}. \tag{1}$$

This motion is caused by the leak alone.

The formula commonly used in checking gages is

$$\frac{m_1}{F_1} = \frac{m_2}{F_2} \tag{2}$$

and is strictly correct only if the system is at equilibrium.

In practice, equilibrium is reached only approximately, and so the result given by (2) is only approximate.

If the system is unbalanced, the liquid in the connecting pipes is in motion. Then, the motion of a piston has two components, namely 1) the natural rate, and 2) an extra rate caused by the inequilibrium. This latter rate is, in general, not constant.

The piston whose load is too high falls the more rapidly; the other piston falls less rapidly than it should, or even rises.

The flow q of the liquid in the tubes is proportional to the difference between the pressures on the pistons, if this difference is small. A change in load on one piston causes a change in flow Δq, which is proportional to the change in pressure difference:

$$C' = \frac{q}{p_1 - p_2} = \frac{\Delta q}{\Delta p}. \tag{3}$$

This C' is a constant for the system of gages, tubes, etc. We shall show below that it is given by

$$C' = \frac{F\Delta v_{av}}{\Delta p}, \tag{4}$$

in which F denotes the referred area and ΔV_{av} is the change in the mean rate of fall of one piston during a given time interval.

If the nominal referred areas are equal, we have a quantity C

$$C \simeq \frac{\Delta v_{av}}{\Delta p}. \tag{5}$$

For brevity, we call C the sensitivity, although this word is also used for characteristics different in nature from the one considered here.

If the referred areas are different, the values of C given by the two gages are not the same.

The sensitivity enables one to estimate the accuracy involved, to compare different systems, and to detect leaks, etc.

In practice C and C' may be found by measuring the rates for two similar loads.

To find C, we must use the equations of motion for the pistons and the liquid in the connecting tube. Let x_1 and x_2 denote the displacements of the pistons caused by the extra motion; let $\underline{x}$ denote the displacement of the liquid in the connecting tube; and let the coordinate axes lie along the directions of the extra motions; then the equations of motion for the pistons are

$$\begin{aligned}
&G_1 - F_1' p_1 - \int_0^{l_1} 2\pi b_1 \mu \left(\frac{du}{dr}\right)_{r=b_1} dl_1 = m_1 \ddot{x}_1, \\
&-G_2 + F_2' p_2 - \int_0^{l_2} 2\pi b_2 \mu \left(\frac{du}{dr}\right)_{r=b_2} dl_2 = m_2 \ddot{x}_2, \\
&F(p_1 - p_2) - \alpha \dot{x} - \rho g F (x_1 + x_2) - \rho g F (v_1 - v_2) t = m \ddot{x}, \\
&F_1' \dot{x}_1 + \int_{b_1}^{a_1} 2\pi r \Delta u_1 dr = F \dot{x}, \\
&F_2' \dot{x}_2 + \int_{b_2}^{a_2} 2\pi r \Delta u_2 dr = F \dot{x},
\end{aligned} \tag{6}$$

where G_1 and G_2 are the weights of the pistons (with loads);

F_1, F_2, and F are respectively the areas of the pistons and the cross-sectional area of the tube;

l_1 and l_2 are the lengths of the pistons;

p_1 and p_2 are the pressures under the pistons;

μ is the dynamic viscosity;

b_1, b_2, a_1, and a_2 are the radii of the pistons and the internal radii of the cylinders, respectively;

ρ is the density of the liquid;

v_1 and v_2 are the natural rates of the pistons, and

$\alpha \dot{x}$ is the frictional resistance in the tube.

Here α is given as $\alpha = 8\pi\mu l$, where l is the length of the connecting tube.

The extra speeds $\dot{x}_1$ and $\dot{x}_2$ cause extra frictional forces to act on the pistons. These forces are caused by the velocity gradients at the surfaces. The flow of liquid through the gaps is also affected. Then the last two equations in (6) become

$$F_1 x_1 = Fx,$$
$$F_2 x_2 = Fx. \tag{7}$$

Here F_1 and F_2 are as above, being the area of the piston proper plus half the area of the gap.

Then (7) transform (6) to

$$M\ddot{x} + 2nx_1 + kx_1 = f + \rho g F_1 (v_2 - v_1)t, \tag{8}$$

in which the coefficients are

$$M = m_1\left(1+\frac{F_1}{F_2}\right),$$
$$n = \pi\mu\left[\frac{b_1 l_1}{h_1} + \frac{b_2 l_2}{h_2}\left(\frac{F_1}{F_2}\right)^2 + 4l\left(\frac{F_1}{F_2}\right)^2\right], \tag{9}$$
$$k = \rho g F_1\left(1+\frac{F_1}{F_2}\right),$$

and f specifies the amount by which the load on the first piston exceeds the equilibrium value.

The second term on the right in (8) is important only if the natural rates are very different, which is not the case here. Therefore (8) may be put as

$$M\ddot{x}_1 + 2n\dot{x}_1 + kx_1 = f. \tag{10}$$

The roots of the characteristic equation corresponding to (10) are

$$z_{1,2} = \frac{1}{M}\left(-n \pm \sqrt{n^2 - Mk}\right). \tag{11}$$

The equation of motion of a piston takes the form:

$$x_1 = C_1 e^{z_1 t} + C_2 e^{z_2 t} + \frac{f}{k}. \tag{12}$$

Here M is proportional to the pressure (see [9]).

Also, n does not depend on pressure if the pressures are fairly low. At high pressures the cylinders are distorted and the viscosity varies along the gap; then, n increases with pressure somewhat less rapidly than exponentially.

The factor k is almost independent of pressure even at high pressures. Therefore, Mk is proportional to pressure.

Further, (9) gives that

$$Mk = \rho F_1^2\left(1+\frac{F_1}{F_2}\right)^2\rho. \tag{13}$$

Thus, the motion is aperiodic from zero pressure up to some pressure $p = p'$, but becomes oscillatory at pressures above p'.

This p' is given by

$$p' = \frac{h^2}{\rho F_1^2 \left(1 + \frac{F_1}{F_2}\right)^2}. \tag{14}$$

In both cases, as $t \to \infty$, $x_1 \to \frac{f}{k}$, i.e., the system tends to some limiting position defined by f, in which position the system will be in hydrostatic equilibrium.

We may calculate C from (5) if the parameters are known.

If a change in load Δf causes a change in position Δx_1 in a time t, we have

$$C = \frac{\Delta v_{cp}}{\Delta p} = \frac{\Delta x_1 F_1}{t \Delta f}. \tag{15}$$

We may find x_1, and hence Δx_1, by using (12) subject to given initial conditions.

In practice, the origin of time is taken as the instant when the extra load is added. Therefore, the initial conditions are $t = 0$, $x_1 = 0$, and $\dot{x} = 0$.

The sensitivity is then found as

$$C = \frac{\left(1 - \frac{z_2}{z_2 - z_1} e^{z_1 t} + \frac{z_1}{z_2 - z_1} e^{z_2 t}\right) F_1}{kt}. \tag{16}$$

The latter term inside the bracket can be struck out, since it is small.

If the working fluid is viscous, with $n^2 \gg Mk$, the above formula can be replaced by:

$$C \approx \frac{1 - e^{z_1 t}}{kt} F_1. \tag{17}$$

Formulas (15), (16), and (17), enable us to estimate the errors arising from inexact balancing.

For instance, if the rate of the piston is put in mm/min and the pressure in kg/cm^2, a gage of MOP-60 type ($F_1 \approx F_2 \approx 1$ cm^2) has a sensitivity of 10^3 - 10^4 units. Therefore, if we allow errors within the limits 0 to 1 mm/min, (15) shows that the error in the pressure measurement will be about 10^{-3} kg/cm^2, which is equivalent to 10^{-3}% or even 10^{-2}%.

Two I-2500 gages ($F_1 \approx F_2 \approx 0.05$ cm^2) working at 2000 kg/cm^2 have a sensitivity of about 10 units. The same limits of error in the rate cause an error of about 10^{-1} kg/cm^2, which is a few thousandths of a percent.

Errors of this magnitude cannot be neglected in standardization work, or in checking first-class instruments.

In conclusion, we point out that the index to the sensitivity proposed here should be used not only with the gages we have considered, but also with any piston gage, since sensitivity is a vital aspect of any measuring instrument. The slight theoretical difficulty in calculating C and C' should not be allowed to stand in the way. These quantities are easily measured by experiment, and calculations are needed only when we have to compare a system with one which is working unreliably.

INVESTIGATION OF THE REASONS FOR THE INSTABILITY OF VARIOUS TENSIOMETER SYSTEMS AT HIGH TEMPERATURES

E. Yu. Nekhendzi

The temperature limit of application of heat-resisting tensiometers is determined by zero drift and unbalance of electrical tensiometric circuits.

Some of the unbalance is caused by imperfection of temperature compensation and instability of the electrical resistance of the wire used in tensiometers. A much greater zero drift, which precludes accurate measurement of even the electrical resistance of the transducer, is due to the deterioration of the insulation properties of cement, which occurs at temperatures above the t_0 characteristic for the given heat-resisting-tensiometric cement.

Thus, for the transducer using heat-resisting cement TsKTI Nos. 1-3 [1], zero drift appears at $t_0 \geq$ 300 to 350° C; for transducers using new heat-resisting cements (on the basis of liquid glass with improved electrical insulation properties), it appears at $t_0 \geq$ 450 to 500° C [2], and for silicon-organic compounds, at $t_0 \geq$ 600 to 700° C [3].

It is considered that the zero drift is irregular and is caused only by the drop of insulation R_i in the cement layer between the transducer and the measured detail [1]. Such an explanation is quite inadequate, since the shunting effect of the cement layer must cause a certain constant lowering of the electrical resistance R of the transducer and should not cause zero drift.

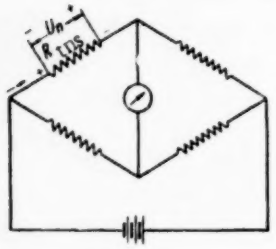

Fig. 1

New cements with a liquid glass base (for instance, mixture No. 2 [2]) possess a resistivity almost 1000 times higher than that of similar old type cements, thus providing a high value for R_i (R_i = 2 meg at 500° C and 0.5 meg at 600° C). Calculation shows that such values of R_i cannot appreciably affect R of the transducer which is equal to 100 to 200 ohms. However, transducers using this cement exhibit a pronounced and incomprehensible zero drift at $t \geq$ 450 to 500° C.

Any further development of tensiometers on a scientific basis requires the investigation of the process taking place in the tensiometer system (wire – cement – detail) and explanation of the reasons for the instability of the measuring circuits.

Such an investigation will provide a clear understanding of the conditions for a further increase in the temperature limit of heat-resisting tensiometers, will fix precise requirements for the cement, and make it possible to select an optimum measuring circuit and methods of applying heat-resisting tensiometers.

Reasons for the instability of a dc bridge circuit. The electrical resistance of tensiometers at various temperatures was measured on dc bridges MTV-1 equipped with a mirror galvanometer GPZ-2 ($C_i \approx 10^{-9}$ amp/mm, $C_u \approx 10^{-6}$ v/mm, T = 2 sec).

Tensiometers using liquid-glass cements, silicon-organic cements and double-layer tensiometers, which were made in two versions. In the first one the grid of the transducer was fixed by a silicon-organic cement and the basic layer consisted of a liquid-glass cement, and in the second the grid was fixed by a liquid-glass cement and the basic layer consisted of a silicon-organic cement.

In all the cases, the observed instability can be described in the following manner:

1. When supplies are switched on and temperature maintained constant $t > t_0$ the measured tensiometer resistance R increases with time and reaches a limiting value R_∞. Thus, a definite regular zero drift is observed with a rising R, a gradual stabilization and attainment of a final position.

2. When the supplies are disconnected, the galvanometer is deflected in the direction of the zero drift and subsequently returns to the zero position.

Instability with such characteristic properties can be satisfactorily explained by relaxation and near-electrode (high-tension) polarization of cement (for polarizations of dielectrics see [4, 5]).

When a heat-resisting tensiometer is connected to a dc measuring circuit a polarization emf $U_n = f(\tau)$ which has an opposite sign to the supply emf and is a function of time is produced in the cement. This is equivalent to connecting in one of the Wheatstone bridge arms an additional polarization voltage which produces a unidirectional zero drift in the galvanometer and increases the tensiometer measured resistance R (Fig. 1). When saturation of polarization is reached $(U_n)_\infty = \text{const}$ (the duration of saturation being τ_∞) the measured R becomes stable. When the supply is disconnected voltage U_n produces, due to the discharge of the polarized cement, an absorption current which is measured by the galvanometer.

The cement in the heat-resisting tensiometer circuit behaves like a charged capacitor. The grid of the tensiometer, the measured detail and separate turns of the grid serve as the electrodes of this "capacitor" (since the potential drops along the length of the wire). When the resistance of a single cement-covered wire is measured, the same instability properties must be observed owing to the back emf of cement polarization.

In order to obtain each of the above components, heat-resisting tensiometers made of nichrome wire of 0.05 mm diameter (base 10 mm long, 0.2-0.6 mm spacing, 5 turns) fixed by means of liquid glass cement to a metal base or a porcelain tube, were tested.

A change in the zero position equivalent to $\alpha_\infty = 0.01$ ohm is taken for the beginning of instability. It was established that (for cement TsKTI No. 3) the temperature of the beginning of instability t_0 is practically the same for transducers and single wires on a metal base; the starting temperature t_0 of a transducer fixed to a ceramic base is about 100° C higher, and increased spacing from 0.2 to 0.6 mm raises it another 30° C; for a single wire on a insulated base the starting temperature is very high, $t_0 \simeq 600°$ C.

These results show that the polarization of cement in the wire-detail circuit is stronger than between the turns of the transducer; the part played by the turns in producing instability is, however, also considerable.

Thus, the instability of the tensiometric dc circuit is caused by cement polarization and not by the shunting effect of the cement insulation layer. It is only the transducers using cements with the lowest insulation properties (the old cement TsKTI No. 3), and then only at temperatures above $t \geq 600°$ C, that exhibit random variations ("floating") of the galvanometer beam caused by the reduced resistance of the insulation layer ($R_i \simeq$ $\simeq$ 100 - 1000 ohms).

On the basis of the above data, it is now possible to formulate new important characteristics for heat-resisting cements:

1) the temperature of the beginning of instability t_0 (see above);

2) the amount of zero drift α (in ohms) during 1 min;

3) the amount of zero drift α_∞ up to polarization saturation;

4) the duration of polarization saturation α_∞ after which the measuring circuit remains stable;

5) the temperature at which the "floating" of the zero due to a low R_i begins.

Instead of determining the size of the drift directly, it is often more convenient to measure the galvanometer kick δ at the instant the bridge supplies are disconnected, i.e., when the polarized cement discharges. Then at the first instant of discharge the same emf U_n operates as for the polarization which caused drift α, and $\delta = \alpha$, since the galvanometer sensitivity in the bridge measuring diagonal is $C_u = C_i R_{ex}$ v/mm (where C_i amp/mm = = const, and R_{ex} = the external resistance of the galvanometer) and is practically the same at the instant of switching in and out of the supply battery (Fig. 2). In carefully conducted tests, it was always found that $\alpha = \delta$. The advantage in using δ instead of α consists in the fact that δ is not affected by the possible instability of the tensiometer wire resistance $R = f(\tau)$.

It follows from the above analysis that the heat-resisting cement must possess not only a high ρ, but also a weak and rapid polarization at high temperatures.

Liquid glass cements with loosely linked mobile ions and a porous heterogeneous structure, are subject, it would appear, to ion-relaxational and so-called high-tension polarization with unfavorable characteristics:

a large drift $\alpha = \delta$ and a long saturation time. Hence, cements of this type [2] even with a high p approaching that of radio porcelain or quartz cannot provide a stable circuit at high temperatures.

It is necessary to use weakly polarized cements on a theoretically different basis, for instance, silicon-organic compounds.

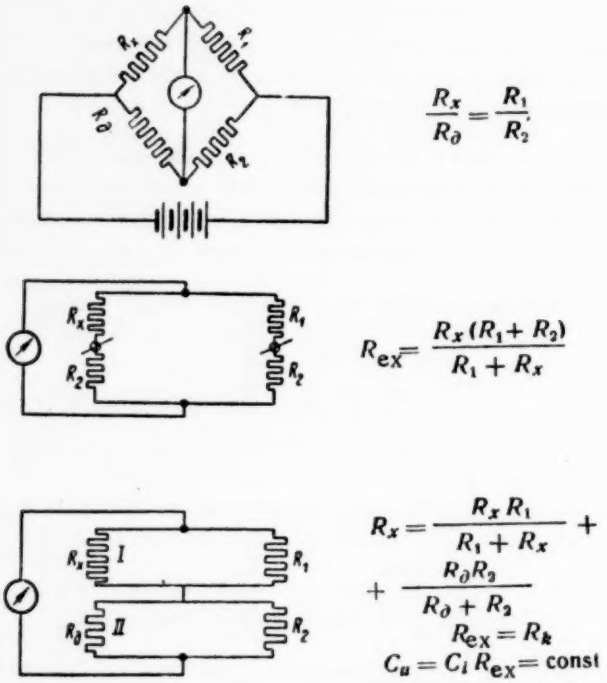

Fig. 2

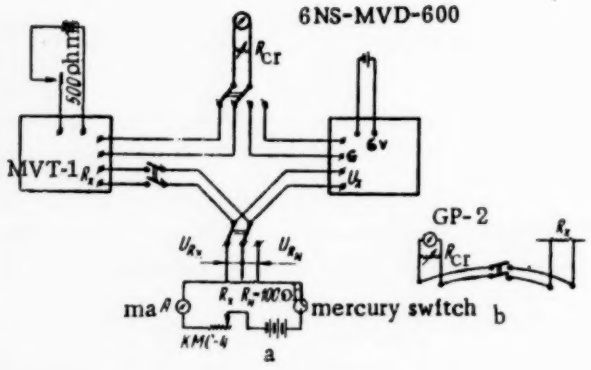

Fig. 3

A method of using liquid-glass cement tensiometers at temperatures up to 700° C. On the basis of the new experimental data, it has become possible to use these tensiometers up to temperatures of 700° C thus exceeding the normal range of such tensiometers in static testing by 200-400° C [2]. This method is, in general, suitable for using tensiometers at temperatures higher than their instability temperature.

In agreement with the above-mentioned explanation of the processes in a heat-resisting tensiometer, this method consists in connecting the tensiometer to the dc supply before the test detail is loaded and passing through the tensiometers the supply current during time τ_∞, until saturated polarization is reached and the zero drift practically eliminated.

According to the data obtained it appears possible to stabilize measuring circuits at high temperatures in 25 min to 3 hours. The time for achieving stabilization is proportional to the bridge supply voltage U, and it is therefore advisable to use as low a supply voltage as possible.

The advantage of new liquid-glass cements [2] consists in the following: 1) the zero drift α_∞ of transducers using these cements is a small fraction of those using old-type cements; 2) with a gradual rise in U the value of α of these transducers does not increase; 3) owing to the high R_i of these cements, no zero "floating" is observed in transducers of this type up to 700° C; 4) the value of τ_∞ for these cements is rather smaller than for the old-type cements.

The above method of using the tensiometers is certainly applicable for static tests under isothermal operating conditions. In order to find out the possibility of using this method under variable temperature conditions, it is necessary to establish the relations between α, τ_∞, and t.

It can be expected that owing to the small value of the zero drift α_∞ tensiometers using cement No. 2 will for small values of the supply voltages U = 0.25 v be usable at variable temperatures.

When tensiometric wire with a high resistance per unit length and higher sensitivity to strain is used, the cement polarization error will decrease.

Investigation of a potentiometer circuit. Measurement of the resistance of heat-resisting tensiometers by the potentiometer method does not theoretically avoid the polarization of cement, since direct current will flow through the tensiometer wire even in a balanced condition.

The effect of polarization in a potentiometer method was verified experimentally.

Figure 3 shows a circuit for a method of measuring R_x on a bridge and a potentiometer, simultaneously. In potentiometer measurements R_x was calculated from the formula $R_x = \frac{U_{R_x}}{U_{RN}} R_N$, where U_{R_x} and U_{R_N} are voltage drops across the potentiometer resistor R_x and the standard resistor $R_N = 100$ ohms, respectively. A battery of alkaline storage cells NKN-45, U - 2.5 v connected in parallel in order to raise their capacity to 270 ampere hours served as the source of supply.

In order to increase the stability of the supply current, the battery was discharged through a resistor of 1600 ohms during 30 min to 1.5 hours before measurements were started, and R_x connected to the circuit. The voltage fell on an average during the discharge of the battery by approximately 10^{-4} v in 30 min, i.e., the supply was sufficiently stable.

The presence of the normal polarization of cement was ascertained by observing the kick on the galvanometer connected straight across R_x (see Fig. 3, b). For instance, for a transducer using cement No. 3 (see [2]) at t = 500° C after passing the current for 1 min a kick $\delta = -50$ mm was observed, which with a critical $R_{cr} = 380$ ohms, $R_x = 120$ ohms, $R_{ex} = \frac{R_{cr} \cdot R_x}{R_{cr} + R_x} = 91$ ohms, $C_u = C_i \cdot 91 = 0.06 \cdot 10^{-5}$ v/mm, $i = 2.5 \cdot 10^{-3}$ amp is equivalent to $\delta R = \frac{\delta U}{i} = 0.012$ ohms. It is significant that this value is similar to the one obtained for δ when the same transducer was tested in parallel on a bridge and a potentiometer: $\delta = 9.5$ mm = 0.0125 ohms (with $S_R = 760$ mm/ohm).

It was established that the long duration of potentiometer measurements can mask the instability of the circuit. For instance, it is impossible to observe by the potentiometer method an increase $R_x = f(\tau)$ due to polarization if $\tau_\infty \leq 2$ min, since consecutive measurements of U_{R_x} and U_{R_N} last over 2 min. This may explain the former conclusions that the potentiometer method of measuring is stable at high temperatures [1]. Such stability, however, is possessed by a simpler bridge circuit after the lapse of time τ_∞.

When the zero drift duration is increased, the potentiometer method similarly (to the bridge method) registers a continuous rise of $R_x(\tau)$ due to the polarization of cement; moreover, both methods produce similar quantitative values of $R(\tau)$.

Investigation of an ac bridge circuit. In measuring the electrical resistance of heat-resisting tensiometers by means of an alternating current the above instability due to polarization should disappear.

At high temperatures, however, an ac measuring circuit also exhibits instability whose causes have not been as yet ascertained.

In the present work, instability tests were made with an electronic ac bridge type ID-2. The instrument was used with a half-bridge consisting of two heat-resisting tensiometers.

Mainly, tensiometers using cement TsKTI No. 3 were tested; however, tensiometers with other cements behave in a similar manner with the exception of different instability starting temperatures.

Above $t \approx t_0$ a pronounced instability of the circuit was observed. Observations of zero indicators in this region lead to the following conclusions:

1. Two distinct types of instability should be mentioned: a large deviation from the zero and rapid small oscillations of the pointer round the reading of the instrument. The latter are observed at high temperatures, do not interfere substantially with measurements and are caused, as in the case of dc measurements, by the drop in the resistance of the cement. The first type of instability is the decisive one.

2. The zero deviations do not depend on the time of the current flow and are, it would appear, of a random nature.

3. The grounding of the detail with the affixed transducers does not decrease instability.

A careful investigation of instability with respect to temperature led to the conclusion that near-zero deviations were produced by small temperature variations of the transducer and the detail.

Thus, at as low a temperature as $t = 425°$ C variations of $\pm$ 0.1 mv = $\pm$ 2.5° C corresponded to an instability of $\Delta\alpha = \pm$ 40 scale divisions. At higher temperatures, the effect of Δt on $\Delta\alpha$ increases rapidly, thus, at $t = 570°$ C, a variation of $\Delta t = \pm$ 0.01 mv produces a deviation of $\Delta\alpha = \pm$ 100-150 scale divisions.

With an ideal isothermic operating condition, an ac circuit can provide a stable reading, i.e., as it was to be expected, there is no unidirectional zero drift in an ac bridge.

At small temperature variations, however, the bridge balance changes considerably, it would appear, due to a large temperature coefficient of the capacity, the insulation resistance, and the loss angle of the cement layer.

It is especially desirable to investigate the effect produced on the instability of heat-resisting tensiometers using different cements by the frequency of the supply voltage at $t > t_0$, and to find the optimum frequency at which the instrument should work.

Since in practice there are always certain variations in the temperature of the detail $\pm \Delta t$, and measurements are conducted in a varying ambient temperature, an ac measuring circuit is considerably less stable at high temperatures than a dc circuit.

SUMMARY

For operation with heat-resisting tensiometers at temperatures above t_0, it is preferable to use a dc circuit.

This important conclusion is of special interest for high temperature dynamic tests in which tensiometers with mechanically tough liquid-glass cements are used at temperatures up to $t \geq 800°$ C, i.e., at $t \geq t_0$. Dynamic measurements are usually made with a carrier frequency. The use of dc circuits should be recommended in this case as well.

LITERATURE CITED

[1] N. G. Tisenko and Yu. M. Margolin, Methods of Manufacturing Heat-Resisting Wire Tensiometers [In Russian] (TsKTI, 1952).

[2] E. Yu. Nekhendzi and N. G. Tisenko, Industrial Laboratory No. 7 (1958).*

[3] E. Yu. Nekhendzi, "Development of heat-resisting tensiometers for measuring static strains at high temperatures," Vol. II, Heat-Resisting Tensiometers up to a Temperature of 700° C [In Russian] (TsKTI, 1956).

[4] N. P. Bogoroditskii, V. V. Pasynkov, and B. M. Tareev, Electrotechnical Materials [In Russian] (1955).

[5] G. I. Skanavi, Physics of Dielectrics [In Russian] (1949).

* See English translation.

AN ELECTROMECHANICAL TENSION DYNAMOMETER FOR 50,000 KG LOADS

O. N. Fofanov

Strain gages are now much used in combination with elastic sensing elements to produce dynamometers. The reason is that strain gages are universally usable, since they serve to transform the force to an electrical signal; they enable one to use dynamometers at remote points and to control forces automatically. But electrical dynamometers need more skill in use than do ordinary ones. Therefore, in some cases, it is better to use mechanical direct-reading dynamometers.

We have designed a universal dynamometer designed to measure tensile loads up to 50,000 kg which has mechanical and electrical reading heads. The two heads may be used together or separately. Used as a mechanical dynamometer only, the instrument is distinguished from ordinary mechanical dynamometers by its using a rod in tension as sensing element. The working of the dynamometer can be checked continuously during use. Discrepancies in the readings exceeding the permitted limits indicate that something is wrong at once. This makes it easier to detect and remove the cause.

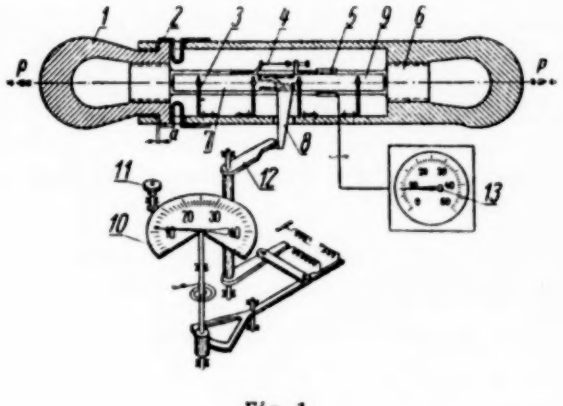

Fig. 1

Figure 1 shows the dynamometer. The forces P applied to the hooks stretch the rod 6. The measuring rods 7 and 9 then move in the spring guides 3 relative to one another under the action of the spring 4, which presses those rods onto the faces of the threaded ends of rod 6, which faces are 520 mm apart. On the other side there are identical rods which act with 7 and 9 to twist the flat spring supports of the arm 8 which is coupled by the lever 12 to a reading mechanism. The force is read on the scale 10. The knob 11 turns scale 10 to set the zero. The stress in rod 6 at 50,000 kg is 40 kg/mm^2. This stress corresponds to an extension of 1 mm, which causes the pointer to turn through 280°. The rod is joined to the body by the springs 2 to protect it from lateral forces. These springs are comparatively soft along the axis of rod 6, but are very stiff in directions normal to that axis. They protect the rod from twisting and bending forces. The instrument is protected against breakage by excessive forces; gap a closes if the force exceeds the upper limit (at which plastic deformation would start), and the body takes up some of the force acting on hook 1.

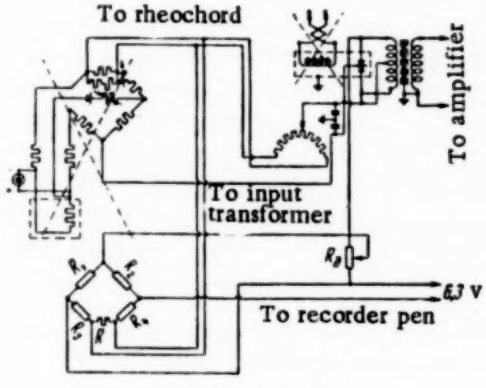

Fig. 2

The electrical signal is provided by a bridge which has four active arms consisting of the strain gages 5. The surface of the rod, in all, holds four independent bridges; if one is found faulty, another can be used simply by changing the connections. The gages are made from 30 μ constantan wire. The base is 25 mm long and is made from capacitor paper; the wire (186 ohms) is fixed with BF-4 glue. This BF-4 glue also holds the gage to the rod.

Standard self-balancing bridges or potentiometers 13 can be used, if they are fitted with new scales graduated in force terms to read the forces acting.

We used an ÉMD-112 bridge or an ÉPD-02 potentiometer. A few minor changes were made in the circuits; the chopper was disconnected, and with it the internal bridge, and the leads were taken to the bridge on the rod. Figure 2 shows the EMD-112 connected to gages R_1, R_2, R_3, and R_4. The shunt R_s is used to set the range. The resistance R is used to set the zero of the pen.

Three of these dynamometers have been made. Each has been calibrated and checked in accordance with instructions 20-49 issued by the Committee on Standards, Measures, and Measuring Instruments. The mechanical reading head and the ÉMD-112 were fitted with graduated scales reading in force units. The readings given by the mechanical head did not vary by more than 200 kg; the electrical head gave variations of only two-thirds of this size. The dynamometers were used at loads up to 50,000 kg over two months, and were each checked three times. The errors at no time exceeded 250 kg at any part of the scale during loading or unloading.

The use of a rod in conjunction with sprung levers makes it easy to make dynamometers for measuring large forces. It is very much easier to design and make rods than it is to make the other sensing elements (membranes, etc.) often used in dynamometers.

If standard electronic bridges or potentiometers are used, the only work needed to make the electrical part of the dynamometer is to glue on the strain gages and fix the sockets needed for connection.

CONVERGENCE OF AUTOMATIC BALANCING IN MEASURING CIRCUITS WITH TWO BALANCING ELEMENTS

V. Yu. Kneller

Both in production testing and laboratory practice there has been felt in recent years an increasing need for changing over from precision manual measurements of electrical ac quantities to automatic measurements.

Since the appearance of automatic balancers and ac bridges—instruments which were most suitable for the purpose—more than 20 years have passed. During this period, many original circuits [1-4] were proposed and sets made; to date, however, there have not been published any descriptions of a sound method for designing such devices, neither does there even exist a clear understanding of the process of automatic balancing and the manner in which it is affected by various bridge parameters. This hinders considerably the development and use of automatic balancers and bridges, in whose design one of the first questions raised is whether the measuring circuit will again balance itself automatically if the balance conditions are disturbed. If the answer is in the affirmative, there arises the question of the quality of the balancing process, i.e., of the speed of balancing, of the oscillations of the balancing elements, etc. The present article deals with analyzing these two problems for automatically controlled balancing by means of two parameters.

General propositions on convergence in automatic balancing. Automatic balancing of measuring ac circuits by means of two balancing elements is different in principle from the manual method.

Manual balancing is done by adjusting each element in turn, so that while one element is varying the other remains constant. The transition by balancing, from one element to the other, is determined by reaching a minimum in the output variable as read on the indicator, and does not depend on time, but only on the parameters of the balancing elements and the indicator. These circumstances provide a simple representation of the balancing process on a topological diagram for its further investigation [5].

Automatic balancing of ac circuits is based on a continuous simultaneous tracking of both measured quantities. Both balancing elements begin their movements as soon as an unbalance appears, and the movement of each is determined not only by the variation of the output variable with changes in the parameters, but also by the effect on the servomechanism of the changes in the parameters, i.e., it is determined by the dynamic properties of the whole system. In this instance, in order to be able to follow the process of balancing, it is necessary to reproduce the entire picture of the movement of the balancing elements from the beginning of balancing, i.e., to make complete calculations of a closed-loop dynamic system. It is obviously impossible to obtain a complete understanding of the process of automatic balancing by means of the topological representation method alone, without taking into account the dynamics of the system. This may explain the phenomenon that in analyzing the operation of one and the same automatic bridge, authors of papers [2] and [3] arrived at diametrically opposite conclusions about its convergence.

In examining manually balanced ac measuring circuits, it is customary to characterize the process of balancing by the concept of convergence, which generally represents the ability of the circuit to approach balance [5]. More often, however, convergence is understood in a narrower sense as the speed with which the circuit can be balanced, represented by the number of consecutive adjustments required to obtain the balance, or by the angle of convergence or coefficient of convergence [6].

All these concepts are based on the characteristics of manual balancing and lose their meaning in automatic balancing. In automatic balancing, however, there remain the same problems, which are described in manual balancing by the concept of convergence, namely: 1) will the circuit attain a balanced state? and 2) how the balancing process is achieved. It is advisable to unite these problems of automatic balancing under the concept of convergence in its broad sense. Henceforth, when the term analysis of convergence is used, we shall mean an investigation conducted with the object of obtaining an answer to both the above questions.

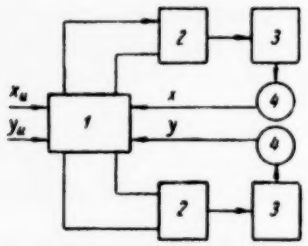

Fig. 1. 1) Measuring circuit; 2) indicator; 3) servoamplifier; 4) servomotor.

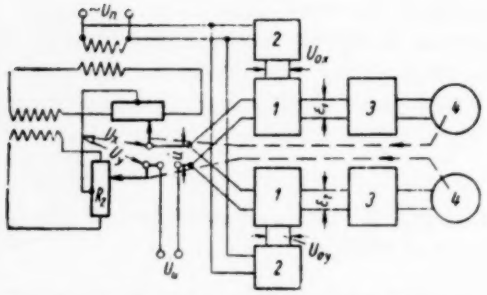

Fig. 2. 1) Phase-sensitive zero indicator; 2) phase-shift circuit; 3) servoamplifier; 4) servomotor.

In order to prove that the automatic balancing is converging, it is necessary to show that with any variation of the measured quantities within the range of the circuit, the latter is automatically returned to a balanced state independently of the previous condition of balance. If every new state of balance is taken as the origin of the coordinates, the question can be put in a slightly different manner: will the circuit be always automatically balanced if the balancing elements are placed in any arbitrary position within the measuring range? This is a typical problem of "over-all" stability in automatic control systems. Thus, in order to be able to answer the first question about the convergence of the system, it is necessary to investigate the "over-all" stability of all the possible points of balance of the measuring circuit.

The most important indication of the quality of the balancing process is its speed. In manual balancing, its speed can be measured by indirect means (coefficient of convergence, angle of convergence, etc.) instead of time; in automatic balancing these parameters have no meaning, and the speed of balancing has to be measured in the time it takes to obtain a balance.

It is, obviously, not expedient to judge all the measuring devices from the point of view of a minimum balancing time and to compare them all on that basis. The time required for balancing is determined in the first place by the operating conditions of the automatic measuring device, and an unjustified striving to increase the speed of operation of the device leads to its unnecessary complication. Having selected, however, a servomechanism for balancing, it is advisable on the basis of the operating conditions to investigate what effect the parameters of the measuring circuit and the indicator have on the speed of operation, and to find out whether the speed of operation has been lowered by a bad choice of these parameters. The problem of ensuring a good convergence for automatic balancing is reduced to a problem of choosing appropriate parameters imposed by the choice of the servomechanism for the measuring circuit and the indicator.

Thus, the problems embraced by the concept of "convergence" in automatic balancing are entirely dynamic and their solution should be sought in the analysis of dynamic systems.

Figure 1 shows a generalized block schematic of a measuring device with automatic balancing by means of two elements. In the most general case, both the measuring part of the device and the servomechanisms can be represented by nonlinear equations of a high order.

In a large number of practical cases, however, they can be represented sufficiently accurately by a system of two nonlinear equations of the first order

$$\left.\begin{aligned} \frac{dx}{dt} &= \Phi_1(x, y, x_u, y_u) \\ \frac{dy}{dt} &= \Phi_2(x, y, x_u, y_u) \end{aligned}\right\}, \qquad (1)$$

where $\underline{x}$ and $\underline{y}$ are the balancing elements;

x_u and y_u are the measured quantities;

Φ_1 and Φ_2 are nonlinear functions which account for the nonlinearity of the characteristic of the measuring part of the device and the limitations of the coordinates in the system.

The investigation of the system represented by (1) can be successfully carried out by constructing a phase trajectory in the $\underline{x}$, $\underline{y}$ phase plane

$$\frac{dy}{dx} = \frac{\Phi_2(x, y)}{\Phi_1(x, y)} \tag{2}$$

for different initial conditions [7]. This diagram of phase trajectories (the so-called phase picture of the system) provides an indication both of the stability of the system and the quality of balancing, i.e., solves completely the question of the convergence of automatic balancing.

Below, we provide phase-plane investigations of the convergence of a wide range of automatic ac measuring systems with linear static characteristics. Such systems include right-angle coordinate balancers and bridges with specially connected control elements described in [8].

The results thus obtained can also be used in the case of ordinary ac bridges when the measuring range forms a small portion of the full values of the measured parameters.

Convergence of measuring circuits with linear static characteristics. In ac measuring systems with two-element automatic balancing and linear static characteristics (ac balancers and others), the servomechanism control signals are formed by dividing the unbalance voltage of the circuit into two components by means of two phase-sensitive zero indicators (PSZI) (Fig. 2).

Let us write the dynamic equation of this circuit in terms of deviations from the balanced state. Let us examine the complex unbalance voltage plane, assuming that the real axis corresponds to the voltage at R_1 (U_x).

The measuring system equation

$$\dot{U} = k_1 (x + jy), \tag{3}$$

where $\dot{U}$ is the complex unbalance voltage;

$\underline{x}$ is the deviation of the balancing element R_1 from the balanced condition;

$\underline{y}$ is the deviation of the balancing element R_2 from the balanced condition.

PSZI equation

$$\varepsilon = kRe\ [\dot{U}e^{-j\varphi}], \tag{4}$$

where ϵ is the voltage at the output of the PSZI; and

φ is the angle between the reference voltage and the voltage across R_1.

If the reference voltage U_{ox} is shifted with respect to U_x by φ and U_{oy} with respect to U_y by ϑ the voltage at the output of the indicator will be:

$$\begin{aligned} \varepsilon_1 &= k_2 Re\,[\dot{U}e^{-j\varphi}] = k_1 k_2 (\cos\varphi x + \sin\varphi x) \\ \varepsilon_2 &= k_3 Jm\,[\dot{U}e^{-j\vartheta}] = k_1 k_3 (-\sin\vartheta x + \cos\vartheta y) \end{aligned} \tag{5}$$

Equations of servomechanisms with balancing elements, neglecting the small time constants of the servo-amplifier and motor take the form

$$\left.\begin{aligned}\frac{dx}{dt} &= -f_1(\epsilon_1)\\ \frac{dy}{dt} &= -f_2(\epsilon_2)\end{aligned}\right\}, \tag{6}$$

where f_1 and f_2 are nonlinear functions accounting for the limited speed of the motors. Usually these functions can be approximated by straight lengths (Fig. 3).

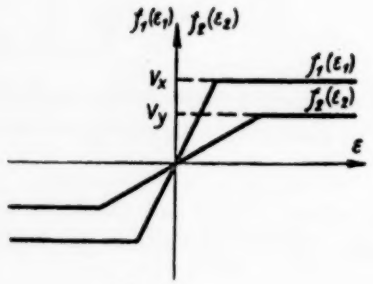

Fig. 3

By substituting (5) in (6), we obtain a system of equations

$$\left.\begin{aligned}\frac{dx}{dt} &= -f_1[k_1 k_2(\cos\varphi x + \sin\varphi y)]\\ \frac{dy}{dt} &= -f_2[k_1 k_3(-\sin\vartheta x + \cos\vartheta y)]\end{aligned}\right\}, \tag{7}$$

which represents the movement of the measuring device when it is deviated from a balanced condition. The following inequalities should be added to (7) in order to account for the limitations in the position of the balancing elements

$$\begin{aligned}X_1 \leqslant x \leqslant X_2,\\ Y_1 \leqslant y \leqslant Y_2.\end{aligned} \tag{8}$$

The above dynamic system has two degrees of freedom. Its condition at any instant is fully determined by two quantities $\underline{x}$ and $\underline{y}$, and hence can be represented by a point on the phase plane $\underline{x}$ and $\underline{y}$ (known as the representative point).

By constructing, for various deviations from the balanced condition, the locus of points representing the conditions of the system after it had been unbalanced (i.e., by constructing phase trajectories), it is possible to study the types of movements of the system in order to solve the question of convergence.

It will be seen from (7) and Fig. 3 that besides the balance condition from which the deviations in $\underline{x}$ and $\underline{y}$ are counted ($x = 0$ and $y = 0$) the system has no other balance position.

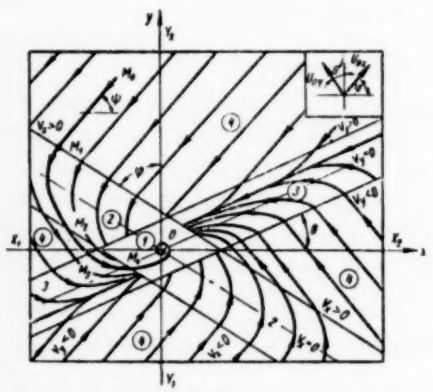
Fig. 4

Let us divide the phase plane into regions in which the system movement has different characteristics.

The equations of boundaries dividing the regions of motor operation at a constant speed and at a speed proportional to ϵ (the so-called transition lines) have the form:

for the X motor:

$$y = \operatorname{tg}(90+\varphi)x \pm \frac{v_x}{k_1 k_2 k_4 \sin\varphi}. \tag{9}$$

and for the Y motor:

$$y = \operatorname{tg}\vartheta x \pm \frac{v_y}{k_1 k_3 k_4 \cos\vartheta}. \tag{10}$$

These straight lines divide the phase plane into domains (Fig. 4).

Domain 1 is a domain of linearity. With deflections $\underline{x}$ and $\underline{y}$ lying within the domain the speeds of the motors do not reach as yet their limiting values of v_x and v_y and are proportional to the controlling voltages ϵ_1 and ϵ_2.

The movement equation of the system in domain 1 is:

$$\left.\begin{aligned}\frac{dx}{dt} &= -k_1k_2k_4(\cos\varphi x+\sin\varphi y)\\ \frac{dy}{dt} &= -k_1k_3k_5(-\sin\vartheta x+\cos\vartheta y)\end{aligned}\right\}. \tag{11}$$

In domain 2 servomotor Y works at its limiting speed u_y and the speed of servomotor X is proportional to ϵ_1.

The movement equation of the system in this domain is:

$$\left.\begin{aligned}\frac{dx}{dt} &= -k_1k_2\epsilon_1(\cos\varphi x+\sin\varphi y)\\ \frac{dy}{dt} &= -v_y\end{aligned}\right\}. \tag{12}$$

In domain 3 servomotor X works at its limiting speed v_X and the speed of servomotor Y is proportional to ϵ_2.

The movement equation of the system in this domain is:

$$\left.\begin{aligned}\frac{dx}{dt} &= -v_x\\ \frac{dy}{dt} &= -k_1k_3k_5(-\sin\vartheta x+\cos\vartheta y)\end{aligned}\right\}. \tag{13}$$

Domain 4 is the domain of saturation. Here both servomotors work at their limiting speeds and the equation of the system movement is:

$$\left.\begin{aligned}\frac{dx}{dt} &= -v_x\\ \frac{dy}{dt} &= -v_y\end{aligned}\right\} \tag{14}$$

The whole phase plane region in which the representative point may be placed is limited according to (8) by straight lines:

$$\begin{aligned}x &= X_1, \quad y=Y_1,\\ x &= X_2, \quad y=Y_2.\end{aligned} \tag{15}$$

Let the system be unbalanced and the deviations from balance be x_0 and y_0. This condition of the system will be represented on the phase plane by point M_0. Let us examine the movement of the system from point M_0.

The differential equation of the phase trajectory in domain 4 is according to (14):

$$\frac{dy}{dx}=\frac{v_y}{v_x}. \tag{16}$$

Thus, in domain 4 the phase trajectory is a straight line passing through point M_0 at an angle $\psi = \tan^{-1}\frac{v_y}{v_x}$ with respect to the X axis. Let us now determine the direction of movement of the representative point along the trajectory. Considering that at point M_0 quantity $v_y > 0$ and $v_x > 0$, it follows from (14) that x and y decrease with time. Hence, their subsequent values will be $x_1 < x_0$ and $y_1 < y_0$, i.e., the movement of the representative point will be in the direction shown in Fig. 4 by an arrow. In domain 2, the representative point movement according to (12) is determined by equation:

$$\frac{dy}{dx}=\frac{v_y}{k_1k_2k_4(\cos\varphi x+\sin\varphi y)}. \tag{17}$$

This trajectory can be constructed by integrating (17). In practice, it is easier to construct phase trajectories in domains 2 and 3 by means of the isocline method [8, p. 537], without solving the differential equations. The direction of movement of the representative point in domain 2 is determined according to (12). In domain 4, past point M_2, the representative point again moves along a straight line at an angle $\psi_1 = \tan^{-1}(-v_y/v_x)$ to the X axis, and in domain 3, past point M_3, along a curve which represents the solution of the differential equation:

$$\frac{dy}{dx} = \frac{k_1 k_4 k_5 (-\sin\vartheta x + \cos\vartheta y)}{v_x}. \tag{18}$$

At point M_4 the representative point enters the linear domain and continues to move according to Eq. (11).

It is not necessary to construct phase trajectories in order to study the movement of the system in the linear domain. It is known that all the phase trajectories in the linear domain tend to the balanced condition providing the roots of the characteristic equation of the system of equations, which represent the movement of the system in this domain, have negative real parts, i.e., providing the solution of system (11) is stable.

The characteristic equation of system (11) is:

$$p^2 + p(k_2 k_4 \cos\varphi + k_3 k_5 \cos\vartheta) k_1 + k_1^2 k_2 k_3 k_4 k_5 \cos(\varphi - \vartheta) = 0, \tag{19}$$

and the condition that its real parts are negative with $k_i > 0$ $(i = 1, \ldots, 5)$ is

$$\cos(\varphi - \vartheta) > 0; \tag{20}$$

$$k_2 k_4 \cos\varphi + k_3 k_5 \cos\vartheta > 0. \tag{21}$$

If conditions (20) and (21) are fulfilled, the representative point will move from M_4 across the linear domain to the point of balance 0. Figure 4 shows a possible trajectory in this domain.

Phase trajectories for other initial deviations from balance are constructed similarly.

It will be seen from Fig. 4 that all the phase trajectories tend to the balance point 0 and hence, at any initial deviation, the circuit will be automatically returned to the state of balance. For a complete solution of the question of convergence, it is necessary to examine the phase pictures of all other points of balance within the measuring range.

Thus, the balancing process is convergent if conditions (20) and (21) are fulfilled, and all the phase trajectories which begin outside the linear domain enter that domain.

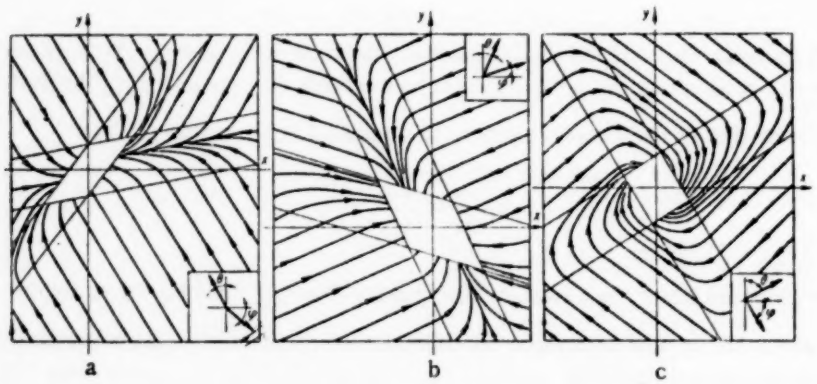

Fig. 5

It is timely now to put the question whether it is sufficient only to fulfill conditions (20) and (21) in order to obtain convergence conditions for the whole measuring range, i.e., whether the necessary and sufficient condition of convergence for the linear domain can be applied to the "over-all" conditions of convergence.

In order to solve the question, it is necessary to examine the behavior of phase trajectories at different balance points with varying measuring device parameters which satisfy conditions (20) and (21).

Figure 4, a, b, and c shows other three phase pictures of the system, plotted for different combinations of relative vector positions of the reference voltages with:

$$90° > \varphi > -90°, \quad 90° > \vartheta > -90°. \tag{22}$$

In all the cases, according to (20), $\dot{U}_{oy}$ leads $\dot{U}_{ox}$ but not more than by 180° and (21) is fulfilled at any values of k_i ($i = 1, \ldots, 5$) by virtue of (22). The variations of quantities φ, ϑ, v_x, v_y, and k_i lead to changes in the basic geometrical elements of the phase picture, the transition line slopes, the width of the linearity domains,and phase trajectories' angles of slope in the saturation domain.

In changing over to a new balance point without varying the parameters of the measuring device, the above geometrical elements of the picture are preserved, but the distances change along the coordinate axes from the balance point to the straight lines,which limit the possible range of deviations from the balanced state. In examining the phase pictures of the systems with various changes of their geometrical elements which correspond to different values of the system parameters, satisfying conditions (20) and (22) it will be seen that in all the cases all the phase trajectories meet in the linear domain 1 as before. Thus, condition (20) is the necessary and sufficient condition of convergence of automatic balancing in the whole measuring range for the above type of measuring devices.

Thus, the first of the two questions, namely whether the balancing process is converging for a given system has a simple solution: it is sufficient to find out whether condition (20) is being fulfilled. For investigating the quality of balancing, it is necessary to construct a phase picture of the system, taking into account the limitations imposed by the choice of the servodrive, and to examine the movement of the system with different values of parameters which can be varied within certain limits. Such an investigation is in the main of a geometrical nature and in each concrete case can be carried out successfully.

The time of operation outside the linear domain is determined as the sum of the operation times in the domains in which the speed of at least one of the servomotors is constant. For instance, the time required for the movement from M_0 to M_4 (Fig. 4) is:

$$t_{M_0 M_4} = \frac{|v_y|}{|y_{M_0}| + |y_{M_3}|} + \frac{|v_x|}{|x_{M_3}| - |x_{M_4}|}. \tag{23}$$

The time of movement in the linear domain can be determined approximately by the real parts of Eq. (19) roots.

The method of investigating the convergence of automatic balancing of measuring circuits with nonlinear static characteristics is similar to the one above. In view of a different character of nonlinear relations of Φ_1 and Φ_2, described in (1), their phase pictures have a different structure and require separate consideration.

LITERATURE CITED

[1] W. Geyger, Archiv für Elektrotchnik 29 (1935).

[2] J. F. Graham, Electronics, No. 2 (1951).

[3] K. B. Karandeev and B. I. Shvetskii, Scientific Notes of the IMA of UkSSR, 2, 2 (1954).

[4] A. H. Foley, Communication and Electronics 11, 33 (1957).

[5] K. B. Karandeev, Bridge Methods of Measurement [In Russian] (Gostekhizdar, UkSSR, Kiev, 1954).

[6] A. D. Nesterenko, Basic Calculations of Balancing Circuits in Electrical Measurements [In Russian] Vol. 12 (Acad. Sci. UkSSR Press, Kiev, 1954).

[7] E. P. Popov, Dynamic of Automatic Control Systems [In Russian] (GITTL, Moscow, 1954).

[8] N. N. Shumilovskii and V. Yu. Kneller, Measurement Techniques No. 4 (1958).

AUTOMATIC TESTING EQUIPMENT OF THE "ELEKTROSCHETCHIK" PLANT

I. N. Osher

Side by side, with the increasing rate of production of electricity meters in the USSR, the automation of their production and testing is also developing.

Fig. 1

The Leningrad Electro-Mechanical plant is using the automatic equipment of the All-Union Scientific Research Institute of the Electrical Industry (VNIIEP) for adjusting electricity meters. It also has the automatic equipment of the Vilnius plant and highly efficient adjusting sets of the Moscow "Elektroschetchik" plant, which are also being used at the Mytishchoi plant.

The automatic racks of the Moscow Electro-Mechanical plant are being used for State testing of three-phase meters.

A new advance in the production and testing of meters was made when a group of the Moscow "Elektroschetchik" plant engineers and technicians developed an automatic set for testing single-phase meters by E. G. Lipshtein's method.

If the meter errors are within the required limits a signal is given automatically by means of two lamps of a different color.

Fig. 2

Description of the automatic equipment. The equipment consists of two parts:

1) an automatic tester attached to the conveyor (Fig. 1); and

2) a rack, carrying all the reference meters and devices which set the testing limits (Fig. 2), placed at a distance from the conveyor.

Such a construction of the tester raises its reliability, since the parts of its circuit which set the limits are removed from sources of vibration and can be easily checked and adjusted by a state inspector.

The tester itself consists of a drum with a hexagonal cross section, mounted on a vertical axle. Each side of the drum holds two meters under test. The meters are connected electrically by means of automatically switched connecting blocks.

The stationary upper part of the tester carries above each meter a photohead consisting of a lamp and a photoconductor which receives the light reflected from the disc of the meter under test.

The disc edge of each tested meter has two diametrically placed bevels with reflecting surfaces.

The drum-motor drive operated by a control relay turns the drum at regular intervals of one sixth of a revolution. In each position the drum remains stationary for 44 sec. During that time, the meters are automatically tested, the meters on each face of the tester being connected to different loads.

In a complete revolution of the drum each meter is tested at all the loads.

The stationary upper part of the tester, on which all the photoheads are fixed (Fig. 1), has the shape of a regular hexagon like the drum itself. Its face, which is opposite the operator's position, has no photoheads, since the position does not serve to test meters but to change tested meters for new ones.

When the drum changes from one position to another, the meters are automatically connected to a different load.

The power circuit of the set is given in Fig. 3 and the relay circuit in Fig. 4.

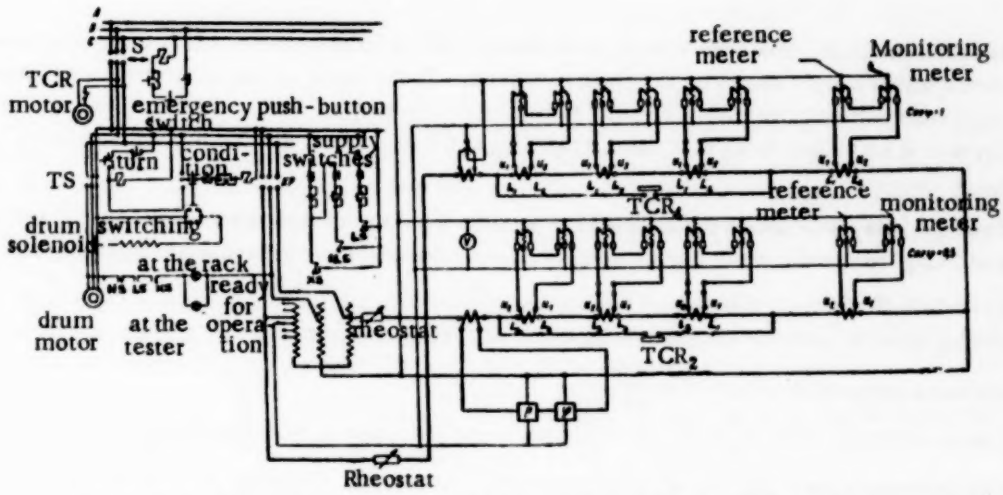

Fig. 3. S is the mains switch; TS is the turning switch; HS is the high-tension switch; LS is the low-tension switch; XS is the heating switch.

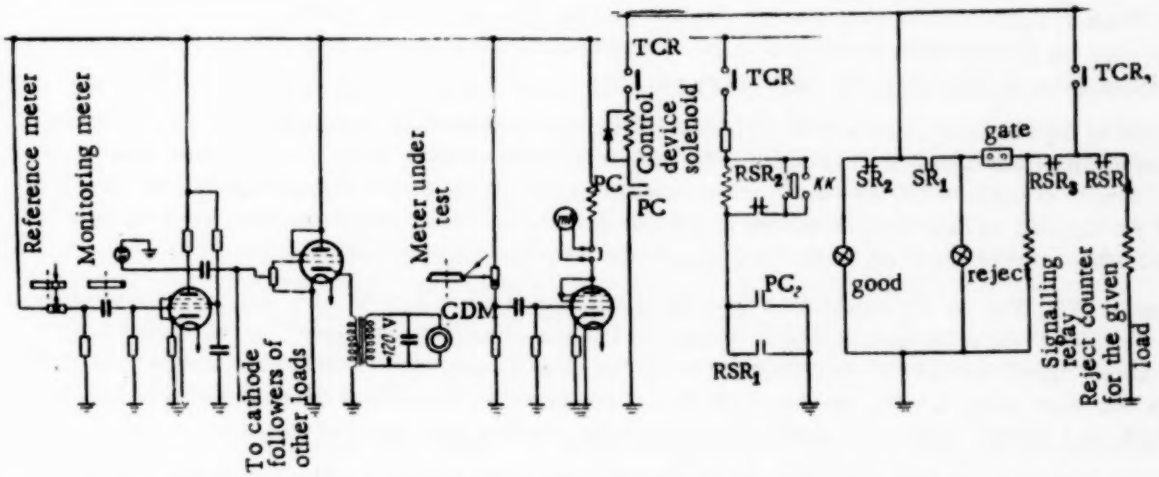

Fig. 4. CDM is the control device motor; PC is the photoconductor; RSR is the references setting relay; SR is the signalling relay.

The series circuits of all the tested meters and of two of the reference meters are connected through current transformers (Fig. 3). The series circuits of the two meters mounted on one side of the drum are connected in series to the same secondary winding of a current transformer. The primary windings of the transformers which serve to check meters at cos $\varphi = 1$ are connected to phase A. The primary windings of the transformers which serve to check meters at cos $\varphi = 0.5$ are connected to phase C so that the relative phase of the current is displaced by 120°.

The primary windings of all the transformers carry a current of 1 amp due to star connected resistive loads.

Since the reactances of the transformers are very small compared with the resistive loads, the currents in the primary windings are in phase with the corresponding voltages.

The shunt coils of all the meters are fed in parallel by voltage U_{A-0}. Thus, the change of cos φ from 1 to 0.5 is made without a phase shifter.

One of the reference meters always operates at cos $\varphi = 1$ and the other at cos $\varphi = 0.5$.

Both reference meters are connected through a current transformer with a ratio of 1/5 amp and operate on full load.

The construction of all the reference meters is the same. The reference meter disc has a row of evenly spaced holes through which a light shines on the photoconductor. As the result of this, an alternating current is induced in the photoconductor circuit; the frequency of this current is proportional to the speed of rotation of the disc. This current is amplified in an electronic amplifier and used to feed the synchronous motors of controlling devices.

The time control relay TCR shorts the transformer primary windings of the meters under test by means of contacts TCR_2 and TCR_4 before the drum begins to revolve, and takes the short off again at the end of the movement.

The controlling devices (two for each load) have the following components:

1) a synchronous motor with a reduction gear;

2) a cam with a friction drive from the synchronous motor reduction gear output axle;

3) a control device solenoid (Fig. 4) which actuates the plunger, thus engaging the cam with the output axle of the reduction gear;

4) contacts KK (Fig. 4) which shunt the winding of the references-setting relay during the whole of the cam revolution with the exception of the time for comparison to the reference standards. Contacts are closed and opened by the cam.

The beam of light from the photohead of the meter under test (Fig. 4) is reflected from the bevel edge of the cam onto the photoconductor, which is in the same photohead. The current pulse thus obtained operates after amplification relay FR, closing its contacts FR_1 and FR_2.

As soon as the revolving drum stops, the contacts of the time control relay TCR_2 and TCR_4 (Fig. 3) open and the meters under test obtain their current. Simultaneously, contacts TCR_8 (Fig. 4) of the same relay close. Therefore, as soon as contacts FR_1 are closed and the circuit of the control device solenoid completed, the plunger of the cam will be actuated, and as soon as the first pulse of the meter under test is received, the cam will start rotating with the speed set by the frequency of the reference meter pulses.

Contacts TCR_9 (Fig. 4) are closed for a fraction of a second at the end of the checking process, and therefore from the instant the relay feeding switch is operated (24 and 48 v) the lamp "good" is lit, but not lamp "reject". Lamp "good" can go out only when the signalling relay SR operates. This can only happen at the end of a test period when contacts TCR_9 are closed. In fact, however, relay SR operates during this time (when the contacts TCR_9 are closed) only if the references-setting relay contacts RSR_3 are also closed.

Contacts RSR_3 are closed or open depending on whether the meter error at a given load is inside or outside the permissible limits. If the error of the meter under test is inside the limits, at the instant the last pulse from the meter under test arrives, when contacts PC_2 are closed, the KK contacts will be riding over the reference-setting cam "tolerance projection" and will remain closed. Hence, the RSR relay will not be shunted. It will

operate closing contacts RSR_1 and opening contacts RSR_2, thus keeping relay RSR operated to the end of the testing period. Moreover, contacts RSR_3 and RSR_4 will be opened, preventing relay SR from operating even if contacts TCR_9 are closed; the lamp marked "good" will continue to glow, but the "reject" lamp will not light and the reject meter will not operate. If, however, the error of the meter under test is outside the limits, at the instant the last pulses from the meter under test arrive, when contacts PC_2 close, contacts KK will not be kept open by riding over the control device cam "tolerance projection" and relay RSR will be shunted. The relay will not operate and contacts RSR_3 and RSR_4 will remain closed. At the end of the testing period when contacts TCR_9 close, relay SR will operate through TCR_3, opening contacts SR_2 and closing contacts SR_1. This will extinguish lamp "good" and light lamp "reject". Moreover, relay SR will remain locked through its own contact SR_1 until this meter is taken off the tester. When the meter is taken off the tester the "gate" contacts are opened and RS released.

Since, when a meter is rejected at any of the loads, RS operates and remains operated until the faulty meter is removed, the lamp "reject" will continue to glow irrespectively of what happens to the testing at other loads.

The part of the circuit shown in Fig. 4 starting with the cathode follower and ending with the reject counter, is the same for each load with $\cos \varphi = 1$. A similar circuit to the one shown in Fig. 4 is used for checking at $\cos \varphi = 0.5$.

The study of the test results of more than 30,000 electricity meters showed that SO-2 grade 2.5 meters of the "Elektrichestvo" plant can be checked quite efficiently at five loads: namely at 150, 50, and 10% of the normal current for $\cos \varphi = 1$ and at 100 and 20% of the normal current for $\cos \varphi = 0.5$%. Hence, the tester is made to check simultaneously five pairs of meters (two per load), with three pairs tested at $\cos \varphi = 1$ and two pairs at $\cos \varphi = 0.5$ at the loads given above.

The synchronous motors of the six control devices are fed by the amplifier which receives pulses from the reference meter working at $\cos \varphi = 1$. The synchronous motors of the remaining four control devices are fed by an amplifier which receives pulses from the reference meter working at $\cos \varphi = 0.5$.

Thus, the meters mounted on the drum of the tester pass through one position in which they are connected and disconnected and five test positions.

At the end of the assembly line, meters run for half an hour on full load. Thus, they arrive at the tester in a heated state. They are warmed up again when tested for sensitivity and creeping.

Checking the operation of the automatic equipment. The operation of the automatic tester is checked by two methods:

1) by rechecking sample meters with grade 0.2 wattmeters and first-grade stop watches;

2) by means of calibrated meters which are also used for setting up the tester.

The first method requires no explanation. The method of calibrated meters consists in the following: For each load at which tests are made, there are two meters adjusted to the limits of the permissible ranges, one as "good" and the other as "reject." The calibrating meters are similar to the normal ones except that they have no counting mechanism, are better made and are run for a long time beforehand in order to increase the stability of their operation. Instead of the normal, calibrated meters are connected to the tester, and if the tester passes the "good" meter and rejects the "reject" one, it is assumed that the set is working correctly. In order to ensure a high stability in the readings of the calibrated meters theyare run continuously on a special rack. Their checking and adjustment is made to stricter limits than the normal ones.

If the operation of the tester is found to be defective, it is possible to adjust it by displacing the KK contacts with respect to the cam.

In order to facilitate this adjustment the control device is provided with a scale over which slides a pointer attached to the KK contacts.

Provision is made for a constant check of the stability of the tester by a stroboscopic method with the help of the monitoring meter, whose series winding is connected in series with that of the reference meter and whose shunt windings are connected in parallel. The disc of the monitoring meter is lit by an instantly operating lamp fed from the amplifier of the reference meter pulses.

The monitoring meter disc appears to be stationary only if the operation of the reference and monitoring meter is stable.

By careful repeated checks, it has been established that the automatic tester is working accurately.

An automatic assembly, adjustment,and testing line for meters. The introduction of this automatic tester led to the establishment of a continuous assembly, adjustment,and testing line of electricity meters right up to the stores of finished meters.

All along this line there is only one means of transport – the conveyor. The meter store receives, on a conveyor, a stream of finished meters stamped by the State inspector.

The work of the State inspectors is carried out in the following way:

The meters before being encased pass internal inspection, which is done by means of sampling. Meters are checked for cleanliness, tightness of screws, the quality of the counting mechanism coupling, etc.

Next, a factory worker places the meter in its case and passes it on to the State inspector who checks it for sensitivity and creeping on a special automatic rack. From here the meters pass to the automatic meter error tester placed next to the previously mentioned machine. Next, the meters are sealed and supplied with fittings and then dispatched by a conveyor to the stores.

Before the automatic tester was introduced,the racks for testing meters occupied 110 m^2. Now the automatic tester takes up 2 m^2 and its auxiliary racks another 3-4 m^2.

Before the establishment of the automatic line 12 inspectors of the Technical Inspection Department were employed, and after the reorganization of the assembly shop only 4 inspectors with a simultaneous doubling of the meter production.

Before the introduction of automatic adjusting sets there were 10 adjusters employed, now only 5,with a doubled production, are needed.

Before the reorganization of the shop there were 7 State inspectors, now there are 6 and both the internal and external inspection has greatly improved in quality.

The All-Union Scientific Research Institute of the Committee of Standards, Measures,and Measuring Instruments is considering the introduction of automatic testers of the Moscow "Elektroschetchik" plant for checking single-phase electricity meters,and automatic installations of the same make for adjusting meters in other establishments as well.

MAXIMUM SENSITIVITY OF A SIMPLE BRIDGE CIRCUIT AT BALANCE

V. A. Kochan

Many papers have been written, for instance [1-4], on the problem of calculating optimum resistance values of simple bridge arms for maximum current, voltage,or power. In addition to above works the present article provides a calculation of optimum bridge arm resistances with a given current I_1 and resistance r_1 for maximum sensitivity (see figure and table).

Existing solutions, in particular solutions with respect to the current in the zero indicator circuit with a given indicator resistance r_g (which is equivalent to determining the sensitivity with respect to voltage or power) cannot be considered complete, since they only hold if the obtained optimum value for current i_1 in resistance r_1 does not exceed the maximum permissible current I_1 for this resistor. A mere increase of some of the

resistance values in the circuit as proposed in [4] if $I_1 > I_1$, can hardly be considered as the most correct solution; it is better to calculate optimum resistances on the basis of a given current I_1. In this case, the following solution applies.

The indicator current (see figure) is equal to:

$$I_g = \frac{E(r_1 r_3 - r_2 r_4)}{r_g r_p r_\Sigma + r_g(r_1'+r_2)(r_3+r_4)+r_p(r_1'+r_4)(r_2+r_3)+R} \quad (1)$$

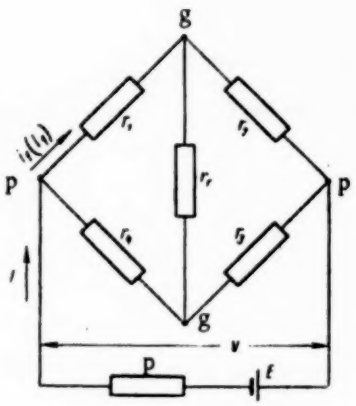

where

$$r_\Sigma = r_1'+r_2+r_3+r_4 . \quad (2)$$

$$R = r_1' r_2 r_3 + r_2 r_3 r_4 + r_3 r_4 r_1' + r_4 r_1' r_2 . \quad (3)$$

Near balance:

$$r_1' = r_1 + \Delta r_1 , \quad (4)$$

where

$$\Delta r_1 \ll r_1 \;\&\; r_1 r_3 = r_2 r_4 .$$

Let us denote *

$$\frac{\Delta r_1}{r_1} = \varepsilon , \quad (5)$$

$$r_2 = m r_1 , \quad (6)$$

$$r_4 = \frac{1}{n} r_1 , \quad (7)$$

$$r_3 = \frac{m}{n} r_1 . \quad (8)$$

Substituting (2) - (8) in (1) and omitting second order quantities, we shall obtain an expression for the indicator current near balance:**

$$I_g = \frac{2 mn r_1 E}{[(1+m)r_1+(1+n)r_p][m(1+n)r_1+n(1+m)r_g]} . \quad (9)$$

* It is known that near balance the indicator current does not depend on which of the bridge arms is varied, providing the condition is fulfilled that

$$\frac{\Delta r_1}{r_1} = \frac{\Delta r_3}{r_3} = \frac{\Delta r_2}{r_2} = \frac{\Delta r_4}{r_4} .$$

** Optimum bridge arm values corresponding to I_g can be obtained by differentiating Eq. (9) with respect to m and n, equating the derivatives to zero and taking into consideration (6), (7), and (8). These values, given below in the first line of the table, were published in [1].

In above instance, for a given current I_1 in resistance r_1, we have:

$$I_1 = I\frac{r_3+r_4}{r_\Sigma} = \frac{E}{r_p+\dfrac{(r_1+r_2)(r_3+r_4)}{r_\Sigma}}\cdot\frac{r_3+r_4}{r_\Sigma} = \frac{E}{(1+m)r_1+(1+n)r_p}. \tag{10}$$

Substituting the value of n from (10) into (9), we have:

$$I_g = \frac{mE\,|E-(1+m)I_1r_1-I_1r_p|}{mr_1|E-(1+m)I_1r_1|+(1+m)r_g|E-(1+m)I_1r_1-I_1r_p|}. \tag{11}$$

The optimum values of the bridge arms for a maximum indicator current are the following.

By differentiating (11) with respect to m and equating the derivative to zero, we have

$$m_0 = \frac{E-I_1r_1-I_1r_p}{I_1r_1}\cdot\frac{\sqrt{r_g}}{\sqrt{r_g}+\sqrt{r_p}}, \tag{12}$$

and in conjunction with (6),

$$r_2 = \frac{E-I_1r_1-I_1r_p}{I_1}\cdot\frac{\sqrt{r_g}}{\sqrt{r_g}+\sqrt{r_p}}. \tag{13}$$

Substituting (12) in (10), we obtain

$$n_0 = \frac{E-I_1r_1-I_1r_p}{I_1r_p}\cdot\frac{\sqrt{r_p}}{\sqrt{r_p}+\sqrt{r_g}}, \tag{14}$$

and in conjunction with (7):

$$r_4 = \frac{I_1r_1\sqrt{r_p}\,(\sqrt{r_p}+\sqrt{r_g})}{E-I_1r_1-I_1r_p}. \tag{15}$$

In a more general case, the resistance of the indicator is not given, only E, r_p and r_1 are given. In this case, in addition to the particular solutions with U = const or I = const [4, 5], let us find a general solution for a maximum power in the indicator.

Let us assume that

$$r_g = k_g r_{gg} = k_g\frac{(r_1+r_4)(r_2+r_3)}{r_\Sigma} = k_g r_1\frac{(1+n)m}{(1+m)n}. \tag{16}$$

where r_{gg} is the bridge resistance looking from the indicator terminals (output resistance).

Substituting (16) in (9) and following appropriate operations, we shall obtain the power dissipated in the indicator:

$$P_g = I_g^2 r_g = \frac{k_g mnr_1E^2}{|(1+m)r_1+(1+n)r_p|^2(1+m)(1+n)}\cdot\frac{k_g}{(k_g+1)^2}. \tag{17}$$

It will be seen from (17) that maximum power in the indicator will be obtained with $k_g = 1$, i.e., with $r_g = r_{gg}$.

We shall obtain optimum values for m_0 and n_0 by equating the derivatives of P_g (17) with respect to m and n to zero. Then

$$(1+m_0)(1-2m_0)r_1+(1+n_0)r_p = 0, \tag{18}$$

$$(1+n_0)(1-2n_0)r_p+(1+m_0)r_1 = 0. \tag{19}$$

From (18) and (19), we obtain:

$$n_0 = \frac{m_0}{2m_0-1} \quad \& \quad m_0 = \frac{n_0}{2n_0-1}, \tag{20}$$

from which it follows that we must always have:

$$n_0 \geq 0.5 \quad \& \quad m_0 \geq 0.5.$$

Solving (18) and (19), we find that each of them has three real roots, but only one for each equation, as determined by the expressions:

$$m_0 = \sqrt{\frac{r_p+r_1}{r_1}} \cos\left[\frac{1}{3}\arccos\left(-\sqrt{\frac{r_1}{r_p+r_1}}\right)\right], \tag{21}$$

$$n_0 = \sqrt{\frac{r_p+r_1}{r_p}} \cos\left[\frac{1}{3}\arccos\left(-\sqrt{\frac{r_p}{r_p+r_1}}\right)\right], \tag{22}$$

has a value greater or equal to 0.5.

Optimum Values of Bridge Arm Resistance

Given values	Operating condition	r_3	r_4	Assuming
E, r_p, r_1, r_g	$I_1 < I_1$	$\sqrt{\frac{r_g r_1}{r_g+r_1}(r_p+r_1)}$	$\sqrt{\frac{r_p r_1}{r_p+r_1}(r_g+r_1)}$	
	$I_1 = \text{const}$	$\frac{E-I_1r_1-I_1r_p}{I_1} \cdot \frac{\sqrt{r_g}}{\sqrt{r_g}+\sqrt{r_p}}$	$\frac{I_1r_1\sqrt{r_p}\left(\sqrt{r_p}+\sqrt{r_1}\right)}{E-I_1r_1-I_1r_p}$	
E, r_p r_1	$I_1 < I_1$	$\sqrt{r_1(r_1+r_p)}\cos\left[\frac{1}{3}\arccos\left(-\sqrt{\frac{r_1}{r_1+r_p}}\right)\right]$	$\frac{r_1\sqrt{r_p}}{\sqrt{r_1+r_p}\cos\left[\frac{1}{3}\arccos\left(-\sqrt{\frac{r_p}{r_1+r_p}}\right)\right]}$	
	$I_1 = \text{const}$	$\frac{(E-I_1r_1)r_1-\sqrt{(E-I_1r_1)(E-I_1r_p)r_1r_p}}{I_1(r_1-r_p)}$	$\frac{I_1r_1r_p(r_p-r_1)}{(E-I_1r_p)r_p-\sqrt{(E-I_1r_1)(E-I_1r_p)r_1r_p}}$	
E, r_p	$I_1 < I_1$	r_p	r_p	$r_1=r_p$
	$I_1=\text{const}$	$r_p\frac{E-2\sqrt{P_1r_p}}{2\sqrt{P_1r_p}}$	$r_p\frac{2\sqrt{P_1r_p}}{E-2\sqrt{P_1r_p}}$	$r_1=r_p$
$P=\text{const}$	$P_1 < I_1^2r_1$	r_1	r_1	
	$I_1^2r_1=\text{const}$	$\frac{\sqrt{Pr_1}-I_1r_1}{I_1}$	$\frac{I_1r_1\sqrt{r_1}}{\sqrt{P}-I_1\sqrt{r_1}}$	

If the value of current i_1 in arm r_1 calculated from Formula (10) is larger than the maximum permissible current I_1, we can obtain by substituting the value of $\underline{m}$ from (10) expressed in terms of I_1 into (17), the following expression:

$$P_g = z^2 I_1^2 r_1 \frac{k_g}{(k_g+1)^2} \cdot \frac{n}{1+n} \cdot \frac{E - I_1 r_p (1+n) - I_1 r_1}{E - I_1 r_p (1+n)} . \tag{23}$$

We obtain maximum power in the galvanometer by differentiating (23) with respect to $\underline{n}$ and taking into consideration (10), if

$$n_0 = \frac{(E - I_1 r_p) r_p - \sqrt{(E - I_1 r_1)(E - I_1 r_p) r_1 r_p}}{I_1 r_p (r_p - r_1)} \tag{24}$$

$$m_0 = \frac{(E - I_1 r_1) r_1 - \sqrt{(E - I_1 r_1)(E - I_1 r_p) r_1 r_p}}{I_1 r_1 (r_1 - r_p)} \tag{25}$$

with

$$r_p \neq r_1$$

and

$$n_0 = \frac{E - 2 I_1 r_p}{2 I_1 r_p} = \frac{E - 2 I_1 r_1}{2 I_1 r_1} \tag{26}$$

$$m_0 = \frac{E - 2 I_1 r_p}{2 I_1 r_p} = \frac{E - 2 I_1 r_1}{2 I_1 r_1} \tag{27}$$

where $r_p = r_1$.

We have the most general case when only the parameters of the supply source E and r_p are given and it is possible to chose not only r_g, but also r_1.

Since, in this case r_1 is an unknown, it is necessary in addition to (18) and (19) also to equate to zero the derivative of expression (17) with respect to r_1, i.e.:

$$(1+n) r_p + (1+m) r_1 = 0 . \tag{28}$$

A simultaneous solution of (18), (19), and (28), provides:

$$m_0 = 1, \quad n_0 = 1, \quad k_g = 1, \quad r_1 = r_p$$

or

$$r_1 = r_2 = r_3 = r_4 = r_g = r_p . \tag{29}$$

If in applying (29), the power in r_1 is found to be greater than the permissible value:

$$P_1 = I_1^2 r_1 , \tag{30}$$

then by substituting I_1 from (30) into (23), we shall obtain:

$$P_g = z^2 P_1 \frac{k_g}{(1+k_g)^2} \cdot \frac{n}{1+n} \cdot \frac{E\sqrt{r_1} - (1+n) r_p \sqrt{P_1} - r_1 \sqrt{P_1}}{E\sqrt{r_1} - (1+n) r_p \sqrt{P_1}} . \tag{31}$$

Similarly to the previous operations, by differentiating (31) with respect to $\underline{n}$ and r_1, and in conjunction with (10), we obtain:

$$\left.\begin{aligned} r_1 &= r_p \\ r_2 &= r_p \frac{E - 2\sqrt{P_1 r_p}}{2\sqrt{P_1 r_p}} , \\ r_4 &= r_p \frac{2\sqrt{P_1 r_p}}{E - 2\sqrt{P_1 r_p}} . \end{aligned}\right\} \tag{32}$$

In [4, 5], the case of constant power consumed by the bridge circuit is also considered. When:

$$P=UI=(1+m)(1+n)I_1^2r_1\,. \tag{33}$$

which, in conjunction with (17) gives:

$$P_g=\varepsilon^2P\frac{k_g}{(1+k_g)^2}\cdot\frac{m}{(1+m)^2}\cdot\frac{n}{(1+n)^2}\,. \tag{34}$$

It will be seen from (34) that the optimum values will be:

$$k_g=1,\quad m=1,\quad n=1$$

or

$$r_1=r_2=r_3=r_4=r_g. \tag{35}$$

If I_1 is given, then, similarly to the preceding operation, we shall obtain from (33) for an optimum case:

$$\begin{aligned} r_2&=\frac{\sqrt{r_1}(\sqrt{P}-I_1\sqrt{r_1})}{I_1}\,,\\ r_4&=\frac{I_1r_1\sqrt{r_1}}{\sqrt{P}-I_1\sqrt{r_1}}\,. \end{aligned} \tag{36}$$

On the basis of above relations, a table was composed which provides formulas for calculating bridge arms for various operating conditions.

It should be noted in conclusion, that in the case of $r_g=\infty$ only the voltage sensitivity of the bridge circuit can be considered. Similarly, current sensitivity should be given as the circuit characteristic in the other limiting case when $r_g=0$. Then, both characteristics can be considered as sensitivity limits with respect to power, i.e., the voltage across the indicator (with $r_g=\infty$) or the current through it (with $r_g=0$) can be expressed as

$$U_0=\lim\left|\sqrt{P_gr_g}\right|\ r_g\to\infty \tag{37}$$

$$I_s=\lim\left|\sqrt{\frac{P_g}{r_g}}\right|\ r_g\to0. \tag{38}$$

By substituting in (37) and (38) appropriate values of P_g we shall obtain U_0 and I_s for an optimum (i_1) or given (I_1) current in a bridge unbalanced by ϵ.

LITERATURE CITED

[1] O. Heaviside, On the Best Arrangement of a Wheatstone Bridge for Measuring a Given Resistance with a Given Galvanometer and Battery. Philosophical Magazine (1873), p. 114.

[2] I. N. Krotkov, Elektrichestvo No. 10 (1951).

[3] K. B. Karandeev, Bridge Methods of Electrical Measurements [In Russian] (Ukrainian Tekhizdat, Kiev, 1953).

[4] A. D. Nesterenko, Basic Calculations of Balanced Electrical Measuring Circuits [In Russian] (Acad. Sci. UkSSR Press, Kiev, 1958).

[5] Wilfried Oesterlin, Maximale Leistungsempfindlichkeit von Wheatstoneschen Brücken in der Nullmethode, ATM, J. 910-5, (June, 1955).

MOVING COIL LOOP VIBRATOR WITH CONCENTRATED LIQUID DAMPING

S. N. Gural'nik and A. N. Zaslavskii

The potentialities of light beam oscillographs with respect to recording rapidly moving phenomena is limited mainly by the natural frequency of loop vibrators.

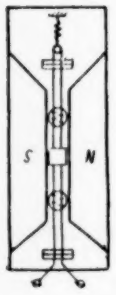

Fig. 1

Raising the natural frequency of vibrators of the existing design is fundamentally difficult since the mass of the moving part is determined not only by the parameters of the loop, and mirror, but also by the mass of the damping liquid which takes part in the movement. The natural frequency of a vibrator with liquid damping usually drops to 0.5-0.4 of its value in air; the upper frequency limit of the oscillograph is reduced in the same proportion.

The vibrator design developed by the authors of the article differs from the "classical" form by using concentrated liquid damping (authors' certificates Nos. 102877 and 106854). The moving part of the vibrator with concentrated liquid damping is not immersed in a container filled with the liquid. Damping is attained by passing the loop in certain limited portions of the air gap through miniature containers of the liquid (Fig. 1). Since in concentrated damping the mirror remains in the air, its effective mass becomes very small.

The natural frequency of such a vibrator with filled containers amounts to 80-100% of its value in air, i.e., it is twice as high as the natural frequency of the same vibrator immersed in the liquid. Hence, with the same frequency characteristic, it is possible to raise sensitivity, or with the same sensitivity to double the frequency range.

Moreover, concentrated damping eliminates the liquid region between the mirror and the lens and avoids chromatism and loss of brilliance; the liquid need no longer be transparent and inert (with respect to glass) and its quantity is reduced to a minimum.

Thus, the possibility arises of using in vibrators liquids with super-low viscosity temperature coefficients.

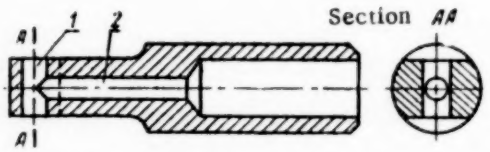

Fig. 2. 1) Operating capillary; 2) auxiliary capillary.

Another important advantage of the new vibrators is the absence of hermetic sealing and the possibility of their mass production with precise frequency characteristics.

The adjustment of the present type vibrators is made at their natural frequency in air, which does not determine accurately their characteristics when they are immersed in the liquid. It is impossible, on the other hand, to adjust vibrators immersed in the liquid under mass production conditions, since this makes very difficult the correction of mirror strains, which often arise when the stress in the loop is changed. In vibrators with concentrated damping, the mirror is in the air and the correction of its strains does not present any difficulties. Thus, adjustments of a damped vibrator become possible.

The condition of the damping liquid at the places of its concentration determines the efficiency of damping and hence the frequency characteristic of the vibrator. This places strict requirements on the liquid container which must ensure an identical amount and a stable position of liquid for all the vibrators.

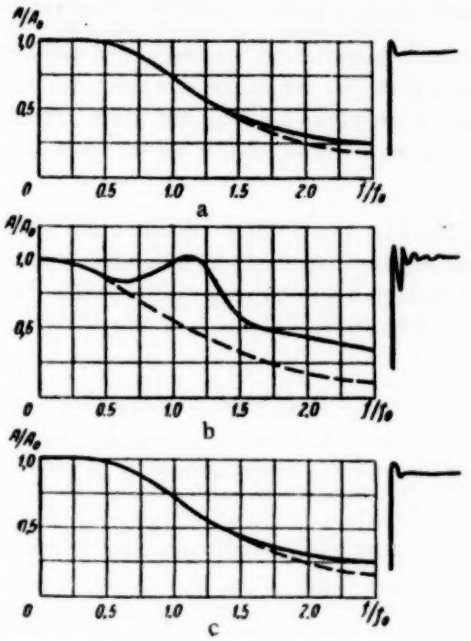

Fig. 3

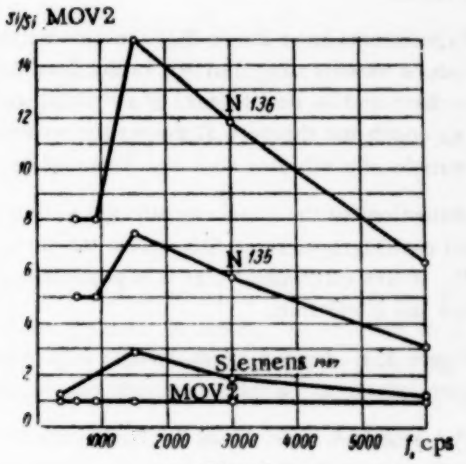

Fig. 4

In developing a production model of the vibrator with concentrated damping a stable position of the liquid was attained by making the operating container in the form of a cylindrical capillary in which the liquid was firmly held by capillary forces.

The identical filling of the operating capillary, through which passes the vibrator loop, is ensured by an auxiliary capillary perpendicular to the first one. Thus, the inaccuracy of filling only results in a level difference of the auxiliary capillaries, whereas the operating capillaries are always equally filled.

Vibrator type	Effective frequency range (± 5%), cps	Sensitivity, mm/ma	Resistance, ohms	Vibrator type of the MOV2 series equivalent in its effective frequency range
N135-0.6	600	52	9	V
N136-0.6		80	9	
N135-0.9	900	20	9	IV
N136-09		30	9	
N135-1.5	1500	6	9	I
N136-1.5		12	9	
N135-2.2	2200	2	4	–
N136-2.2		4	3	
N135-3	3000	1	4	II
N136-3		2	3	
N135-6	6000	0.16	2	VII
N136-6		0.2	1.5	

The container looks like a miniature glass whose axis is perpendicular to that of the loop.

Extensive testing under load of sample vibrators with such glass-shaped dampers showed that their life is practically unlimited and that the stability of their characteristics is not inferior to normal vibrators.

If the glass-shaped dampers are made entirely of a nonmagnetic material, the magnetic flux and hence the sensitivity of the vibrators is slightly reduced owing to the holes made for the dampers in the poles. In vibrators with an operating length less than 20 mm, the sensitivity is decreased by 20% and more. For such vibrators, it is advisable to make glass-shaped dampers with soft iron segments which fill the cut-outs in the poles (Fig. 2).

Experiments have shown that the concentration of the damping liquid in limited volumes along the loop may produce various irregularities in the frequency characteristic. Figure 3, a shows an amplitude-frequency characteristic and an oscillogram of switching on a direct current through a normal loop oscillograph; the curves approach the theoretical shapes for systems with one degree of freedom. Figure 3, b shows a distorted characteristic of a vibrator with concentrated damping.

Distortions of the characteristic are very undesirable, especially for general purpose vibrators used in a universal oscillograph, since this makes the interpretation of oscillograms and the use of corrections more difficult. It was established that it is possible to choose the number and position of dampers so as to practically eliminate the distortions.

Figure 3, c shows a characteristic of a vibrator with concentrated damping and an optimum positioning of dampers, whose shape coincides with that of a normal vibrator.

The attached table shows the basic parameters of two series of loop vibrators with concentrated damping, types N135 and N136, whose production is being undertaken by the "Vibrator" plant.

The N135 vibrators are designed to work with type MPO2 oscillographs. Vibrators N136 have a larger magnet and are designed for new types of oscillographs.

Comparative sensitivities of various loop vibrators are shown in Fig. 4. The effective frequency range in which the sensitivity does not differ from that at a direct current by more than 5% is plotted along the X-axis; and the ratio of the sensitivity of vibrators of a given type to that of type MOV2 vibrators equivalent to them in their effective frequency range is plotted along the Y-axis. It will be seen from the diagram that the vibrators with concentrated damping are much more sensitive than both home-manufactured and the best foreign-made loop vibrators.

Moreover, vibrators with concentrated damping have a four times greater permissible deflection at frequencies above 3,000 cps as compared with loop vibrators of other types.

HIGH AND ULTRAHIGH FREQUENCY MEASUREMENTS

A STANDARD PULSE-SERIES GENERATOR FOR CHECKING DISCRETE-OPERATION COMPUTERS IN MEASURING INSTRUMENTS

G. L. Grin and M. A. Zemel'man

The wide application of discrete-operation electronic and electromechanical devices in various spheres of measurement and automatic control has raised the problem of testing their accuracy. In addition to the general requirements peculiar to measuring instruments, these devices should be checked for speed of operation, reliability of their computer circuits, and the effect of the input pulse parameters (amplitude, duration and steepness of edges) on the operation of the devices.

It is essential to determine the reliability of operation, or accuracy of the computer readings. Usually the indications of the electronic computers are taken to be correct. When, however, the operating limits of the computer are approached with respect to the repetition frequency, shape of the incoming pulses, or other parameters (aging of tubes, etc.), mistakes in their work are possible. In particular, missing of counts is possible as well as self-operation of trigger units, i.e., "extra" counts. These irregular operations cannot always be detected by inspection.

A study of the technical characteristics of existing discrete-action instruments has shown that for checking the greater part of them, it is advisable to have a device which would produce a given number of pulses of different polarities with controllable repetition frequency, duration, and amplitude. On the basis of industrial measuring instruments of discrete action which use digital computers (operating with electromechanical, gas discharge or electronic elements) with a top frequency limit of 20-30 kc, the laboratory of electronic instruments of the All-Union Scientific Research Institute of the Committee of Standards, Measures, and Measuring Instruments developed and produced a model of a standard pulse-train generator. This instrument produces a definite number of pulses set by the operator with different polarities, durations, amplitudes, and repetition frequencies.

The standard pulse-train generator (SPSG) is a photoelectronic device with a revolving disc, and it consists of three separate units (Fig. 1): an opticoelectromechanical unit, an electronic unit and a unit setting the number of pulse series.

The opticoelectromechanical unit, which serves to convert light into electrical pulses, consists of motor 1, with disc 2, two illuminators 3, and two photoelectric stages 4. The circumference of a disc fixed to the axle of the motor (Fig. 2) contains closely spaced, narrow, rectangular holes (channel I), and closer to the center of the disc, one hole (channel II). In front of the disc there are two incandescent lamps with focusing lenses. When the disc is rotated, light pulses corresponding to the passing of the light through both sets of holes are fed to the photoelectric elements. When the disc is turned through one revolution, the first channel receives a series of pulses corresponding to the number of holes placed along the circumference of the larger radius, and the second channel receives one pulse. Thus, the number of pulses passing through the second channel is equal to the number of revolutions of the disc. The speed of the disc rotation determines the frequency of pulses entering either channel.

The electronic control unit is also divided into two channels. Channel II of this unit serves to shape the low repetition frequency pulses and consists of a level trigger 5, for transforming the bell-shaped pulses of the

photoelectric cell into rectangular pulses, a biased blocking oscillator 6, for tripping the next stage, kipp oscillator 7, and a trigger for controlling gate 8. The gate consists of a tube stage which either blocks or transmits the operating signal, depending on the control signal it receives. The kipp oscillator generates negative pulses controlling the operation of unit 9 which sets the number of pulse series. Channel I consists of similar shaping elements. The last tube (7) of channel I also serves as a gate. The control grid of this tube is fed with a blocking or operative dc voltage from the output of the gate control trigger, whose input receives pulses from the unit setting the number of pulse series. Negative output pulses of controlled duration and amplitude are taken off the anode load of the first channel kipp oscillator 7 output tube. Positive output pulses of controlled duration and amplitude are taken off the anode load of the next tube which operates as a phase inverter.

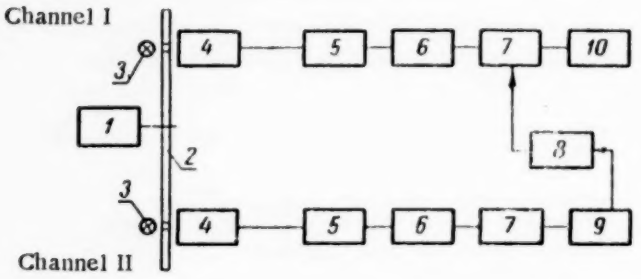

Fig. 1

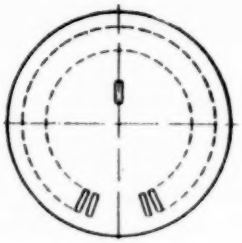

Fig. 2

The setter of the number of pulse series consists of an electronic computer. Its input is fed from the output of the second channel electronic control unit. The number of pulse series fed to the output of channel I is determined by the conversion factor of the setting circuit.

Supplies for the electronic circuit of the device can be obtained from any mass-produced stabilized power pack (for instance type UIP-1).

Before testing a computer 10 (Fig. 1), the disc is made to revolve at the required speed. The clearing switch of the setter of the number of pulse series is then in position "Cleared," channel I gate is closed and the computer under test does not receive any signals. Next the clearing switch is thrown to the operating position. When the disc revolves a number of times equal to the conversion factor to which the setter is adjusted, the gate will receive a clearing signal and pulse series will be transmitted to the output of channel I. The number of pulse series which are fed to the computer under test is equal to the conversion coefficient to which the setter of the number of pulse series is adjusted. As soon as the set number of series has been registered, the gate will close again and the computer under test will stop receiving pulses. Next, the clearing switch should be again thrown to the "cleared" position and the reading of the computer under test compared with a number equal to the number of transmitted series multiplied by the number of holes in the disc.

In order to avoid the possibility of losing pulses or the appearance of "extra" pulses at the output of channel I due to the delay in transmitting pulses through channel II and the operating time of channel I gate, the closely spaced holes are not placed round the entire circumference of the larger radius, but over an arc of approximately 345°. The pulse from the single hole placed nearer to the center appears during the interval between the series of closely spaced pulses.

The SPSG parameters are chosen to provide pulses between 1 and 30 μsec duration and an amplitude of 80 v. The disc is of 250 mm in diameter and it has 300 closely spaced holes, which at its maximum speed of 6000 rpm corresponds to a frequency of 30,000 cps. A binary computer is used as the setter of the number of pulse series. Its conversion factor can be set on the binary scale from 1 to 128.

A large rise in the pulse repetition frequency is difficult to achieve by this means (for instance a threefold rise in the frequency). For checking extremely high-speed computers other probably purely electronic devices will have to be used.

The number of pulses transmitted by the SPSG depends both on the number of holes in the disc and the correct operation of the electronic circuit,especially the setter of the number of pulse series.

The operation of the latter is checked by means of the SPSG itself. For this purpose the setter of the number of series is connected to the output of channel 1 instead of the computer under test. Its operation is checked by the method described above, by means of visual counting of the number of turns of the disc (at speeds up to 1 rps). The final checking of the SPSG is done by taking oscillograms of the output signal at frequencies up to 10,000 pps and then counting the number of pulses on the oscillogram. The accuracy of operation of the SPSG at frequencies between 10,000 and 30,000 pps is determined by oscillograms of the processes in various units of the set taken on a cathode-ray oscilloscope.

The SPSG was used as a standard for checking, during State inspection, computer BK-3 and other electronic computers.

Technician S. A. Zhubenko took part in the work.

IMPEDANCE MEASUREMENTS BY MEANS OF DIRECTIONAL COUPLERS

A. I. Zykov

Measurement method. Directional couplers with a matched load in one of the arms of a secondary waveguide are widely used in the microwave range for finding the reflection factor modulus ρ in the main waveguide by the ratio of the signal amplitudes in the opposite arms of the coupler [1, 2]. With this method, it is impossible to measure the phase of reflection and difficult to measure small values of ρ, since the sensitivity of the elements varies usually according to the square law. Hence, the ratio of the signal amplitudes is equal to ρ^2 and with small values of ρ an indicator with a wide dynamic measuring range is required.

The study of a directional coupler with a reflecting plunger in a loaded waveguide shows that this arrangement is free of above defects.

The wave propagated toward the indicator in the coupler secondary waveguide with a short-circuit (Fig. 1) can be represented in relative units as follows:

$$\vec{E}=\frac{\vec{\tau}_1\left(1-\vec{\rho}e^{-j2\beta l}\right)+\vec{\tau}_2\left(\vec{\rho}-e^{-j2\beta l}\right)}{1+\vec{\rho}_u e^{-j2\beta l}}. \qquad (1)$$

where $\vec{\tau}_1=\tau_1 e^{-j\varphi_1}$ is the propagation constant of the coupler in the forward direction;

$\vec{\tau}_2=\tau_2 e^{-j\varphi_2}$ is the propagation constant of the coupler in the reverse direction;

$\vec{\rho}=\rho e^{-j\varphi}$ is the reflection factor in the main waveguide;

$\rho_u=\rho_u e^{-j\varphi_u}$ is the reflection factor in the main indicator;

$\beta=\frac{2\pi}{\lambda_{\partial_2}}$, λ_{∂_2} is the wavelength in the secondary waveguide; and

l is the distance from the short circuit plane to the coupler border plane.

If the coupler has an ideal directivity ($\vec{\tau}_2=0$) and the indicator is matched ($\vec{\rho}_u=0$), we shall obtain the expression:

$$E^2=\tau_1^2\left[1-2\rho\cos\left(2\beta l+\varphi\right)+\rho^2\right]. \qquad (2)$$

It follows from (2) that the ratio of the maximum and minimum readings of the indicator, measured by displacing the reflecting plunger, is equal to $\frac{1+\rho}{1-\rho}$, i.e., it is equal to the standing-wave ratio in the main waveguide. Thus, the range of standing-wave ratios nearest to 1, the most important range for matching, becomes more readily attainable with a short-circuited coupler.

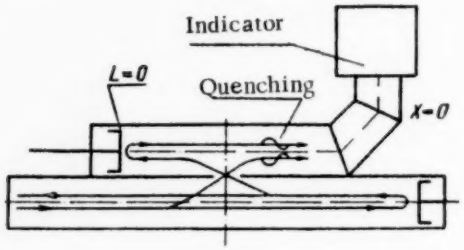

Fig. 1

For instance, if for the measurement of ρ a coupler with a matched load in the secondary waveguide is used, then with a standing wave ratio = 1.04, it would be necessary to measure signals with a ratio of $\frac{4}{10{,}000}$. If, on the other hand, a directional coupler with a reflecting plunger is used, it will be necessary to measure a ratio of $(1.04)^2 = 1.08$, which can be measured with greater accuracy. It is also possible to measure with a short-circuited directional coupler the phase of the reflected wave with respect to the chosen basic plane in the main waveguide. Let plane X = 0 in Fig. 2 be taken as the origin of reckoning and let plane L = 0 correspond to it in the coupler waveguide. When the plungers are placed in these planes the indicator reading is zero. The displacement of the plunger in the coupler waveguide with respect to plane L = 0, for obtaining a minimum reading of the indicator at a load of the main waveguide with a reflection $\vec{\rho} = \rho e^{-j\varphi}$, and the displacement of the minimum electric field in the main waveguide with respect to plane X = 0 are related by the expression:

$$\Delta X = \frac{\lambda_{\partial_1}}{\lambda_{\partial_2}} \Delta L, \tag{3}$$

where λ_{∂_1} is the wavelength in the main waveguide; and

λ_{∂_2} is the wavelength in the coupler waveguide.

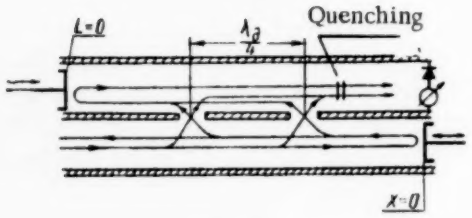

Fig. 2

The short-circuited directional coupler has the advantage over an ordinary measurement line in eliminating the errors due to the irregular insertion of the probe along the line, and in being insensitive to small reflecting plunger misalignments, which do not alter the reflections caused by the plunger.

Measurement errors. Since actual couplers have a finite directivity ($\vec{\tau}_2 \neq 0$) and the matching of indicators may not be perfect ($\vec{\rho}_u \neq 0$), errors may occur in the measurement of impedances, and these errors can be evaluated from (1).

From (1) we obtain:

$$E^2 = \frac{K - 2(B\cos 2\beta l - C\sin 2\beta l)}{1 + 2\rho_u \cos(2\beta l + \varphi_u) + \rho_u^2}. \tag{4}$$

where

$$\begin{aligned} K &= 1 + \rho^2 + A^2 + \rho^2 A^2 + 4\rho A \cos\varphi \cos\alpha, \\ B &= \rho(1 + A^2)\cos\varphi + A(1 + \rho^2)\cos\alpha, \\ C &= \rho(1 - A^2)\sin\varphi + A(1 - \rho^2)\sin\alpha, \end{aligned} \tag{5}$$

$$A = \frac{\tau_2}{\tau_1},$$

$$\alpha = \varphi_2 - \varphi_1.$$

By equating to zero the derivative $\frac{d}{dl}[E^2]$ we obtain an expression for determining the extreme values of l_{ext}:

$$M \sin 2\beta l_{ext} + N \cos 2\beta l_{ext} = D, \tag{6}$$

where

$$\begin{aligned} M &= B(1+\rho_u^2) + K\rho_u \cos\varphi_u, \\ N &= C(1+\rho_u^2) + K\rho_u \sin\varphi_u, \\ D &= 2\rho_u (B \sin\varphi_u - C\cos\varphi_u). \end{aligned} \tag{7}$$

From (6), we find:

$$\begin{aligned} \cos 2\beta l_{max} &= \frac{ND - M\sqrt{M^2+N^2-D^2}}{M^2+N^2}, \\ \cos 2\beta l_{min} &= \frac{ND + M\sqrt{M^2+N^2-D^2}}{M^2+N^2}, \\ \sin 2\beta l_{max} &= \frac{MD + N\sqrt{M^2+N^2-D^2}}{M^2+N^2}, \\ \sin 2\beta l_{min} &= \frac{MD - N\sqrt{M^2+N^2-D^2}}{M^2+N^2}. \end{aligned} \tag{8}$$

By substituting (8) in (4), we obtain an expression for the square of the maximum to the minimum amplitude ratio of the signals fed to the indicator:

$$\left(\frac{E_{max}}{E_{min}}\right)^2 = \frac{1+\frac{2(BM+CN)}{K\sqrt{M^2+N^2-D^2}} \cdot \frac{1+\frac{2\rho_u}{(1+\rho_u^2)} \cdot \frac{M\cos\varphi_u + N\sin\varphi_u}{\sqrt{M^2+N^2-D^2}}}{1-\frac{2(BM+CN)}{K\sqrt{M^2+N^2-D^2}} \cdot \frac{1-\frac{2\rho_u}{(1+\rho_u^2)} \cdot \frac{M\cos\varphi_u + N\sin\varphi_u}{\sqrt{M^2+N^2-D^2}}}{}}. \tag{9}$$

In a general case when $\rho_u \neq 0$ and $A \neq 0$, expression (9) is cumbersome and difficult to inspect. It is, however, possible to obtain from it an expression for the maximum error in measuring the standing-wave ratio when $\varphi = \alpha = \varphi_u = 0$. Then:

$$\frac{E_{max}}{E_{min}} = \frac{1+\rho}{1-\rho} \cdot \frac{1+A}{1-A} \cdot \frac{1+\rho_u}{1-\rho_u} = KK_{cpl}K_u,$$

where k is the standing-wave ratio in the main waveguide;

k_u is the standing-wave ratio at the indicator; and

k_{cpl} is the standing-wave ratio due to the finite directivity of the coupler and measured with a matched load in the main waveguide and with a matched indicator.

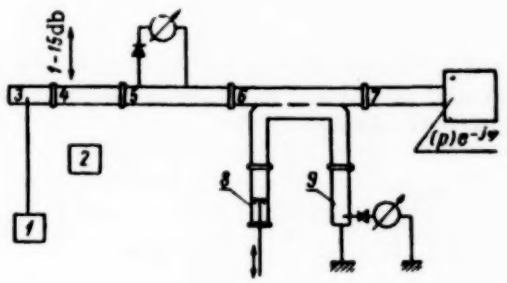

Fig. 3

The maximum possible error in measuring the standing-wave ratio in the main waveguide is:

$$\delta K_{max} = \left(\frac{KK_{cpl}K_u - K}{K}\right) \cdot 100\% = (K_{cpl}K_u - 1) \cdot 100\%. \tag{10}$$

It should be pointed out that the maximum error of a directional coupler with a reflecting plunger is equal to the one with an absorbing load if the mismatching of the indicator and load are the same.

In fact, the maximum error in determining the standing-wave ratio when measuring the ratio of signal amplitudes in opposite arms of the coupler is:

$$\delta\kappa_{max}=\left[\frac{1+\frac{\rho\tau_1+\tau_2+\rho_N(\tau_1+\rho\tau_2)}{\tau_1+\rho\tau_2+\rho_N(\rho\tau_1+\tau_2)}\cdot\frac{1-\rho}{1+\rho}-1}{1-\frac{\rho\tau_1+\tau_2+\rho_N(\tau_1+\rho\tau_2)}{\tau_1+\rho\tau_2+\rho_N(\rho\tau_1+\tau_2)}}\right]\cdot 100\%= \tag{11}$$

$$=\left(\frac{1+A}{1-A}\cdot\frac{1+\rho_N}{1-\rho_N}-1\right)\cdot 100\%=(\kappa_{cpl}\,\kappa_N-1)\cdot 100\%,$$

i.e., it coincides with (10) when $k_u = k_H$. Thus, with respect to the value of the error when measuring the standing-wave ratio both methods are equally good.

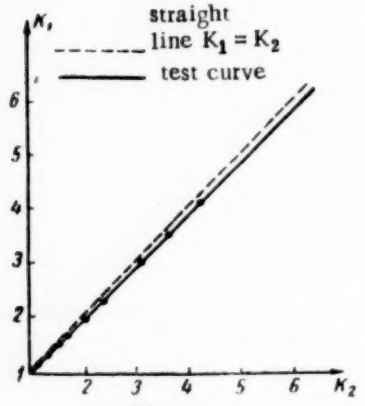

Fig. 4

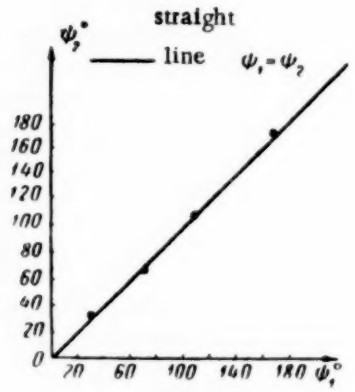

Fig. 5

From (8), we obtain:

$$2\beta\,(l_{min}-l_{max})=\arccos\left[\frac{2D^2}{M^2+N^2}-1\right], \tag{12}$$

from this it follows that if the indicator is mismatched, the distance between the extremal positions of the short circuiting device will not be equal to quarter of a wavelength. This phenomenon can be utilized for checking the matching of the indicator during measurements.

In the case of a narrow-band indicator, an improvement can be obtained by using a decoupling attenuator, as the power fed to the indicator is considerably higher than in the case of reflected power measurements. With $\rho_u = 0$, the error in measuring the reflected phase is determined by the expression:

$$\delta\varphi=\left(\frac{\arccos\left\{\frac{\rho(1+A^2)\cos\varphi+A(1+\rho^2)\cos\alpha}{\sqrt{[1+2A\rho\cos(\varphi+\alpha)+A^2\rho^2]\cdot[\rho^2+2A\rho\cos(\varphi-\alpha)+A^2]}}\right\}}{\varphi}-1\right)\cdot 100\% \tag{13}$$

When $A \ll \rho$

$$\delta\varphi_{max}\sim\left\{\frac{\arccos\left[\left(1+\frac{A}{\rho}\right)\cos\varphi+\frac{A}{\rho}\right]}{\varphi}-1\right\}\cdot 100\%. \tag{14}$$

Test results. The schematic of comparative impedance measurements by means of a directional short-circuited coupler and a measurement line IVL-1 are shown in Fig. 3.

The directivity of the coupler with $\lambda_0 = 10.7$ cm was equal to 40 db. Measurements were made under continuous operating conditions.

Figures 4 and 5 show the relations between $k_0 = f(k_u)$ and $\varphi_0 = f(\varphi_u)$, where k_0 and φ_0 are respectively the standing-wave ratio and the reflected phase found by means of a short-circuited directional coupler, and k_u and φ_u are the same quantities found by means of a measurement line. The standing-wave ratio of the indicator was equal to 1.02. The difference between k_0 and k_u did not exceed 3%. The phase-measurement error was still smaller.

LITERATURE CITED

[1] R. A. Valitov and V. N. Sretenskii, Radio Measurements at Super-High Frequencies [In Russian] (Moscow, 1951).

[2] D. Sausvort, The Principles and Application of Waveguide Transmission [In Russian translation from English] ("Soviet Radio" Press, Moscow, 1955).

CALCULATION OF ERRORS IN COMPARING FREQUENCIES BY MEANS OF LISSAJOUS FIGURES

M. I. Shatalov

Lissajous figures are widely used for comparing frequencies in radio measurements and in particular in the checking technique. The application of Lissajous figures can be reduced to the following two fundamental cases:

for tuning oscillators to a frequency which bears a definite relation to another frequency used as a standard;

for determining errors in a frequency compared with a standard frequency, when the ratio of the frequencies is not an exact integer.

In the first instance, when the problem is reduced to obtaining a stationary Lissajous figure characteristic for the given frequency ratio, usually no difficulties arise, since the frequency relation is fairly simply determined by known methods [1] even with complicated figures.

In the second instance, the error is determined accurately only with the simplest frequency ratio of 1/1. The error for this frequency ratio is determined by the quotient of the number of complete cycles in the changes of the figure shape ("revolutions of the figure") $\underline{k}$ over the time $\underline{t}$ during which the number of cycles was counted, i.e.:

$$\Delta f = \frac{k}{t} \text{ cps} \qquad (1)$$

Experience has shown that with more complicated frequency ratios difficulties often arise and errors are committed when determining the frequencies. One of the reasons for these difficulties and errors is the inaccuracies committed in textbooks on radio measurements [2, 3] when dealing with Lissajous figures.

Lissajous figures for the most common frequency ratios are given in this article. The instantaneous values of the lower frequencies are plotted along the X-axis and of the higher frequencies along the Y-axis. All the figures are plotted for the case when the phase of the second frequency is leading the first. The phase difference

Lissajous Figures for the Most Common Frequency Ratios

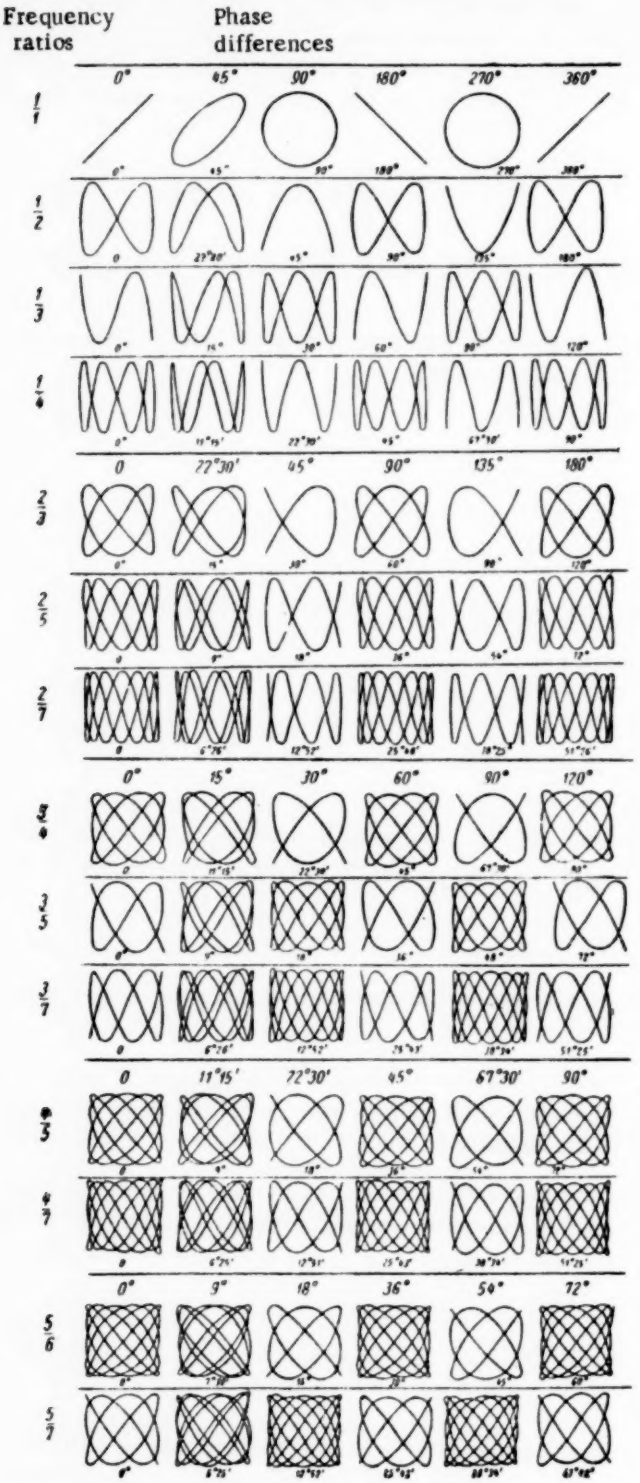

corresponding to each figure is expressed in fractions of a period (degrees) of the higher frequency and is shown for each group of figures. Below each figure the absolute value of the phase difference is shown in fractions of a period (degrees) of the lower frequency.

Henceforth, any frequency ratio will be shown by a fraction of the form of $\frac{m}{n}$, where m and n are mutually prime integers of a series starting with unity. With this notation ratio $\frac{1}{n}$ will be a particular case when m = 1, in relation $\frac{1}{1}$, therefore, m = n = 1.

The figure-changing cycle at any frequency ratio occurs when the phase (φ) of the voltage, whose frequency is proportional to m, changes by an angle equal to:

$$\varphi_m = \frac{360^\circ}{n} \tag{2}$$

And for the second frequency, we have the relationship

$$\varphi_n = \frac{360^\circ}{m} \tag{3}$$

Hence, the phase shift of a voltage, whose frequency is proportional to m, by 360° corresponds to n cycles of figure shape changes and a 360° phase shift of the second frequency (proportional to n) corresponds to m cycles of figure shape changes.

From the above, it is possible to find a general expression for the frequency error at any frequency ratio $\frac{m}{n}$. If the frequency proportional to n is the standard frequency, the quotient of the number of cycles of figure changes over time (sec) must also be divided by n, i.e. (1) takes the form:

$$\Delta f_m = \frac{k}{tn} \text{ cps} \tag{4}$$

For the case when the frequency proportional to m is taken as the standard expression (1) takes the form:

$$\Delta f_n = \frac{k}{tm} \text{ cps} \tag{5}$$

As an example, let us take the case when the Lissajous figures are used at a frequency ratio of 2/3 for determining the error of a frequency which is approximately equal to 66 cps, measured against a standard frequency of 100 cps.

If $\frac{k}{t}$ = 1 rps, the error $\Delta f_{66} = 0.33$ cps.

If the same frequency ratio is used for determining the frequency error at about 150 cps against a standard frequency of 100 cps, the error for the same value of $\frac{k}{t}$ = 1 rps will be: $\Delta f_{150} = 0.5$ cps.

For the beginning of the reckoning of figure changes, the simplest characteristic figures corresponding to the given frequency ratio are usually used. These figures correspond to a phase shift expressed in terms of fractions of a period (degrees) of the higher frequency equal to 0° or $\frac{360^\circ}{2m}$, if m and n are both odd numbers and $\frac{360^\circ}{4m}$ or $\frac{3 \cdot 360^\circ}{4m}$, if either m or n is an even number.

LITERATURE CITED

[1] G. A. Remez, Textbook of Fundamental Radio-Technical Measurements [In Russian] (1955).

[2] Terman and Pettit, Measurement Technique in Electronics [In Russian translated from English] (Foreign Literature Press, 1955).

[3] A. Hund, High-Frequency Measurements, (Mc Graw-Hill, 1951).

A V. T. VOLTMETER FOR A RADIO-NOISE MEASURING DEVICE WITH INTERNATIONALLY RECOMMENDED PARAMETERS

I. M. Furmanov

In measuring radio noise, reactive quasi-amplitude detectors are used. Owing to the high resistance of the detector load, (of the order of 6-12 meg) it is practically impossible to measure the voltage across it directly by means of an indicating instrument. Hence, the voltage across the detector is measured in noise measuring instruments by means of a tube voltmeter. Typical Soviet made noise measuring sets use in their tube voltmeter (dc amplifier) circuits tubes with an extended characteristic (of the variable μ type), which provide a nonlinear, so-called semilogarithmic, scale on the output-indicating instrument [1]. Foreign noise-measuring instruments mostly use automatic gain control (AGC). Our sets do not use AGC because it introduces distortion when pulse interference is measured. The requirements of the Special International Committee for Radio Interference (CISPR) with respect to the linearity of the high-frequency channel preceding the detector exclude the use of AGC in measuring interference [2].

The basic characteristic of a CISPR tube voltmeter consists in obtaining an overload point of the dc amplifier, connected between the detector and the indicating instrument, 12 db above the voltage level of the full scale indicating instrument reading with a deviation from ideal linearity of no more than 1 db. The requirements of linearity and a margin of overloading in the tube voltmeter are due to the necessity for measuring low pulse repetition frequency interference. With accepted values for time constants of the interference measuring detector (for charging — 1 μsec, and for discharging — 160 μsec) the rectified voltage fed to the tube voltmeter will vary within large limits. A tube voltmeter with a moving coil instrument and the time constants quoted above will provide readings corresponding to a certain fraction (down to $-$ 12 db) of the peak voltage value. Hence, when measuring a low repetition frequency pulse interference which causes a full deflection of the indicating instrument, a peak voltage exceeding that read on the instrument by about 12 db will be impressed on the input of the tube voltmeter. For a correct measurement of radio noise, it is therefore necessary to provide an overload margin of 12 db. The linearity requirement of the tube voltmeter excludes the use of nonlinear tubes in it so as to obtain a nonlinear scale of the indicating instrument. It is true that the decisions of the Brussels Conference of the CISPR (1956) note that the use of an indicating instrument with a nonlinear scale is permissible, if the technical requirements are preserved [3]. The use of an indicating instrument with a nonlinear characteristic would provide a semilogarithmic scale for the instrument. This method, however, appears inadmissible to us, especially if it is considered that in this case all the indicating instruments would have to be made with identical characteristics which would involve considerable technical difficulties. Thus, for the fulfilment of the CISPR requirements, it is necessary to produce a linear tube voltmeter with a linear indicating instrument.

Other requirements of a CISPR voltmeter are the critical damping of the indicating instrument and its mechanical time constant which should be equal to 160 μsec. This requirement is due to the discharge time constant of the CIPS detector circuit being taken as 160 μsec, which the mechanical time constant of the

indicating instrument must not affect to any considerable extent. It is, in practice, very difficult to make an indicating instrument with a smaller time constant. In Soviet noise measuring sets whose discharge constant of the detector circuit is 600 μsec, the mechanical time constant of the indicating instrument must lie between 200-400 μsec [4].

It is known that for a critically damped instrument the equation of its moving system can be the following:

$$T^2\frac{d^2\alpha}{dt^2} + 2T\frac{d\alpha}{dt} + \alpha = k, \tag{1}$$

where α is the deflection of the moving system of the instrument;

$T = \frac{j}{A}$;

j is the polar moment of inertia;

A is the coefficient of friction;

k is the coefficient of sensitivity; and

i is the current flowing in the instrument.

If at rest, the current through the instrument is $i = I$, Eq. (1) will take the form:

$$\alpha = kI\left[1 - \left(1 - \frac{t}{T}\right)e^{\frac{t}{T}}\right]. \tag{2}$$

Quantity T has the dimensions of time and assumes the value of the mechanical time constant.

It is possible to deduce from (2) a practical method of determining the mechanical time constant of the instrument. It is equal to the duration of a rectangular pulse (of a constant amplitude) which causes a deflection of the instrument 35% of that produced by a direct current of the same amplitude as the rectangular pulse. The damping of the indicating instrument is in practice adjusted so that the overshoot of the pointer does not exceed 5% of the steady state value.

The value of the internal noise of the measuring set changes greatly with the frequency to which it is tuned. The set is calibrated by a sinusoidal unmodulated signal. It can be considered with sufficient accuracy that the internal noises add to the signal in quadrature. Hence, the increments to the rectified voltage across the detector load with a signal of the same value but with different internal noise will differ:

$$U_{ad} = 1.41k\left(\sqrt{U_c^2 + U_n^2} - U_n\right), \tag{3}$$

where U_{ad} is the voltage increment across the detector load due to an input signal;

U_c is the signal voltage;

U_n is the internal noise of the set referred to its input; and

k is the total gain of the set from the detector input.

Thus, addition in quadrature of the signal to the internal noise can lead to a considerable error in the reading of the indicating instrument depending on the frequency of measurement.

Internal noises of the set are not specified by the CISPR. Neither is the signal-to-noise ratio given. The CISPR requirements limit the "noise background" of the receiver by stating that it must not introduce an error of measurement exceeding 1 db. With a linear tube voltmeter and a linear indicating instrument the requirements of a limitation of the "noise background" reduce mathematically to the equation:

$$k\sqrt{U_n^2 + U_c^2} < \frac{k}{3.16}\sqrt{U_n^2 + (3.16 \cdot 1.12U_c)^2}, \tag{4}$$

where

U_n is the voltage of the internal noise of the set referred to its input with a normal gain at the intermediate frequency;

U_c is the input signal voltage at which a decrease of the intermediate frequency gain by 10 db with a simultaneous equivalent increase in the input signal will produce an error of 1 db in the indicator reading; and

k is the normal set gain from the detector input.

The solution of this equation provides the permissible signal-to-noise ratio:

$$\frac{U_c}{U_n} > 1.86. \tag{5}$$

It is obvious that (5), in conjunction with other factors (in the main, the variations of the detector circuit time constant when detecting small voltages) will determine the maximum sensitivity of the measuring set.

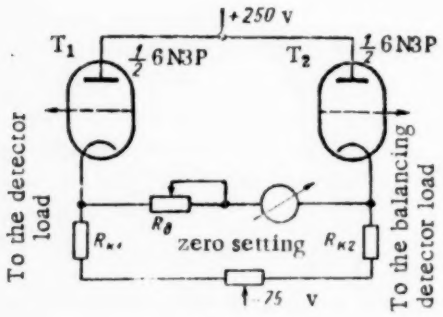

Fig. 1

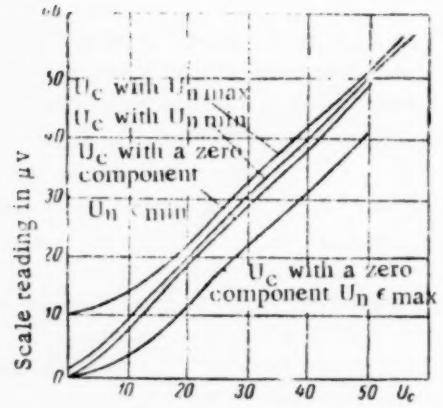

Fig. 2

In order to decrease the effect of internal noise on the set readings, it is advisable to set the zero in the absence of noise, for which purpose, it is possible, for instance, to lower the intermediate gain during the zero setting. The set will read the quadrature sum of the signal and the internal noise. With this adjustment, the indicating instrument will, in the absence of a signal, read the internal noise of the set. With a signal 5.4 db (1.86 times) higher than the internal noise, i.e., with a signal corresponding to the nominal sensitivity of the set from the point of view of limiting the "background noise", the error of the indicating instrument will not exceed 1 db, which meets the technical requirements of the CISPR. This method of measurement does not exclude the possibility of measuring weaker signals with a greater error as is the case with typical Soviet-made instruments. For this purpose, it is only necessary to set the zero of the tube voltmeter with the presence of internal noise.

In the balanced CISPR tube voltmeter (Fig. 1) the rectified voltage from the detector is fed to the control grid of tube T_1. Tube T_2 is used for balancing, and it receives its voltage from a balance diode. The balance tube provides zero stability of the voltmeter. A type M-24 200 μamp microammeter is used as an indicating instrument. Shunting of the instrument movement provides an almost critical damping. The full scale deflection is 500 μamp.

In the absence of a signal or internal noise, the tube voltmeter will only receive the diode contact voltage. By means of the "zero setting" potentiometer the set is adjusted to zero. When the signal voltage appears at the input of the tube voltmeter the internal resistance of tube T_1 is changed, the bridge is unbalanced, and the indicating instrument connected in the bridge diagonal reads a current which is a function of the input voltage.

It is known that the current in the indicating instrument of a bridge circuit is determined by equation [5]:

$$I_g = \frac{R_{i1}R_{k2} - R_{i2}R_{k1}}{R_g(R_{i1} + R_{i2})(R_{k1} + R_{k2}) + R_{i1}R_{k1}(R_{i2} + R_{k2}) + R_{i2}R_{k2}(R_{i1} + R_{k1})}, \tag{6}$$

where R_1 and R_2 are the internal dc resistances of the tubes;

R_{k1} and R_{k2} are the corresponding cathode loads; and

R_g is the resistance in the instrument circuit.

By means of the analytical-graphical method, it is possible to easily analyze this circuit. Figure 2 shows the relations between the readings of a linear tube voltmeter and the input signal with varying internal noise in the set with and without zero compensations of the indicating instrument in the presence of internal noise. In these calculations, the minimum internal noise referred to the input was taken as 1.9 μv and the maximum noise as 10.55 μv, the indicating instrument's full scale reading corresponds to a voltage of 50 μv at the input; the total gain of the set from the input to detector was taken to be $7.1 \cdot 10^4$. The assumed value of internal noise of the set is determined by the characteristic of its input circuits. It will be seen from Fig. 2 that with the assumed maximum internal noise of the set (curve U_c at $U_{n\,max}$) the minimum measurable voltage from the point of view of the "background noise" is 20 μv. In the absence of an input signal the indicating instrument reads the internal noise voltage of the set. When it is necessary to measure voltages smaller than those due to internal noise of the set, it is possible to compensate for the noise of the tube voltmeter (curve U_c with zero compensation, $U_n \epsilon_{max}$). With this adjustment, however, the indicating instrument reading error rises rapidly both when measuring small and large signal voltages.

LITERATURE CITED

[1] I. A. Fastovskii and I. M. Furmanov, Conventional Instruments for Measuring Radio Noise [In Russian] (Sudpromgiz, 1958).

[2] International Electrotechnical Commission, CISPR, 302, Draft Specification for a CISPR Radio Interference Measuring Apparatus for the Frequency Range of 0.15 Mc to 30 Mc (January, 1958).

[3] International Electrotechnical Commission, CISPR, Report of the Plenary Session Held in Brussels on July 24-27, 1956.

[4] Permissible Limiting Values of Industrial Interference [In Russian] (Svyaz'izdat, Moscow, 1954).

[5] A. D. Nesterenko, Basic Calculation of Balanced Electrical Measuring Circuits [In Russian] (Acad. Sci. UkSSR Press, Kiev, 1954).

APPLICATION OF HIGH PRECISION 44-I WAVEMETERS

V. Ya. Volodarskii

Instrument 44-I is a wavemeter of high precision in the three-centimeter wave range (frequency range of 8,900-10,000 Mc) with the measurement of frequency made on the tenth harmonic of a decimeter oscillator.

The circuit and the construction of the instrument provide for its application over a wider range of 100 to 10,000 Mc, working on harmonics both of the signal and the decimeter oscillator.

Since for frequencies below 8,900 Mc the waveguide of the 44-I instrument is working at its limit and introducing large attenuation, the measured signal should be fed directly to the mixer, for which purpose it is advisable to insert into the waveguide an insulated wire long enough to touch the crystal detector. Tests have shown that the sensitivity of the wavemeter over the whole range is of the order of 100 μw.

Frequencies in the 100 to 10,000 Mc range are measured in the normal way. In order to determine which harmonics of the signal and the decimeter oscillator are producing beats, it is necessary to know in advance the approximate value of the frequency to be measured. This can be done by means of a resonance wavemeter of an appropriate range.

RADIATION MEASUREMENTS

ASSAYING RADIUM PREPARATIONS FOR RADIUM CONTENT

G. V. Gorshkov, F. M. Karavaev, and N. S. Shimanskaya

The amount of radium in a preparation is not usually assayed by direct weighing, since the radium is seldom sufficiently free from barium and other impurities. Many extra recrystallizations are needed to get preparations containing less than 0.2% impurity. Various indirect methods, especially ionization ones, are used to assay the preparations. The gamma-ray fluxes from the preparation and from a standard containing a known weight of radium are compared in terms of their ionization effects, which are measured (usually) with an ionization chamber. The measurements made at the All-Union Metrology Research Institute employ two State Standards, X and XI, whose radium contents (for 1957) are taken as 29.37 and 14.27 mg. These measurements give us not the amount of radium in the source, but the equivalent of that amount in gamma-ray terms, i.e., the amount of radium that would under those conditions give the same gamma-ray flux as the preparation [1]. This gamma-equivalent makes no allowance for self-absorption in the source.

In such measurements, we have always to bear in mind the errors that may arise from differences between the absorption in the preparation and that in the standard. These errors can be reduced if filtered gamma-rays are used. A spherical ionization chamber with lead walls 2 cm thick is used at the Institute. These walls absorb the soft gamma-rays from Ra (B + C) almost completely, so only the hard gamma-rays are effective; these rays are absorbed very little by the glass ampules and by the radium itself. Differences between the thicknesses of the ampules, or in the amount of self-absorption in the salt, have less effect on the result than is usual in routine laboratory measurements, in which the filter is 5 mm of lead and the walls of the chamber are thin. Under the latter conditions, the error in the result may be large unless corrections are made for the differences in the absorption of the gamma-rays from Ra.

We have established how accurate the ionization methods in current use are for standard radium preparations. For this purpose, we have used three pure samples meant for calorimetric measurements on the half-life of Ra^{226} [2]. These were recrystallized. Spectral analysis showed that none of them had more than 0.2% impurity by weight. The weight data on the $RaBr_2$ in these samples (with allowance for the spectral analyses) are given in the table.

Preparation	Wt. of salt P (mg)	Wt. of Ra, p (mg)	Gamma equivalent (mg-eq.)			$\frac{p}{I_n}$
			VNIIM	maker	RIAN	
1	2	3	4	5	6	7
Ra I ($RaBr_2$)	274,8	160,7	157,0	158	157,7	1,023
Ra II ($RaBr_2$)	305,8	178,8	175,6	176	135,6	1,018
Ra III ($RaBr_2$)	256,3	149,9	147,7	148	149,0	1,015
Ra III' ($RaSO_4$)	211,9	148,7	–	145,3	–	1,020

The table also gives the weights of the $RaSO_4$ and Ra in preparation Ra III', which was subsequently made by precipitation from the bromide (which was done in order to check the bromide for constancy of composition during preparation, as was indicated by special experiments with barium bromide). Columns 4, 5, and 6 give results for the gamma equivalents of all these preparations obtained by the original maker, by the Institute (VNIIM), and by the Radium Institute, Academy of Sciences of the USSR (RIAN). Column 7 gives the ratio of the weight of radium p to the milligram-equivalent (from VNIIM measurements). In all four cases, this ratio is larger than one, the excess being always about 2%. These results show that ionization measurements result in values too low, even when heavy filtration (2 cm Pb) is used. The cause is that the

XI (main) standard used at NVIIM in these measurements (14.27 mg) contains much less radium than do our preparations, and is not enclosed in a second glass safety ampule, as in the case of the standard preparations.

The latter fact, in view of the differences in the wall thicknesses, would imply an apparent reduction in the radium content of our preparations of 0.5-0.7% (under the filtration conditions used). Our calculations show that the difference between the self-absorption factors for 15 mg of $RaCl_2$ and 150 mg of $RaBr_2$ is also appreciable. We have assumed an effective absorption coefficient $\mu = 0.65$ cm^{-1} and that the density of the $RaCl_2$ in the standard and of the $RaBr_2$ in the preparations is $\rho = 1.5$ g/cm^3. The range and absorption curves for the gamma rays for these preparations show that the effective self-absorption in standard XI is 0.9%, while that in 150 mg of $RaBr_2$ is 1.7%, i.e., that there is a difference of 0.8%. These results agree with experimental measurements of the absorption factors of radium preparations [3, 4]. Our estimate of the total discrepancy between I and p (1.3-1.5%) is near to, but somewhat less than, that actually found.

The table also shows that the gamma equivalents I_0 found by using 2 cm Pb filters do not differ appreciably from I_1 and I_2, which have been measured under the conditions usually used in the USSR (5 mm Pb). This is to be expected, since the secondary radium standards calibrated by VNIIM and used at RIAN and elsewhere have a standard packing and a radium content that is roughly equal to the radium contents of these preparations.*

Thus, our results show that the ionization methods used in the USSR systematically underestimate the radium contents of our preparations because the absorption conditions for the State Standards differ from those for our preparations. The error depends on the activity and reaches about 2% for preparations containing 150-175 mg of radium. To increase the accuracy, it would be best to make new primary standards whose contents might be 1, 5, 10, 25, 100, 200, and 500 mg Ra. Then, self-absorption effects could be largely eliminated. It is clear that the absorption conditions used in ionization measurements must be as closely as possible the same for the sample as they are for the standard. The lead filters should not be thinner than 1-1.5 cm.

Until new primary and secondary standards are made it would be best to use the following approximate formula for preparations of activity 20-300 mc:

$$p = I\left(1.006 + 3.6 \cdot 10^{-3} \sqrt[3]{I}\right),$$

where I is the milligram-equivalent of the unknown; the terms in the bracket represent, respectively, the differences in the absorption conditions in the safety ampules.

This formula ensures an accuracy of 0.3-0.5%, at least for standard preparations.

The problem of assaying a preparation of any shape and activity exactly is one that may be resolved fairly easily by calorimetric methods [5, 6], and so we may consider that the question whether the ionization methods should be replaced entirely by calorimetric ones has been settled.

LITERATURE CITED

[1] K. K. Aglintsev, Z. P. Balon, et al., Atomic Energy for Peaceful Purposes [In Russian] (GEI, 1957), p. 145.

[2] G. V. Gorshkov, Z. G. Gritchenko, and N. S. Shimanskaya, Zh. Eksper. Teor. Fiz. 34, 576 (1958).

[3] W. Perry, Proc. Phys. Soc. 57, 178 (1947).

[4] Keyser, Can. J. of Phys. 29, 301 (1951).

[5] W. Mann, J. Res. Nat. Bur. Stand. 53, 277 (1954).

[6] G. V. Gorshkov and N. S. Shimanskaya, Atomnaya Energiya 1, 5, 86 (1956).

* The State Standards X and XI are also secondary international standards, because the radium they contain has been measured not by direct weighing (they contain about 10% $BaCl_2$) but by comparison with a primary standard. The absorption in that standard is very similar to the absorption in the State Standards, so the latter have been assayed accurate to about 0.2%, as the certificates state.

VISCOSITY MEASUREMENTS

A PORTABLE ELECTROVISCOMETER

P. A. Ivanov

Until recently, there has been no equipment available for measuring the viscosities of insulating varnishes, enamels, etc., directly in the feed tanks at their working temperatures.

Our EVI-56P portable viscometer was designed to fill this gap. It is meant for use on the plant; it can measure viscosities in the range 0 to 100 poise at temperatures from + 15 to + 300° C. The unit works by transforming the viscosity to a phase shift of a voltage, which shift is then measured [1]. The main parts are the control panel and the synchronous head, whose axle carries one of a set of interchangeable dippers.

Table 1 gives the sizes of these various dippers.

TABLE 1

Dipper No.	Range in centipoise	Scale division P, centipoise	Remarks
1	0-50	0.5	$p = \frac{\eta_{k\,max}}{m}$, where m = 100 is the number of divisions on the scale of the potentiometer, and $\eta_{k\,max}$ is the maximum viscosity for that range
2	0-250	2.5	
3	0-500	5	
4	0-1000	10	
5	0-10,000	100	

In the new model EVI-57P the first and second ranges have been combined into one (200 cp nominal), and so have the third and fourth (1000 cp nominal).

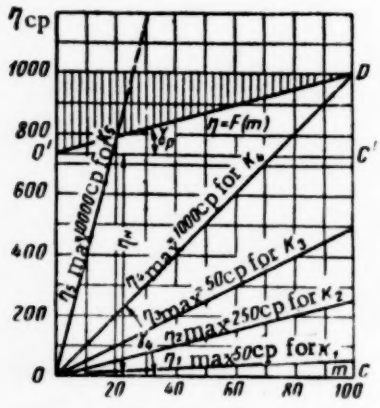

Fig. 1

Figure 1 shows calibration curves.

For each range the viscosity η satisfies the equation

$$\eta = \frac{M}{K\omega}\,\max \tag{1}$$

where K is a constant, M is the torque, and ω is the speed.

The purpose of the unit is such that the viscosity is measured in vessels with $D \gg R$ (where R is the dipper's radius). Therefore, we may neglect effects from the walls of the vessel.

Then, we have

$$\kappa = 4\pi R^2 H,$$

where H is the dipper's height.

Each range has its corresponding constant K_1, K_2, etc.

In Fig. 1 the slopes of the η (m) lines give the values of one such scale division on the potentiometer for the corresponding ranges, i.e., the constants P_K.

The limiting viscosity is

$$\eta_{\kappa\ \max} = m \operatorname{tg} \gamma_\kappa.$$

Hence, one scale division is

$$\operatorname{tg} \gamma_\kappa = \frac{\eta\ \max}{100} = P_\kappa. \tag{2}$$

Any intermediate viscosity within a range is

$$\eta_x = \operatorname{tg} \gamma_\kappa\, m_x = P_\kappa\, m_x. \tag{3}$$

The ÉV1-56P (Fig. 2) is such as to enable one to reduce P_K for any part of a range. Thus, for the fourth range (Fig. 1) the reading corresponding to the initial viscosity η_i can be brought to the zero (point 0') by turning the stator appropriately. Then any new changes in viscosity will lie on the line O'D. It is clear that γ_p (the angle between that line and O'C) is less than γ_4, i.e., that the sensitivity has been increased.

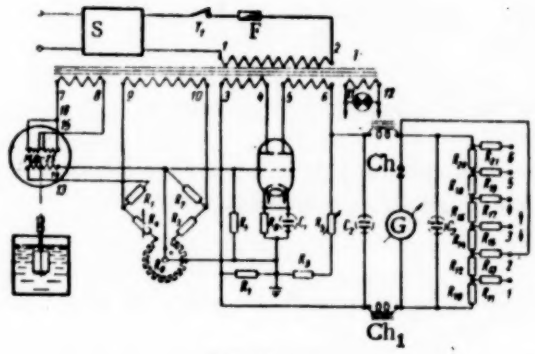

Fig. 2

Figure 1 shows directly that

$$P_p = \operatorname{tg} \gamma_p = \frac{\eta_{4\max} - \eta_i}{m} = P_4 - P_1, \tag{4}$$

where P_4 is the original scale constant (value of one scale division).

Then, for the new range $\eta_{4\max} - \eta_i$ any intermediate point is

$$\eta_x = P_p m_x. \tag{5}$$

Figure 3 explains how the zero is shifted on the potentiometer scale.

When a viscosity η_i is being measured, the rotor is displaced through an angle θ_i, and the position of the emf vector for the generator relative to the voltage U applied to the motor is as in Fig. 3, b. A transfer from O to O' is equivalent to a mechanical displacement of the generator's stator through the same angle θ_i (Fig. 3, c). Then, the emf vector takes up the initial position, for which the angle between U and that vector is 90°.

When η_i has been balanced out, any new change M caused by change in the viscosity (which occurs along O'D in Fig. 1) can be deduced from Fig. 3, d. The emf vector E_g is turned through an angle $\theta = M$.

This method of increasing the sensitivity at any part of the range is a major advantage of the synchronous electric system.

The main errors in the readings arise from the functioning of the transducer head.

The loss equation for the transducer takes the form

$$\sum P = a\omega + \beta\omega^2 + I^2 R + I_g^2 R_g. \tag{6}$$

where $a\omega + \beta\omega^2$ are the losses in the steel and the mechanical losses caused by friction in the bearings.

I^2R is the copper loss in the motor, and $I_g^2 R_g$ is the copper loss in the generator.

The first two terms in (6) are reduced to zero (in effect) by balancing the no-load torque M_0.

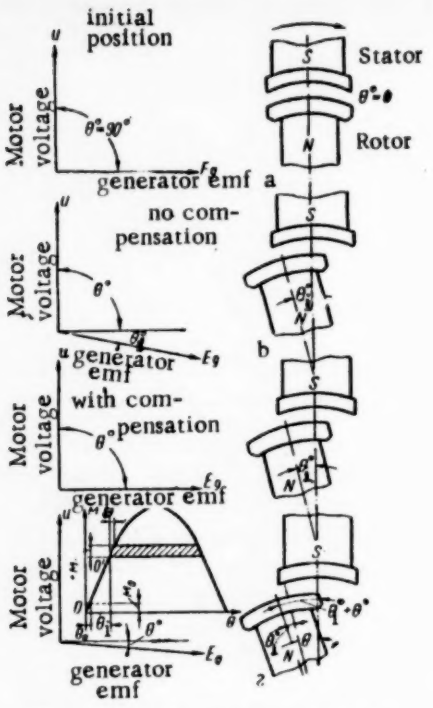

Fig. 3. a) No-load position, no losses, M = 0; b) motor on load; E_g takes up a new position, since the rotor takes up a fresh position at θ_i; c) electrical compensation (the generator's stator is turned through θ_i – the machine has two poles only; d) change in torque caused by viscosity; θ is measured by a phasemeter.

The speed of the rotor (n = 100 rpm) is constant, so the loss in the steel is constant. Armature reaction is neglected, because the poles of the rotor are made of a magnetic alloy.

But, if the transducer becomes heated, the friction in the bearings is reduced, so the torque is altered and the phase changes. Then, although η = const, the bridge

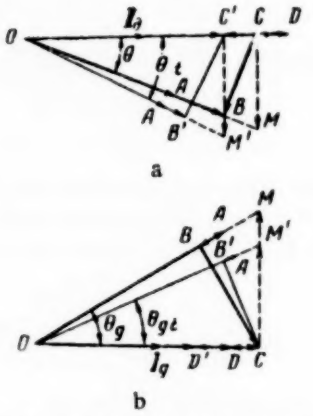

Fig. 4. a) Motor; b) generator.

goes out of balance, and the result is to introduce into the measured quantity a systematic error:

$$\gamma_F\,\% = \frac{-\Delta M_F}{M_{t_1}}, \qquad (7)$$

where M_{t_1} is the torque corresponding to a viscosity η at a bearing temperature t_1;

$\Delta M_F = M_{t_2} - M_{t_1}$ is the change in the friction torque in the bearings when M_0 has been balanced out, and M_{t_2} is the torque produced at temperature t_2, with $t_2 > t_1$.

These torques M_{t_1} and M_{t_2} are found by experiment.

The error for the first range ($\eta_{1\,max}$ = 50 cps) is $\gamma_F\,\% = -1.1\%$.

The third term in (6) may be considered in relation to Fig. 4. The stator coils in the motor become hotter, so the voltage absorbed by their resistance $-\overline{DC} = IR$ rises to $-\overline{DC'} = I_t R_t$, so for a fixed torque M = const (with η = const) we have that Θ (the angle between $\overline{OC}$ and $\overline{OA}$) increases to Θ_t.

The phase change is $\Delta\Theta_t = \Theta_t - \Theta$ and is given by the torque equation (the angles are small, so we may put $\sin\Theta \approx \Theta$):

$$M\eta = C_1 U_1 \Theta + C_2 U_1^2 \cdot 2\Theta_\sigma, \qquad (8)$$

where

$$C_1 = \frac{E_0}{\omega x d};$$

$$C_2 = \frac{xd - xq}{\omega 2 x d\, xq};$$

x_d and x_q are the longitudinal and transverse reactivities;

Here $\overline{OD} - \overline{DC} = U_c - IR = U_1$ is the voltage on the cold motor (the volts lost in the resistance, IR, have been allowed for).

For the hot coils, we have

$$M_t = C_1 U_t \Theta_t + C_2 U_t^2 \cdot 2\Theta_t \tag{8a}$$

where $U_t = U - I_t R_t = \overline{OD'} - \overline{DC'}$; and U is the line voltage.

Then (8) and (8a) give us that

$$\Theta_t = \Theta \frac{C_1 U_1 + 2C_2 U_1^2}{C_1 U_t + 2C_2 U_t^2}. \tag{9}$$

Now the rotors of motor and generator have a common axle, so the phase of the generator's voltage shifts by $\Delta\Theta_t = \Theta_t - \Theta$.

But the last term in (6) shows us that, if the generator's coils become hot, the phase is shifted in the opposite direction, i.e., that the phase error is reduced. The latter phase shift $\Delta\Theta_{gt} = \Theta_g - \Theta_{gt}$ is found from the diagram for the generator (Fig. 4):

$$-\Delta\Theta_{gt} = \operatorname{arctg}\frac{MC}{OD+DC} - \operatorname{arctg}\frac{M'C}{OD'+D'C}. \tag{10}$$

The first term in (10) gives Θ_g, the angle for the cold generator, whereas the second gives Θ_{gt}, the angle for the hot generator.

The notation we shall use for the vectors in this equation is

$$\overline{MC} = I_g x_q.$$

Here x_q is the synchronous inductive impedance of the transverse axis;

I_g is the generator's load current;

$\overline{OD} = U_g$ is the generator's voltage;

$\overline{DC} = I_g R_g$ is the voltage lost in the resistance (cold); and

$\overline{D'C} = I_{gt} R_{gt}$ is the same for the resistance hot, where $I_{gt} < I_g$.

The current is

$$I_{gt} = I_g \frac{(R_M + R_g) + jx_p}{(R_M + R_{gt}) + jx_p}, \tag{11}$$

where $R_M = R_1 + R_2 + R_3 + R_0 + R_4$ is the total resistance of the compensating bridge;

x_p is the impedance of the leakage inductance;

$\overline{OD'} = U_{gt}$ is the voltage of the hot generator.

$$U_{gt} = U_g \frac{(R_M + R_g) + jx_p}{(R_M + R_{gt}) + jx_p}. \tag{11a}$$

Therefore, the relative error caused by the phase drift is

$$\gamma_{\theta t}\% = -\frac{\Delta\Theta_t - \Delta\Theta_{gt}}{\Theta_g} \cdot 100\% = -\frac{\Delta\Theta_t}{\Theta_g} \cdot 100\%. \tag{12}$$

The MD-25 unit used in the EVI-56P gives $Y_{\theta_t}\% = -0.3\%$.

Now (9) and (11) show that Y_{θ_t} depends on the resistances. Therefore, the error will be reduced if these can be reduced. Not only so; we can minimize the $-\Delta\Theta_t$ indicated by (12) by choosing R and R_g, appropriately.

The change in generator resistance, which is in series with R_1 (Fig. 2), causes an error

$$Y_{Z_t}\% = \frac{\Delta Z_t}{Z_1} \cdot 100\%, \tag{13}$$

where

$$\Delta Z_t = Z_2 - Z_1;$$
$$Z_1 = (R_g + R_1) + jx_p;$$
$$Z_2 = (R_{g_t} + R_1) + jx_p.$$

In our instrument $R_1 = 50$ kΩ. Now, ΔZ_t does not exceed 10 ohms within the permissible temperature range, so Y_{Z_t} can be neglected.

We now deal with the errors caused by change in line frequency.

Modern power grids show frequency changes that are small and that occur only at certain times of day. The frequency $\nu = \text{const}$ during normal working hours.

TABLE 2

η, cp	5	10	15	20	25	30	35	40	45	50	First range
Y_{K_1}, %	3,8	2,25	3,2	1,5	2,5	3	2,4	2,25	2,1	2	

η, cp	10	20	30	40	50	60	70	80	90	100	110	120	130	140	150	Second range
Y_{K_2}, %	1	0,5	1,4	1,7	1,1	0,5	0,6	0,7	0,5	0,2	0,4	0,7	0,7	0,6	0,6	

Now if ν increases, the error $Y_\nu\% = \frac{\Delta\nu}{\nu} \cdot 100\%$ will to a certain extent be balanced out by the errors Y_F and Y_{θ_t}.

The errors considered above vary linearly. The total error for any given range is

$$\sum Y\% = Y_F\% + Y_{\theta_t}\% + Y_\nu\% = Y_K\% . \tag{14}$$

The errors may be expressed in scale divisions on the potentiometer or in viscosity units, i.e., as

$$\Delta m_Y = Y_K m, \tag{15}$$

$$\Delta\eta_Y = Y_K \eta \max . \tag{16}$$

The total systematic error for the first range is $Y_{K_1} = 1.4\%$.

We have not considered errors caused by inaccuracy or changes in the bridge resistances, by thermal changes in the dimensions of the dipper, or by calibration errors. Therefore, the actual error is slightly larger than the one given above. But, if the measurements have to be very precise, the error Y_{K_1} may be balanced out by adjusting R_4 (Fig. 2).

We have tested the ÉVI-56P by measuring repeatedly a standard viscosity with the instrument hot. Table 2 indicates the errors found for the first and second ranges.

The error becomes correspondingly less for the latter (2nd) range, as is clear from Table 2.

The ÉVI-56P may be found useful in metallurgy, and in the chemical, cable, radio, electronics, oil, and textile industries.

LITERATURE CITED

[1] P. A. Ivanov, Zavodskaya Lab. (1957), No. 4.

DYNAMIC PROPERTIES OF DEVICES FOR MEASURING UNSTABLE TEMPERATURES

G. P. Katys

The optical devices used for measuring temperatures of unstable flames and gaseous media are usually photoelectric systems operating under dynamical conditions. The accuracy of measurement of rapidly changing temperatures depends very much on the principle adopted for the measuring system of the device and on the dynamical properties of its components. However, in designing or examining such devices the dynamical properties of measuring systems are not usually taken into account. As a result, the dynamical errors may reach the size of the errors of the method and even exceed them.*

1. Various types of brightness pyrometers are given in Fig. 1. Figure 1, a shows a system not involving the obturation of the light flux. The dynamical properties of such systems are relatively high, but the need to use wide band amplifiers which have many operational shortcomings results in a certain instability of indications in time. In order to improve the stability of indications, circuits operating on the carrier frequency are employed in brightness pyrometers. The systems with an optical obturation in the light flux [4-6] using a revolving or vibrating obturation (Fig. 1, b) or systems in which the sensing element operates on alternating voltage (Fig. 1, c), are used for this purpose. Resonance amplifiers, which are characterized by a good stability of indications in time, are used in such devices. The system shown in Fig. 1, c has better dynamical properties than the system shown in Fig. 1, b. This is due to the fact that the optical obturation of the light flux prevents an increase of the carrier frequency above a certain limit, while at the same time the carrier frequency of the supply to the sensing element can be sufficiently high, for example, 4000 cps [6].

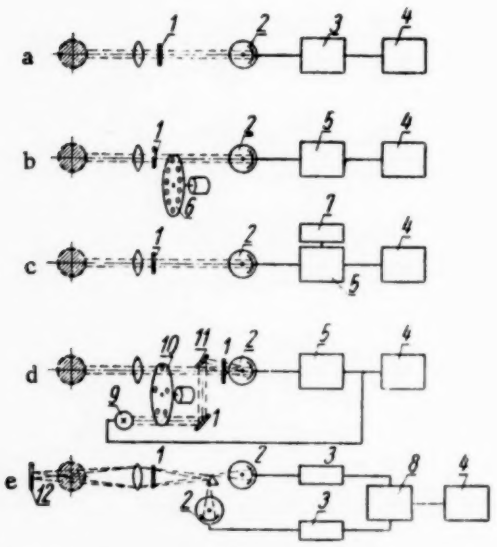

Fig. 1. Schematic diagrams of brightness pyrometers. 1) Filter; 2) sensing element; 3) amplifier; 4) recording device; 5) amplifier-converter; 6) obturator; 7) generator; 8) conversion circuit; 9) lamp; 10) modulator; 11) mirrors; 12) blackbody.

Balancing systems with the feedback from the light flux (Fig. 1, d) are also used sometimes in brightness pyrometers. This eliminates the influence of the parameters of the system upon the indication of the device. However, the use of such systems renders the device somewhat complicated and has a deteriorating effect upon its dynamical properties.

The brightness pyrometer can measure directly the actual temperature of the flame if a mirror and a black screen, which reflect the radiation into the pyrometer objective (Fig. 1, e), are placed behind the flame. The optical system of this device is made in such a manner that the radiation of the flame on the background of the blackbody is passed to a photomultiplier, while the

* This article does not deal with the problem of the methods of measurement of unstable temperatures which have already been considered in technical literature in sufficient detail, for example in [1-3].

radiation coming from the section of the flame behind which the mirror is arranged falls onto another photomultiplier. The measuring signals from both photomultipliers can be fed to a conversion circuit and then to a recording device. This method is relatively simple and can be used in measuring rapidly changing temperatures.

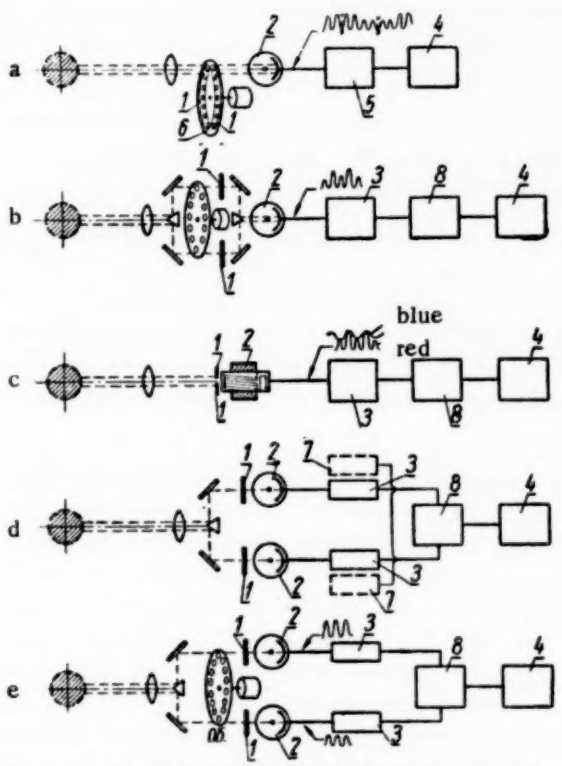

Fig. 2. Schematic diagrams of color pyrometers. 1) Filter; 2) sensing element; 3) amplifier; 4) recording device; 5) amplifier-converter; 6) light modulator; 7) generator; 8) conversion circuit.

The method, with its modifications, of balancing the brightnesses – the method of absorption and emission [2] – also makes possible the direct measurement of the actual temperature of the flame with a brightness pyrometer. In the method of absorption and emission the brightnesses are not balanced, and the actual temperature is determined by measuring three quantities: the brightness of the standard light source, the brightness of the flame, and the brightness of radiation of the light source which has passed through the flame. This method is used in the case of a relatively wide band of spectral radiation as supplied by ordinary light filters, as well as in the case of the monochromatic region of the D-line of the sodium spectrum. In the latter case, prism spectroscopes are used as monochromators. However, the general design of optical commutation devices and the principle of operation of the measuring units are the same in both cases.

2. Schematically, the color pyrometers (Fig. 2) can be of a single- or double-channel type.

In the single-channel type, two different spectral fluxes are directed alternately onto the same photoelectric receiver by means of a light commutator [8 to 10]. The changes in the characteristics of the elements of the device and of the feed voltage simultaneously affect both signals and therefore have no effect upon the indications of the device. For this reason, the requirements presented to the stability of the characteristics of these parts and of the feed voltage need not be high. However, the introduction into the measuring system of a commutator considerably restricts the frequency range of the device in which case a change takes place from a continuous to a discrete measurement.

In the majority of cases the light commutator is in the form of a rotating disk which has on its periphery a certain number of holes into which light filters are inserted (Fig. 2, a). When the commutator revolves, an amplitude-modulated electric signal of a constant frequency is formed in the photocell circuit. The dynamical range of such a device is determined by the frequency of commutation of the color ratio used and by the transmission band of the electronic measuring circuit. In order to improve the dynamical properties of the device, it is desirable to use an alternating rather than a "block" arrangement of light filters in the holes of the commutator disk.

Types of color pyrometers [9] are in use in which the radiations being investigated are divided into two beams, which pass through different light filters and are then alternately fed onto the same sensing element (Fig. 2, b) by means of the light obturator. The dynamical properties of this system are the same as those of the system with an undivided beam in which the light commutator is made as shown in Fig. 2, a.

The commutators made as electromagnetic vibrators to which light filters are secured can also be used in color pyrometers.

The replacement of an electromechanical device for switching color fluxes by means of electromagnetic commutation of the photoelectron fluxes is a very promising development from the point of view of increasing the speed of operation of the device. In the case of electronic commutation of signals corresponding to brightness

temperatures, the radiation is continuously received by the cathode of a special photocell (Fig. 2, c); the variation of the magnetic field by means of a coil which encloses this photocell makes it possible to direct electron fluxes from different sections of the photocathode onto the anode [10]. Two light filters are arranged in front of the photocathode in such a manner that the first half of the photocathode receives radiation of one color and the other half radiation of the other color. This produces in the photocell circuit an amplitude-modulated electric signal, the frequency of which determines the dynamical properties of the device. In the case of an electromagnetic commutation the frequency can be made considerably higher than when opticomechanical commutators are used.

Kerr cells can be used as the light commutator in single-channel pyrometers; they enable an inertia-free modulation of the light flux to be performed by means of a controlling electrical signal. With two Kerr cells, it is possible to pass alternately on to the sensing element two different light fluxes.

For measuring highly unstable temperatures two-channel color pyrometers are used (Fig. 2, e), whose dynamical properties are considerably better than those of the single-channel type (due to the absence of light commutation). In such devices, the measuring signal of each spectral range being investigated is passed simultaneously over two independent channels; the instantaneous color temperature of the object is determined from the ratio of strength of these signals [11]. In order to use resonance amplifiers both sensing elements can be supplied with an alternating voltage produced by a tube generator; the frequency of the supply voltage may be rather high.

Some two-channel color pyrometers make use of optical commutators of light flux. In this case, no light filters are placed into the holes of the rotating disk and the holes are used merely for the purpose of obturation of the flux without a spectral dispersion (Fig. 2, e). Before reaching the obturator, the flux is divided into two beams by means of a semitransparent mirror or prism and directed through suitable light filters into two photocells. The measuring signals of photocells are passed into amplifiers operating on the carrier frequency and into the corresponding conversion system. The main difference between this instrument and its single-channel counterpart (Fig. 2, b), is that the electrical pulses being measured and which correspond to the light signals, are formed in the phototube, simultaneously, whereas in the case of the disk commutation of the flux these signals are shifted in time. The fact that the signals are simultaneous results in a certain improvement in the accuracy of measurements because in this case the measuring signal represents a mean taken over a shorter period of time. However, the two-channel color pyrometer with optical commutation cannot be considered the best type of its kind. Because of the presence of two measuring channels the system makes it possible, in principle, to measure highly unstable temperatures. But the use of the optical obturation of light fluxes substantially reduces the dynamical properties of the device. The use of two-channel light pyrometers without the optical commutation of fluxes is more rational.

3. Figure 3 shows schematic diagrams of quick-acting devices based on several variations of the method of inversion of the spectral line of an alkali metal (for example, sodium) introduced into the flame. The devices can be divided into two groups: a) systems operating on the emission-absorption method within the region of the line of sodium; b) systems operating on the method of balancing the brightness of the sodium line.

The schematic diagram of a device of the first group is given in Fig. 3, a. The measuring system consists of prism-monochromators, an opticomechanical interrupter with two disks, a photomultiplier with an amplifying converting unit, and a recording device [13, 14]. The radiation emitted by the tungsten lamp placed behind the flame is interrupted during the measurements with a frequency of 300 cps by means of the revolving disk with holes which is placed between the tungsten lamp and the flame. The radiation arriving in the device from the flame is interrupted with a frequency of 60 cps by means of a second disk with holes on the periphery. These disk obturators are placed on a common axis and rotate at the same speed. The different frequencies of obturation are obtained by having holes of a different size and shape in the disks. The photomultiplier placed at the outlet slit of the spectroscope receives the suitably modulated monochromatic light flux. Figure 3, a shows the measuring signal of this device obtained from a changing temperature of the flame. At the beginning of the measuring process, before the flame appears, the calibration signal is recorded — this is obtained by modulating the radiation of the tungsten lamp by means of the disk interrupter. When the flame being investigated appears, the measuring signal becomes modulated twice by two rotating disk obturators. By measuring the dimensions a, b, and c of the signal obtained, it is possible to determine the actual temperature T_f of the flame being investigated:

$$\frac{a-b}{c} = e^{c_{2\lambda}\left(\frac{1}{T_f} - \frac{1}{T_{st.l}}\right)}$$

This method was used for measuring rapidly changing temperatures, in which case the frequency of modulation of the radiations being investigated, which was effected by means of the rotating disks, was increased to 10 kc [13].

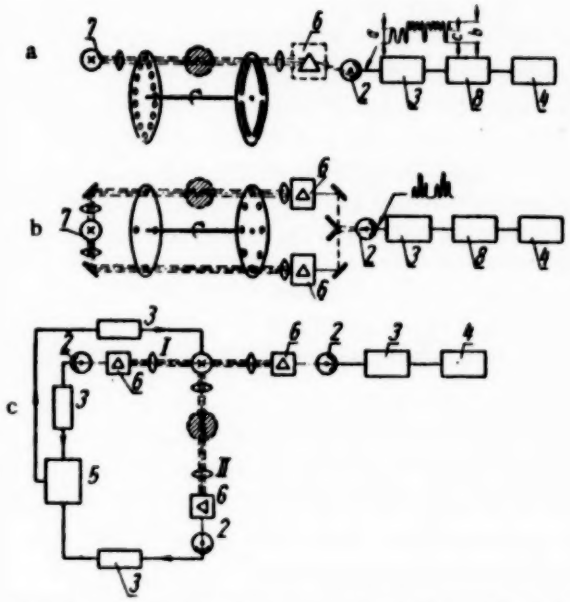

Fig. 3. Schematic diagram of devices based on the inversion method. 1) Filter; 2) sensing element; 3) amplifiers; 4) recording device; 5) bridge; 6) monochromator; 7) lamp; 8) conversion circuit.

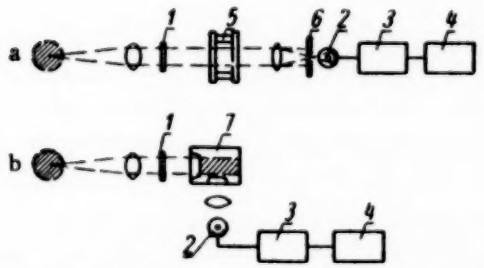

Fig. 4. Schematic diagrams of devices with interferometers. 1) Filter; 2) sensing element; 3) amplifier; 4) recording device; 5) interferometer; 6) diaphragm with a central hole; 7) resonance tube.

The same principle is employed in the device [14], whose schematic diagram is given in Fig. 3, b. The radiation of the standard light source is divided into two beams by means of a system of mirrors and lenses. The path of the lower beam is equal to the length of the path of the upper beam, the only difference being that it does not pass through the flame. The disk interrupters, which have a common axis, alternately direct the light beams coming from the top and the bottom optical channels onto the photomultiplier. The shape, size, and mutual positions of the holes on the disk interrupter are chosen in such a manner that the photomultiplier receives radiations of three types at regular intervals. This produces in the measuring signals groups of impulses containing three peaks: the first peak represents the radiations of the flame, the second – the radiations of the standard source, and the third, the radiation of the standard light source which has passed through the flame plus the radiation of the flame. The general principle of determining the temperature of the parameters of the measuring signal is in this case the same as in the instrument considered above. This device makes possible the taking of 3000 discrete measurements per second.

The basic difference between this device and the one considered above is that in the former, the measuring signal contains marks whose amplitude is proportional to the intensity of radiation of the standard source, in addition to the marks whose amplitude is proportional to the intensity of radiation of the flame and to the intensity of radiation of the standard light source which passed through the flame. The introduction into the measuring signal of impulses proportional to the intensity of radiation of the standard light source, which characterizes the stability of operation of the device, renders the measurements more accurate as compared with those made with the above system.

The dynamical qualities of the devices considered are determined by the frequency of commutation of the radiation being investigated. An increase of the commutation frequency is restricted by the need to perform an accurate balancing of the rotating disks and also by the need to make the holes on the commutation disks with great precision. In the majority of devices of this type, the time required for one discrete measurement is 0.01-0.001 sec, but in some instruments it has been reduced to 0.0001 sec.

The use in the devices already considered of electronic conversion circuits which automatically determine the temperature from the signals received from the photomultiplier, appear to be very promising. The output signal of such an electronic circuit must be an electrical signal proportional to the temperature.

In one of the devices operating by the method of balancing the brightness of the sodium line, the monochromatic brightness of the standard light source (sodium gas discharge tube) varies automatically with the flame temperature. The regulation of the monochromatic brightness of the standard light source is effected in such a manner that the sodium line radiated by the unstable flame is in a continuous process of inversion on the background of the spectrum of the standard light source [16]. The device operates on the principle of automatic balancing of the spectral brightness of the sodium line in two radiation beams (Fig. 3, c). The first beam 1 consists of monochromatic radiations of the standard sourcethat are continuously fed onto the sensing element, and the second beam 2 consists of the radiation of the same standard source which has passed to the flame and is partially absorbed by it. If the temperature of the flame is equal to the temperature of the standard source, a continuous inversion of the sodium line will take place. In this case, the intensity of both light beams will be equal, since the sodium vapors contained in the flame will radiate the amount they absorb. The photomultipliers which receive the first and the second light beams are connected to a bridge-type measuring circuit. A disturbance of the temperature balance between the flame and the tube will cause an unbalance in the bridge. The unbalance signal thus obtained is fed into the gas-discharge tube and changes its brightness until the temperature equilibrium between the tube and the flame is restored. The spectral brightness of the gas-discharge tube is recorded by means of a third photomultiplier which is connected into a separate measuring system. The strength of the measuring signal produced by this photomultiplier is proportional to the temperature of the flame.

The dynamical range of this device is determined mainly by the dynamical properties of the system which controls the operation of the sodium tube, and by the transmission band of the system used for measuring the spectral brightness of the sodium tube. It appears that a device of this type incorporating a tungsten lamp operating in stable conditions as a standard light source has good prospects of success. In this case, the inertia-free regulation of its brightness can be effected by means of an optical element (e.g., the Kerr cell), the coefficient of absorption of which varies with the strength of the controlling electrical signal.

4. Systems in which the temperature is determined from the intensity of the central part of a saturated spectral line of an alkaline metal (e.g., sodium) introduced into the flame* [17] can be used for measuring unstable temperatures.

Here a spectral apparatus must be used which makes possible the dispersion of the flame into a spectrum, and the separation from the spectrum of the sodium line, and from this line its central part. In recent years, in addition to the ordinary optical spectral systems, the Fabry-Perot interferometers and the sodium resonance tube have been increasingly used.

The schematic diagram of the device incorporating an interferometer [18] is shown in Fig. 4, a. In order to separate a section of black radiation of a spectral line, this device contains a diaphragm with a centrally located hole which separates the central spot of interference fringes. The radiation of the saturated section which has passed through the aperture of the diaphragm is received by the cathode of the photomultiplier. The electrical signal thus produced is passed through the amplifier and then into the measuring device.

The background produced by the flame, which contains a solid spectrum of radiation, has a deteriorating effect upon the sharpness of interference fringes and produces an additional error. A very promising development in this case is the use of modulation methods which make possible the measuring of useful signals with the background taken into account. If a piezoelectric ring placed between the plates of the interferometer is used as a modulator, it is with an alternating voltage which varies with a definite frequency. This causes a change in the distance between the plates of the interferometer, and the interference fringes obtained become modulated with the same frequency. In this case, the photoelectric receiver will receive alternating radiation from the upper part of the spectrum line and from its background, which produces a modulated electrical signal; this signal

* A detailed consideration of this method, of the optimum range of its application and the accuracies being achieved, is given in [1, 3, 17, 18, 19].

makes possible the measurement of the intensity of the spectral line, with its background taken into account.*

The dynamical properties of the device being considered are determined by the transmission band of the amplification system and can be sufficiently high. The use of the modulation methods of measuring will not substantially reduce the dynamic properties of the device since the frequency of modulation of the measuring signal can be made very high.

The sodium resonance tube which responds only to the radiation of sodium vapor contained in the flame, and which in this case emits resonance radiation [19], can be used as a highly monochromatic light filter for separating the central portion of the spectral line.

The schematic diagram of the device incorporating the resonance tube is shown in Fig. 4, b. The radiation of the flame is directed by means of the objective into the inlet window and the interior of the tube. The excited resonance radiation of sodium vapors emerges through the other window of the tube and is received by the photomultiplier. In the device being described, the direction of the exciting radiation and of the resonance radiation which is being measured are mutually perpendicular. The signal produced by the photomultiplier is amplified and passed into the measuring device.

The use of the resonance tube as the monochromator has certain advantages, such as the simpler design and compactness of the apparatus. This measuring system has high dynamical properties. However, the shortcomings of the resonance tube include the presence of dissipated light and the need to maintain a constant temperature.

If an element with a lower excitation potential, e.g., potassium, is introduced into the flame instead of sodium, the lower limit of application of this method can be as low as 1500° C. The upper limit of application of the method can be increased by the use of elements with a high excitation potential (e. g., calcium) to 10,000° C.

LITERATURE CITED

[1] A. E. Kadyshevich, Measurement of Temperatures of Flames [In Russian] (Moscow, 1954).

[2] I. I. Kirenkov, Measurement of Temperatures of Flames [In Russian], Proceedings of the All-Union Research Institute of Metrology 5, 65 (1949).

[3] N. N. Sobolev, Proceedings of the FIAN (1956), Vol. 7.

[4] Automobile Engineer 10, 437-438 (1955).

[5] P. M. Sudakov, Photoelectrical Pyrometer [In Russian] Instruments and Test Stands, (Izd. INI AN SSSR, Moscow, 1955).

[6] Ya. I. Merson and A. I. Kadyshevich, Coll.: Measurement of Temperatures of Flames, [In Russian] (Moscow, 1954).

[7] G. H. Hett, Jet Propulsion 25, 3 (1955).

[8] W. Brown, J. Sci. Instrum. 31, 12 (1954).

[9] A. F. Gibson, J. Sci. Instrum. 28, 153-155 (1951).

[10] G. P. Katys, Author's Certificate No. 114,791 (1958).

[11] G. M. Auble, Jet Propulsion 25, 9 (1956).

[12] A. E. Kadyshevich, Coll.: Measurement of Temperatures of Flames, [In Russian] (Moscow, 1954).

[13] G. H. Millar, J. Opt. Soc. 43, 609 (1953).

[14] G. S. Sutherland, Jet Propulsion 25, 10, 537 (1955).

* This method of modulation has been developed at the Khar'kov State Institute of Measures and Measuring Devices.

[15] A. Moutet, Recherche Aeron 27, 21 (1952); 28, 21 (1952).

[16] M. H. Wakil, Transactions ASME 74, 2, 255 (1952).

[17] V. V. Kandyba, Author's Certificate No. 99,901 (1955).

[18] L. M. Kutsina et al., "Measurements of temperatures of flames by means of the resonance tube," Proceedings of the Conference on Pyrometry, Leningrad (VNIIM, 1957).

COMMITTEE OF MEASURING STANDARDS, MEASURES, AND MEASURING DEVICES

I. NEW STANDARDS FOR MEASURES AND MEASURING DEVICES APPROVED BY THE COMMITTEE

New Standard Specifications

(Registered in the Period December 1958 to February, 1959)

GOST 2823-59. "Mercury glass thermometers, commercial grade." Replaces GOST 2823-45.

GOST 5334-59. "Spectacle glasses. Classification." Replaces GOST 5334-50.

GOST 8916-58. "Mechanical ship chronometers." New standard.

GOST 9016-59. "Optical dividing heads. Types, basic characteristics and dimensions. Standards of precision." New standard.

GOST 9017-59. "Diamond styli for profilometers and profilographs." New standard.

GOST 9018-59. "Fuel distributing columns." New standard.

GOST 9020-59. "Wagon scales." New standard.

GOST 9030-59. "Portable devices for measuring hardness of metals. Types and basic characteristics. Technical specification." New standard.

GOST 9031-59. "Standards of hardness." New standard.

GOST 9032-59. "Laboratory measuring transformers. Technical specification." New standard.

GOST 9038-59. "Block gages." Replaces GOST 85,000-39.

II. MEASURES AND MEASURING DEVICES APPROVED BY THE COMMITTEE ON THE BASIS OF OFFICIAL TESTS AND ADMITTED FOR USE IN THE USSR

(Registered in the period between December, 1958 to January, 1959).

Generator of meter waves, maker's designation GMV of the Kiev Council of National Economy. State registration No. 1226-58.

Master device for frequency measurements, maker's designation "Avangard," Moscow-Region Council of National Economy, State registration No. 1227-58.

Impulse tube voltmeter, maker's designation VLI-2, Gorkii Council of National Economy. State registration No. 1228-58.

Dc potentiometer unit, maker's designation U302, of the Krasnodar Council of National Economy. State registration No. 1229-58.

Photoelectronic color pyrometer, maker's designation TsEP-3 of the Kaluga Council of National Economy. State registration No. 1230-58.

Device for measuring gamma radiation, maker's designation "Kaktus," Belorussian Council of National Economy. State registration No. 1231-59.

Electromagnetic panel ammeters, maker's designation M 224, to combine with the earlier approved electromagnetic panel-type microammeters with maker's designation M 494. Omsk Council of National Economy. State registration No. 419.

Radar-tester, maker's designation RT-10, for the frequency range 2700-2100 Mc of the Leningrad Council of National Economy. State registration No. 1232-59.

Radar-testers, maker's designation RT-10A, for the frequency range 3060-3390 Mc, Leningrad Council of National Economy. State registration No. 1233-59.

Beta-gamma radiationmeter, maker's designation DP-11-B, Moscow City Council of National Economy. State registration No. 1234-59.

AMENDMENTS TO THE INSTRUCTIONS NOW IN OPERATION FOR THE INSPECTION OF MEASURES AND MEASURING DEVICES

N. N. Staroverov

Instruction 220-55 on the inspection of the G4-1 and the G4-1M heterodyne frequency meters has been extended by adding an appendix explaining the inspection of the G4-1M devices without the use of the "Avangard" unit. This inspection must be carried out in the following order:

a) first, the multiplicity of a division of the frequency (10 Mc) of the G4-1M quartz generator is checked by means of a multivibrator;

b) the frequency of the G4-1M quartz generator is now checked against the standard frequency signal transmitted by radio, or against the frequency of the reference quartz generator;

c) this is followed by checking the measuring generator against the frequency of the G4-1M quartz generator.

Amendments were made to Instruction 210-54 concerning the checking of tube voltmeters; they simplify the checking process of the device and realize the efficiency suggestion of A. D. Taranenko.

For tube voltmeters used in dc measurements an instruction for setting the device for dc-operation has been added. Here, for measuring the dc voltages 1 mv - 300 v, the same circuit is used as for ac measurements, which is given in Fig. 1 of the Instruction; in this circuit the ac source with a filter has been replaced by a dc source of variable voltage.

A second variant of the tables has been added to the Instruction for checking the VKS-7, VLU-2, LV-9, MVL-1, and MVL-2 tube voltmeters.

Both types of auxiliary tables can be used in the inspection. The alternative tables simplify the process of setting the necessary division factors and also the calculations, but increase the number of switching operations on the master device scale.

In order to accelerate the process of checking tube voltmeters, wire-type voltage dividers should be used with the division factors 10, 100, and 1000.

In Instruction 36-55 on testing road tankers, paragraph 22 has been amended; the new version says that a reduction of water level in the neck section after a 5-minute drive can be increased to 0.15% of the nominal capacity of the tank instead of 0.5% as specified earlier. This amendment was necessary because the Instruction specifies an average temperature of 10-30° C for the calibration and inspection of the tank by the volume method. Within this temperature range, the volume of water in the tank changes over in a wider range than allowed for settling.

In Instruction 64-56 concerning the checking of quadrants, the permissible error of quadrants is equal to the value of a division; the penultimate paragraph 5 of the Instruction has been altered to this effect.

Instruction 49-57 concerning the checking of mobile scales with unequal arms has been expanded by a note reading as follows: "In checking 150 kg and smaller scales the allowance for the stability of the no-load equilibrium position is doubled."

According to GOST 1643-56 ("Spur-gear transmissions. Allowances.") the classes of accuracy specified in GOST 1643-46 were replaced by the grades of accuracy in the book "Inspection of Devices for Measuring Gears."

In Instruction 120-53 on the inspection of gear-measuring micrometers, amendments were made which take into account amendment 2 to GOST 6507-53. This amendment eliminated the division of gear-measuring micrometers into classes and made changes in the permissible error of these devices; as a result the table of paragraph 9 was changed as follows (see table).

No.	Type of error	Micrometer measuring range, mm	Permissible error, μ
1	Deviation of measuring faces from flatness;	all ranges	0.9
2	Deviation of measuring faces from parallelism	Ditto	3
3	Total indication error of micrometers	Ditto	± 5
4	Deviation of the setting gage length from the nominal dimension	25 mm	± 1
		50 and 75 mm	± 1.5
5	Deviation of the faces of setting gages of all dimensions from parallelism		Should not exceed the accuracy standards set for third class block gages (according to OST 85,000-39)

The indication error of the gear-measuring micrometers is determined by means of block gages of 5th grade or of second-class accuracy.

Instruction 120-53 has been extended by a note permitting the use of micrometers with indication errors exceeding by not more than two times the values specified in the Instruction.

These micrometers are considered as belonging to the second class and should be marked "II cl.".